"Design, Synthesis And Evaluation Of Metal complexes of Medicinal Agents"

Thesis submitted for the degree of

Doctor of Philosophy (Ph.D.) in

Pharmaceutical Sciences

BY

Mr. DINESHCHANDRA G. DESAI, M.Pharm.

Guide:

Dr. A. K. SETH, Ph.D.

Department of Pharmacy

SUMANDEEP VIDYAPEETH

JULY 2011

SUMANDEEP VIDYAPEETH, PIPARIYA, GUJARAT

Certificate

I certify that the thesis entitled **"Design, Synthesis And Evaluation Of Metal Complexes Of Medicinal Agents"** submitted for the Degree of Doctor of Philosophy by **Mr. DINESHCHANDRA G. DESAI** is the record of research work carried out by him under my guidance and supervision and that this research work has not formed the basis for the award of any degree, diploma, associateship, fellowship or other similar titles in this University or any other University or institution.

Dr. A.K. SETH
Dean,
Dept. of Pharmacy,
Sumandeep Vidyapeeth,
Piparia.

Date :
Place : Pipariya.

SUMANDEEP VIDYAPEETH, PIPARIYA, GUJARAT

Certificate

I declare that the thesis entitled **"Design, Synthesis And Evaluation Of Metal Complexes Of Medicinal Agents"** submitted by me for the Degree of Doctor of Philosophy (Ph.D.) is the record of research work carried out by me under the guidance of **Dr. A. K. SETH** and has not formed the basis for the award of any degree, diploma, associateship, fellowship or other similar titles in this University or any other similar institution of higher learning.

Mr. DINESHCHANDRA G. DESAI
Research Scholar,
Dept. of Pharmacy,
Sumandeep Vidyapeeth,
Pipariya.

Date :
Place : Pipariya.

ACKNOWLEDGMENT

It gives me immense pleasure today when I take an opportunity to acknowledge all those personalities who contributed directly or indirectly to my project. This research would not have been possible without the whole hearted encouragement, guidance, support, and cooperation of my beloved family, teachers, friends, well wishers and relatives. Probably I would have never achieved this without their support and blessings. With profound appreciation, I acknowledge to one and all.

I wish to express my sincere thanks, with a deep sense of gratitude, to my respected guide **Dr. A. K. Seth**, M.Pharm, Ph.D., Director, Faculty of Pharmacy, Sumandeep Vidyapeeth, Pipariya. for his valuable guidance, supervision, creative suggestions and meticulous attention, sustained interest, immense guidance, dedicated support he has bestowed upon me for the timely completion of this work. I am extremely indebted to **Seth Sir** for his motivational inspiration, kind expertise during the writing up of my thesis and the scientific attitude he has nurtured in me which will definitely stand in all my future endeavours.

Dr. K. I . Molvi, Principal, Ali-Allana College of Pharmacy, Department of Pharmaceutical Medicinal Chemistry, Akkalkuawa, Nandurbar, Maharashtra, India, has always remained a source of inspiration for me. He is the person who has inspired me to start this work and I always remain indebted for the continuous encouragement he gave me during my research work.

I am grateful to Dr. B. N. Suhagia, M. Pharm, Ph. D., F.I.C., Professor and Head, Department of Quality assurance, L. M. College of Pharmacy for providing all necessary help ,support and cooperation he gave during the course of my work.

I am deeply grateful to Dr. Mansukh Shah, Dr.Dixit Shah, Dr.Purvesh Shah, Dr.Jayshree Mehta and Mr. N. N. Shah, Sumandeep Vidyapeeth for providing facilities required in completing the work.

I am very much thankful to Rathod Sir and Mr.Been Prajapati for their technical and moral support they provided in my research work.

Thanks are also due to my colleagues and friends Mr.Mustakim Mansuri and Mr.Javid Mansuri for their continuous support and everlasting smile.

A special thanks to honorable trusties of Sanskar Education Trust, Principal, P. & M. Kansara Pharmacy College Pipariya, Teaching and non teaching staff of the college for their help.

I am thankful to Dr.B.N.Patel, Mrs.Chauhan, Mr.K.N.Patel, Mr.Tejas Ghelani and Dr. Anwar Shaikh for their support and help.

I thank Mr.Rajubhai Patel, Macbay Pharmaceutials, for free gift of chemicals

I am indebted infinitely to love, care and trust being showered on me by my mother, my wife and my sons Krutang, Krupesh and Krutesh without their consistent prayers, affection, selfless care and endless confidence in me, I would have never come to the stage of writing this acknowledge. This is a modest beginning and with the encouragement and support of my contributors it should be possible for me to continue my mission.

Last, definitely not the least I pay reverence to the almighty, omniscient, omnipresent, omnipotent, supreme soul who has perpetually patronize me with the contentiousness and love.

July 2011 (Dineshchandra G.Desai)

CONTENTS

LIST OF TABLES

LIST OF FIGURES

LIST OF CHARTS

ABBREVIATIONS

ACs	Actinomycins
ABLM	Activated Bleomycin
ADP	Adenosine diphosphate
ATP	Adenosine triphosphate
ATCC	American Type Collection Culture
AC	Anthracycline
BC	Before Christ
BLM	Bleomycin
Cx	Cinoxacin
CFT	A type of ionic bondig model
CFU	Colony forming unit
°C	Degree celcius
DFO-Ga	Desferrioxamine-gallium
DMF	Dimethyl formamide
DMSO	Dimethyl sulfoxide
FTIR	Fourier Transform Infra Red Spectroscopy
gm	Gram
hr	Hour
HCl	Hydrochloric Acid
M	Metal
µ	Microgram
MO	Metal-Oxygen
MIC	Minimum inhibitory concentration
M.W.	Molecular weight
NCTC	Natural Collection Type Culture
NIM	Nitroimidazole
NMR	Nuclear Magnetic Resonance

PPM	Parts per million
%	Percentage
PFD	Pirfenidone
SN	Streptonigrin
TC	Tetracycline
TMS	Tetramethyle silane
ie	That is
tnz	Tinidazole
UV	Ultraviolet

ABSTRACT

Nitroimidazoles, especially tinidazole (tnz) was a therapeutic agent of choice for amebiasis and also used in combination with other antimicrobial drugs against yeast infections. Under anaerobic conditions inside the cell, it was reduced to a cytotoxic nitro radical and binds nonspecifically to the organism's DNA and enzymes, which were thus inactivated. High doses or long-term administration of tinidazole can cause a peripheral neuropathy with sensory disturbances, and the emergence of resistance to this drug is known in many pathogenic bacteria and protozoa. Other available drugs have their own limitations, and today, parasite resistance is also a global problem. Metal based drugs such as Au(I) complexes have been used successfully for the treatment of various diseases including P_{38} leukemia. Many neutral palladium (II) and palladium (IV) complexes were found to exhibit potential antitumour activity. Moreover, Ru complexes of chloroquine act as potential antimalarial agents against *P. falciparum*. So it is well-known that coordination of metal ion has a positive effect on drug efficacy. A series of Pd, Pt, Cu, Au, and Ru complexes of metronidazole (mnz) was prepared shows good activity.

A series of metal complex with 2-substutituted nitroimidazole (tinidazole and dimetridazole) analogues were prepared with the various transition metals like nickel, cobalt, cadmium and copper etc.

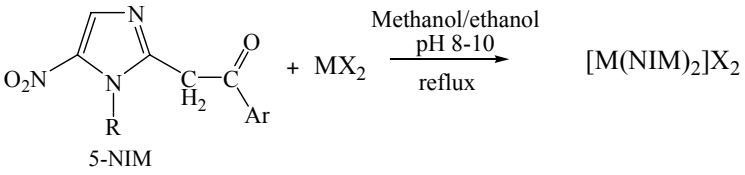

5-NIM

Ar = phenyl, *p*-cl phenyl, *m*-cl phenyl,
o-cl phenyl, furoyl
R = $-CH_3$, $-CH_2CH_2SO_2CH_2CH_3$

The Nickel complex with 2-substituted nitroimidazoles were designed, synthesized and characterized by IR, ^{1}HNMR, MASS, UV and conductivity measurements. The IR frequency for ligand and complex was compared; it was found that frequencies for CH_2, NO_2 is matching with peak of complex. The frequency for carbonyl is changed drastically as it is useful band in the infrared spectra of carbonyl ligand in metal

complexes is that due to C–O stretching. The later gives very strong sharp bands which are separated from the bands of other ligand that may be present. The stretching wave number for a terminal carbonyl ligand in a complex correlates with the 'electron-richness' of the metal. The band position is determined by the bonding from the d Orbitals of the metal into the π* anti-bonding Orbitals of the ligand (known as *backbonding*). The bonding weakens the C–O bond and lowers the wave number value from its value in free CO thus its show lower frequency ranging 2250-2000cm^{-1} The M-O streching is observed near 600-480 Cm^{-1}. Characterization by spectral analysis reveals that divalent nickel transition metal binds the bidentate ligand (2-substituted nitroimidazoles) in the ratio of [M:L;1:2] was confirmed by the MASS, which shows the double in the mass of the molecules. The conductivity measurement shows negligible conductance which is indication of non electrolytic behavior of the complex. Thus characterization shows that the nickel complexes of nitroimidazoles may be tetrahedral in nature.

Cobalt complex with 2-substituted nitroimidazoles were designed, synthesized and characterized by IR, ^{1}HNMR, MASS, UV and conductivity measurements. IR frequencies of the complexes shows, the broad peak near 3600-3500 cm^{-1} which indicates the water of crystallization of cobalt nitrate salt, C-H streching (3096-2800 cm^{-1}), >C=O (2250-2000 cm^{-1}) , NO_2 (1570-1540 and 1366-1358cm^{-1}), M-O (600-480 cm^{-1}) indicates the coordinate covalent bond formed between ligand and metal. All other characteristics were same as the metal complexes of nickel. The cobalt complex also reveals the tetrahedral structure of complex due to binding of metal to ligand in the ratio of 1:2

All the $[Cd(NIM)_2]Cl_2$ complexes were light yellow to dark brown in color and are soluble in DMSO,DMF and insoluble in all other solvents. The complexes are stable solid with melting point ranging from 212 - 248°C. IR frequencies of the complexes shows the C-H streching (3096-2800 cm^{-1}), >C=O (2250-2000 cm^{-1}), NO_2 (1570-1540 and 1366-1358cm^{-1}), M-O (600-480 cm^{-1}) indicates the coordinate covalent bond formed between ligand and metal in the ratio of 1:2.

Copper (II) ion is well known to modify the radiation response in both mammalian and bacterial cells. The radiosensitizing mechanism in mammalian cells may involve reduction of copper (II) to copper (I). More recently, it has been found that: radiosensitization process may be related to radiation induced DNA damage, biological damage sensitized by copper ions might involve nucleobases; and copper complexes with different structural features can bind with double-helical DNA and promote double-strand DNA damage. Copper complex with 2-substituted nitroimidazoles were designed, synthesized and characterized by IR, ^{1}HNMR, MASS, UV and conductivity measurements. IR frequencies of the complexes shows the, the broad peak near 3700-3500 cm^{-1} which indicates the water of crystallization of copper chloride salt, C-H streching (3096-2800 cm^{-1}), >C=O (2100-1900cm^{-1}) , NO_2 (1570-1540 and 1366-1358cm^{-1}), M-O (600-480 cm^{-1}) indicates the coordinate covalent bond formed between ligand and metal. It is also confirms that copper -nitroimidazole complex having tetrahedral structure.

All the synthesized and characterized compounds of 2-subtitutednitroimidazole complexes of metals were studied for their antimicrobial study against Gram negative bacteria (*S.Aboney*) and Gram positive bacteria (*S.auerues and B.Pumulis*) using tinidazole and ciprofloxacin as standard control drug by cylinder plate method. The results were expressed in zone of inhibiton (mm) at 100 µ/ml concentration.

The complexes from each series having the ligand NIMF, NIMDF and NIMDP that mean complex $[Ni(NIMF)_2]Cl_2$, $[Ni(NIMDF)_2]Cl_2$, $[Ni(NIMDP)_2]Cl_2$ with Nickel as metal, $[Co(NIMF)_2(NO_3)_2]6H_2O$,$[Co(NIMDF)_2(NO_3)_2]6H_2O$, $[Co(NIMDP)_2(NO_3)_2]6H_2O$ having Cobalt as metal, $[Cd(NIMF)_2]Cl_2$, $[Cd(NIMDF)_2]Cl_2$, $[Cd(NIMDP)_2]Cl_2$ with Cadmium as metal and $[Cu(NIMF)_2Cl_2]2H_2O$, $[Cu(NIMDF)_2Cl_2]2H_2O$, $[Cu(NIMDP)_2Cl_2]2H_2O$ with Copper as metal were found to be active against Gram positive bacteria (*B. Pumulis and S. aureus*). Among all the synthesized complex, $[Ni(NIMDF)_2]Cl_2$ was found most active and having zone of inhibition (25mm) comparable to the standard ciprofloxacin having zone of inhibition (30) as show in the figure and chart 1. It was also observed that all the metal complexes of 2-substitutednitroimidazole were remain inactive against the gram negative bacteria.

Zone of inhibition against

***B. Pumilus* for *[*Ni(NIM)$_2$]Cl$_2$**

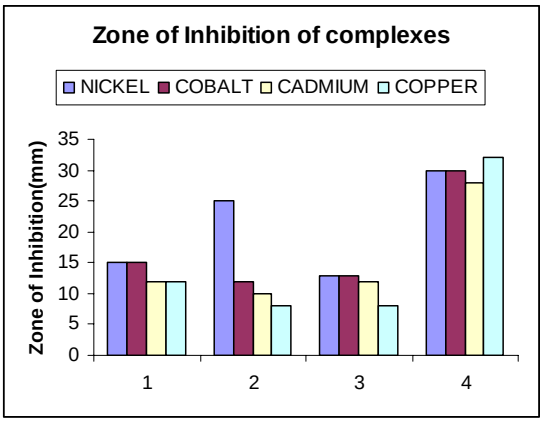

Zone of inhibition of active Complexes(*B. Pumulis*)

(Where 1; NIMF, 2: NIMDF 3: NIMDP and 4: Ciprofloxacin)

It was the finding that the metal complexes of nitroimidazole show tetrahedral structures with divalent transition metals observed in the ratio of [M: L; 1:2]. The antimicrobial study shows the most potent acitivity was observed in the nickel metal amongst all the divalent transition metal against Gram positive bacteria. Nitroimdiazoles are the drug specifically used for the treatment of anaerobic bacteria; surprisingly the preparation of its nickel complex shows good aerobic antibacterial activity against gram positive bacteria which is almost comparable to standard drug ciprofloxacin. Thus the nitroimidazole complex of nitroimidazole may be considered as better choice for treatment of anaerobic and aerobic infections.

CHAPTER I
INTRODUCTION

1.1 Introduction to coordination chemistry

Coordination chemistry is a branch of chemistry under which the "complex" compounds are studied. Complex is formed by the association of the metal with ligand. The ligand may be an atom or a molecule or a group of other ligand is said to donate electron pair(s) whereas, metal accepts them. In a more sophisticated manner, the complex is an association of Lewis base with Lewis acid. Since the appearance of water on earth, aqua complex ions of metals must have existed. The subsequent appearance of life depended on and may even have resulted from, interaction of metal ions with organic molecules.

The history of coordination chemistry encompasses a great deal of diversity of substances and phenomena. Perhaps the earliest known of all the coordination compounds is the bright red alizarin dye, a Ca-Al chelate compound of hydroxyl anthraquinone. It was first used in India and is known to the ancient Persians and Egyptians long before it was used by Greeks and Romans.

Alizarin was mentioned by Herodotos' (ca 450 B.C.). It was probably red dye used by Alexander the great to win a battle against a much larger army of Persia 120 years later. He dyed his soldiers' clothing with blood-like splotches and enticed the Persians into heedlessly attacking what they thought were a demoralized force of badly wounded men. In more recent times muddy dyes were an integral part of American revolutionary history, being the dye used in the British redcoats (Martin and Martin, 1964)

The compounds, which played vital role, in the development of coordination chemistry, later on may be described as hexamincobalt (III) ion (Tassaert, 1798), tetraamminecopper (II) ion (Libavious, 1710), prussian Blue, Gmalin Compounds (Gmelin, 1822), vaquelin's Salt and mangnus grin salt (Vaquelin, 1813).

Thomas Graham was the first to introduce the theory of metal amines, so-called ammonium theory (Kauffman, 1972), in which metal amines were considered as substance ammonium compounds. He attempted to explain the constitution of $Cu(NH_3)_2\ Cl_2$. He suggested that, one H atom from each ammonia molecule had been displaced by the Cu atom.

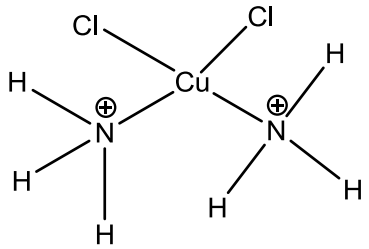

Fig 1: Coordinate complex

The theory, thus resembles to the modern Lewis acid base approach to the formation of coordinate covalent bonds. The theory was further modified by several other chemists such as Gerhardt. (Gerhardt 1850; Wartz, 1850; Von Hoffman, 1851 and Weltzein, 1856).

Some important theories put forward, and which played an important role in the domains of understanding the metal-ligand bond may be listed as conjugate theory,1814 (Reiset, 1855), Clauis ammonia theory, 1856 (Berzelius, 1841), The Biomsim Jorgenson Chain Theory,1889 (Claus, 1856), Werner's coordination's Theory,1896 (Werner, 1893), Effective Atomic Number, 1923 (Sidgwick, 1923), Atomic Orbital or Valence Bond, 1931 (Pauling, 1937), Principle of Electro neutrality of Atoms, 1947 (Pauling 1948), Molecular Theory, 1935 (Van vleck, 1935) and Crystal Field Theory,1929 (Bethe, 1929).

1.1.1 Coordination chemistry in biological system

The chemistry of metal atoms in biological systems is indeed the coordination chemistry of these metal atoms. Most of the essential metals (except Na, K, Ca) can not occur in the biological systems as free metal ions as under the prevailing pH conditions, these would be hydrolyzed and precipitated. These must therefore, be transported in the form of highly stable chelates. In body fluids, animals and plants, various simple chelating agents like, citrate, tartarate, malate, lactate, amino acids etc. are present to effectively complex the metal ions (Banerji, 1993).

The following are the few important metal complexes found in biological systems, which illustrates the significance of coordination in biochemistry, iron containing hemoglobin, ferritin, transferring and hemosiderin; Mg-containing chlorophyll; Co-containing vitamin B_{12} ; Cu containing ceruplasmin and plastocyanin; Mo containing xanthine oxidase and nitro-reductase.

Generally speaking, in biological systems coordination complexes may be said to play the following roles;

(I) Act as catalyst in many metabolic processes of the living bodies which involve; (a) Redox reactions with change in metal valency of the complex (b) Reaction of the acid-base type in which metal ion acts as a Lewis acid and combining with a substrates accelerate the reaction.

(II) Act as agents for the transmission of energy in plant metabolism.

1.1.2 Coordination chemistry in medicines

The important application of metal complexes is in the field of therapy. Many of the complexes are known to be used in drugs in certain type of diseases and also for metal detoxification in the case of metal poisoning. Ca-chelate, Na_2EDTA is used in Pb poisoning, Fe poisoning and also in the excretion of Zn and radioactive Sr, the chelating agent, 2,3 dimercaprol is used in the treatment of poisoning by Hg, As, Bi, Sb and penicillamin is used to mobilize and excrete copper in the treatment of Wilson disease. Disferrioxamine is used to accelerate the urinary excretion of Al and slow the progress of Alzheimer's disease (Nielends, 1966).

The organic mercurials $(R\text{-}Hg)^{+}$ are used in the medicine as diuretics. The organic arsenicals and antimonials are well known, antipyretic action of salicylates; aminopyrin etc. is associated with the chelated transport of Cu^{+2} ion, which is released from intracellular sites in pyrexia process. The use of metal complexes and ligands fighting against disease in general has been reviewed. The use of gold complexes in the treatment of tuberculosis and arthritis is known. After the discovery of antitumor activity of some Pt compounds by Rosenberg, there have been several reports on Pt complexes in cancer chemotherapy. $Pt(NH_3)_2Cl_2$ or cis-platin has been found most effective against cancer.

1.1.3 Coordination chemistry in medicines (antibiotics)

Metal ion also plays a key role in the action of antibiotic drugs. They are involved in specific interaction with antibiotic, proteins, membrane components, nucleic acid and other biomolecules (Ming, 2003). DNA can also bind many different biomolecules and synthetic compounds including proteins, antibiotics, polyamines, metal complexes and organometalic compounds. In such specific interactions, transcription is regulated to turn on and/or off a specific biological process. DNA is also a target for therapeutic treatment of various disorders and diseases such as cancers via direct ligand binding to it or binding to DNA regulating biomolecules. Several clinically used anti-cancer antibiotics such as bleomycin, streptomycin are DNA binding agents. Keflin interact with Co(II), Cu(I), Ni(I) and Zn(II) metal ion leading to complexes of the type $M(Keflin)_2Cl_2$ and $M(Keflin)Cl_2$ which have been characterized by physicochemical and spectroscopic methods (Tassaert, 1798).

Ciprofloxacin is a 4-quinolone derivative related to the cinoxacin (C_x), norfloxacin, nalidixic and oxilinic acid. These compounds are antibacterial agents employed as specific inhibitors of the bacterial DNA-gyrase and it has been suggested that their activity could be mediated by copper or iron ions. Structurally these compounds have a common moiety and their activity and mechanism of action should be related to this. Solid state IR studies of $M(NaI)_n$ complexes suggest that they are formed by interaction through the carboxylate group with no apparent interaction of keto group. The synthesis and crystal structure of the complex $[C_o(C_x)_3\ ]\ N_a6H_2O$ and chemical behavior of the cinoxacinate anion in complexes $[M(C_x)_2(DMSO)_2]4H_2O$ [(M= $N_i^{\ II}$,$Z_n^{\ II}$) & $Cd_2\ (C_x)_4\ (DMSO)_2\ ]\ 2H_2O$ reveals that in all the compounds the cinoxacinate ion act as bidentate ligands through one carboxylate oxygen atom and the exocyclic carbonyl oxygen atom. The metal is bonded to six oxygen atoms in slightly distorted octahedral environment.

Nitroimidazoles, which belong to the nitroheterocyclic drug family and consist of a common imidazole ring structure with a nitro group at position 5, have a unique position in heterocyclic chemistry was introduced in the late 1950. 5-nitroimidazoles are now widely used as trichomoniacidal, antibacterial and antiprotozoal agent (Ahmad *et al.,* 2009). The most common of these are dimetridazole [1–2– dimethyl–

5–nitroimidazole], metronidazole [1-(2-hydroxyethyl)–2-methyl–5- nitroimidazole] (Tiwari *et al.,* 2006), ornidazole [1-(3-Chloro-2-hydroxy-propyl)-2–methyl–5–nitroimidazole] and tinidazole, 1-(2–ethylsulphonylethyl)–2–methyl–5-nitroimidazole (Cosar *et al.,* 1966 and Howerd *et al.,*1969). These compounds have various substitutions , usually a methyl group, on the imidazole ring either on nitrogen at position 1 or on the carbon at position 2 and have been used as hypoxic cell markers in the body (Miller *et al.,* 1970).

1.2 Introduction to transition metal

1.2.1 History

Humans have been aware of the existence of some of the transition elements for thousands of years. Decorative beads made from iron meteorites date back 6000 years to 4000 BC and the use of copper almost certainly predates this. However, it is only in the 20^{th} century that the complete set of stable elements has been identified and samples of pure metal isolated from each. The isolation of technetium, for example, was not achieved until 1937, within living memory for some. Such work continues to this day in studies of the formation and atomic properties of the 6*d* transition elements. In broad terms, the discovery of the transition elements can be divided into four phases which reflect both the chemical nature of the elements and the development of human knowledge. The first metals to be discovered were those which can exist on Earth in native form that is as the elemental metal. The iron beads mentioned above are not a typical example, in that iron is normally found on Earth in combination with other elements, particularly oxygen or sulfur. However, iron-rich meteorites provide an extra terrestrial source of impure metallic iron which was discovered at an early stage. The transition metals more typically found in native form are copper, silver and gold. These so-called being lustrous and malleable would be conspicuous among other minerals to ancient peoples, gold in particular being prized for its luster and resistance to corrosion. The use of copper probably dates back to *ca.* 5000 BC and it is thought that the Egyptians were using a form of gold coinage as early as *ca.* 3400 BC.

The second phase of transition element discovery involved those which could readily be released from minerals through heating or reduction by hot charcoal. Again copper in the carbonate mineral malachite, silver in the sulfide mineral argentite and mercury as the sulfide in cinnabar might first have been obtained in metallic form from

minerals mixed with the glowing embers of a camp fire. The formation of metallic copper through charcoal reduction appears to have been known by 3500 BC. The copper tin alloy bronze is said to have been discovered before about 3000 BC, leading to the 'Bronze Age'. Brass, another copper alloy formed with zinc, appeared in Palestine around 1400 BC. Iron is superior to bronze or brass in that it is hard but can be worked when hot, and sharpened to a fine cutting edge which can be resharpened when necessary. The reduction of iron ores is more difficult than for copper, requiring higher temperatures than arise in a simple fire. However, by using bellows to increase the temperature of burning charcoal it was possible to obtain metallic iron from minerals. The smelting and use of metallic iron appears to have been developed in Asia Minor (modern Turkey) by *ca.*2000 BC. However, this technology did not become widespread until much later, so that the 'Iron Age' did not really begin until about 1200 BC. Since that time, a huge variety of alloys based on iron have been developed and countless common place modern items contain ferrous metal components.

The third major phase of discovery of the transition elements came about during the 18^{th} and 19^{th} centuries. This was stimulated by the increasing understanding of chemical transformations and the improved methods of separation developed by the alchemists. The appearance of Dalton's atomic theory in 1803, followed by the periodic table in 1868, gave further impetus to the search for new elements and many new transition elements were discovered during this period.

The fourth phase of discovery came with the more detailed knowledge of atomic and nuclear structure and the discovery of radioactivity, which arose at the end of the 19^{th} and beginning of the 20^{th} centuries. Although cerium had been isolated in 1839, the concept of an *f* series of elements did not exist at that time. Thus it was not until 1913 that the lanthanide elements were found to constitute a new series. Until then, the similarity in the properties of these elements had led to their mixtures being thought of as single elements. However, in 1918 it was recognized by Bohr that these elements actually constituted the series of 4*f* elements. Among the actinides, thorium was found in 1829 and uranium in 1789, although uranium metal was not isolated until 1841. The more radioactive 5*f* elements protactinium, neptunium, plutonium, americium and curium were only discovered in the 20^{th} century. The production of the

full series of 6*d*-block elements has only been achieved in the later part of the 20th century.

Initially, the transition metals presented a chemical puzzle because their halides could form compounds with molecular species such as ammonia, despite the fact that the valencies of all the elements in the metal halide and the ammonia molecule are already satisfied. The problem over the nature of these *'complex compounds'* or complexes of the transition metals led to much debate near the end of the 19th century.

The matter was finally resolved through the work of Alfred Werner who was awarded the 1913 Nobel Prize. Werner proposed the concept of a primary valence and a secondary valence for a metal ion. Werner also showed how the number of compounds formed by a transition metal which have the same formula but different properties, *i.e.* the number of isomers, can reveal structural information. The subsequent theoretical work of Bohr, Schrodinger, Heisenberg and others in the early part of the 20th century provided the basis for a more detailed understanding of the electronic structures of atoms. The directionality in the bonding between a d-block metal ion and attached groups such as ammonia or chloride can now be understood in terms of the directional quality of the d orbitals. In 1929, Bethe described the (CFT) model to account for the spectroscopic properties of transition metal ions in crystals. Later, in the 1950s, this theory formed the basis of a widely used bonding model for molecular transition metal compounds. The CFT ionic bonding model was since then superseded by (MO) theory, which make allowance for covalency in the bonding to the metal ion. However, CFT is still widely used as it provides a simple conceptual model which explains many of the properties of transition metal ions. The interactions between transition elements and organic molecules through metal carbon bonds to form compounds also became a topic of intense interest during the 1950s. In due course, as research in this area reached fruition, it resulted in the award of two Nobel prizes. The first went to K. Ziegler and G. Natta in 1963 for their work on the polymerization of alkenes using organometallic catalysts. The second was awarded in 1973 to G. Wilkinson and Fischer for their work on organometallic chemistry, in particular on 'sandwich compounds', or in which a transition metal forms the filling between two planar cyclic alkenes in a sandwich-like structure.

1.2.2 The *d*-block elements

The atomic radii of the first row *d*-block elements do not decrease smoothly across the row as might be expected. This is because the increase in electron–electron repulsions across the series counteracts the effect of the increase in *Z*eff. The first, second, and third ionization enthalpies increase across the first row *d*-block elements with increasing *Z*eff, though there are some anomalies. These are due to the greater electron–electron repulsions between paired electrons than between unpaired electrons, and also losses in exchange energy. In a particular triad, the atoms of the second and third row *d*-block elements are larger than the atoms of the first row element, though of similar size to each other. The similarity in sizes of the second and third row atoms is caused by the lanthanide contraction. Metals on the left hand side of the *d* block exist naturally as oxides and are obtained from the ores by reduction. Metals on the right hand side of the *d* block occur naturally as sulfides, and are obtained by conversion to the oxide followed by reduction.

1.2.3 Chemistry of the first row *d*-block elements

Although most *d*-block elements contain *s* electrons in addition to *d* electrons, in both ions and compounds the *s* orbital is of higher energy than the *d* orbitals. This means that the electronic configuration of a *d*-block element in a compound is *always dn* and *never dn*–2 s^2. With the exceptions of Groups 3 and 12, *d*-block elements have more than one possible oxidation state, and this is reflected by the different oxides and halides in the elements form. For the first row *d*-block elements the +3 oxidation state is more stable than the +2 oxidation state on the left-hand side, but the +2 oxidation state is more stable than the +3 oxidation state on the right-hand side. The availability of different oxidation states is a factor in the catalytic activity of many *d*-block compounds.

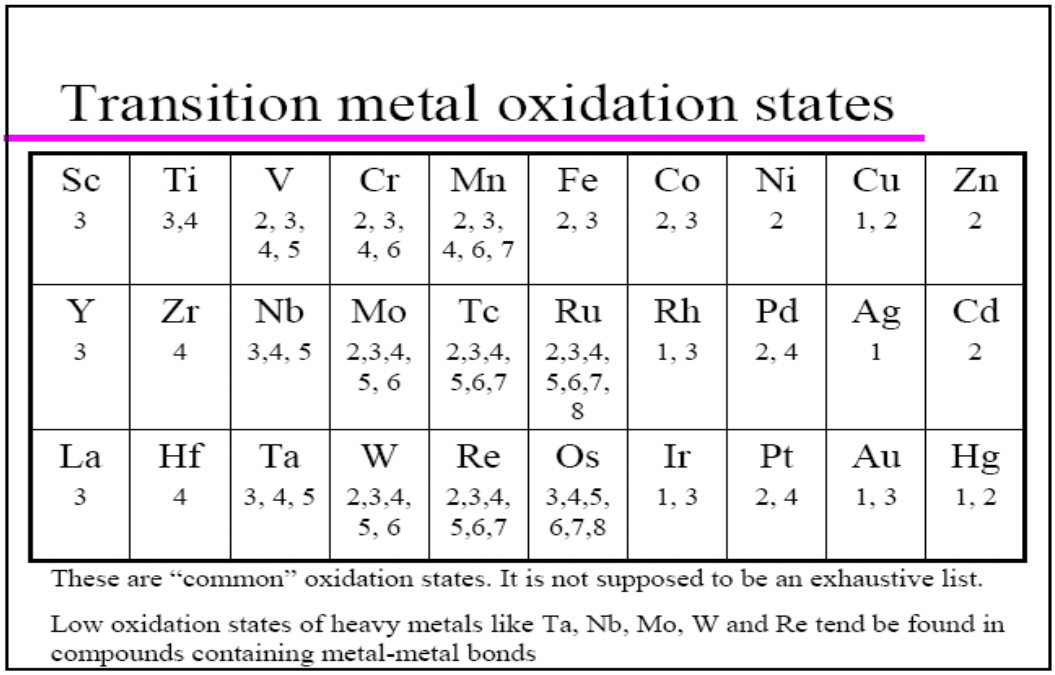

Transition metal oxidation states

Sc	Ti	V	Cr	Mn	Fe	Co	Ni	Cu	Zn
3	3,4	2, 3, 4, 5	2, 3, 4, 6	2, 3, 4, 6, 7	2, 3	2, 3	2	1, 2	2
Y	Zr	Nb	Mo	Tc	Ru	Rh	Pd	Ag	Cd
3	4	3,4, 5	2,3,4, 5, 6	2,3,4, 5,6,7	2,3,4, 5,6,7, 8	1, 3	2, 4	1	2
La	Hf	Ta	W	Re	Os	Ir	Pt	Au	Hg
3	4	3, 4, 5	2,3,4, 5, 6	2,3,4, 5,6,7	3,4,5, 6,7,8	1, 3	2, 4	1, 3	1, 2

These are "common" oxidation states. It is not supposed to be an exhaustive list.

Low oxidation states of heavy metals like Ta, Nb, Mo, W and Re tend be found in compounds containing metal-metal bonds

Fig 2: Transition metal oxidation states

1.2.4 Coordination chemistry

In a coordination complex, ligands are generally coordinated to a metal centre through electron pairs on their donor atoms. Monodentate ligands coordinate through one donor atom, whereas polydentate ligands coordinate through more than one donor atom, giving rise to chelate rings. The total number of donor atoms coordinated to a metal ion is known as the coordination number. For a first row *d*-block complex, this can vary from 2 to 8, but 4 and 6 are the most common. 4-coordinate complexes can be tetrahedral or square planar and 6-coordinate complexes are almost always octahedral. Structural isomers and stereoisomers are possible for coordination complexes. Ionization isomers hydrate isomers, coordination isomers, and linkage isomers are types of structural isomers. Geometric isomers and configurational isomers are both types of stereoisomers. Metal ions and ligands can be divided into hard and soft classes. Hard metals have high charges or high charge densities, whereas soft metals are larger, with lower charges, and more polarizable. Hard ligands have small electronegative donor atoms such as N, O, or F, whereas soft ligands have larger, more polarizable donor atoms. Hard metals form more stable complexes with hard ligands and soft metals form more stable complexes with soft ligands.

1.2.5 Crystal field theory

Crystal field theory is an electrostatic model of bonding in coordination complexes that considers the ligands as point charges. Electrostatic attraction between the metal ion and the point charges holds a complex together. Electrostatic repulsion between the ligands and the metal *d* orbitals causes the *d* orbitals to lose their degeneracy and split into sets of different energies. In an octahedral complex, the *d* orbitals are split into two sets, with three orbitals stabilized (the t^2g set) and two orbitals destabilized (the *eg* set). The crystal field splitting energy is the gap between these sets, and in an octahedral complex it is given the symbol Δo. In an tetrahedral complex, the *d* orbitals are split into two sets, with two orbitals stabilized (the *e* set) and three orbitals destabilized (the t^2 set). The crystal field splitting energy is Δt. The crystal field splitting energies Δo and Δt are related by the expression Δt = 4 9 Δo. The *d*-orbital splitting diagram for a square planar complex is obtained from that for an octahedral complex by stabilizing all of the orbitals with a *z*-component and destabilizing those without a *z*-component.

1.2.6 Filling the *d* orbitals

Uneven occupation of the *d* orbitals means that the electrons in a transition metal complex are generally at a lower energy than in the free ion in a spherical field. The difference is called the crystal field stabilization energy. Octahedral complexes with the electronic configurations *d*4–*d*7 have two possible arrangements, and the one that is adopted depends on the values of Δo and *P*, the pairing energy. If Δo > *P*, a high spin complex is formed and, if Δo < *P*, a low spin complex is formed. The ranking of ligands in order of decreasing Δ is called the spectrochemical series. Ligands with large values of Δ are called strong field ligands, and those with small values of Δ are called weak field ligands. Low spin complexes are favored by a high charge on the metal ion and the presence of strong field ligands. Low spin complexes are more prevalent for second and third row *d*-block metals. Jahn-Teller distortions occur when there is a degenerate ground state. This is particularly significant for octahedral complexes in which the *eg* orbitals are unevenly filled, which occurs in *d*4 and *d*9 configurations.

1.2.7 Color in coordination compounds

Many *d*-block complexes are colored because photons of visible light give rise to electronic transitions between the two sets of *d* orbitals. The color observed for a complex ion is complementary to the color of the light absorbed. The intensity of absorption is affected by three selection rules- the Laporte, parity, and spin selection rules. The more selection rules that are broken, the less intense the absorption. Charge-transfer absorptions do not involve *d–d* transitions, so they generally give rise to intense colors. As a result of the parity selection rule, tetrahedral complexes are generally more intensely colored than octahedral complexes.

1.2.8 Magnetic properties

The magnetic moment of a first row transition metal complex is related to the number of unpaired electrons through the spin-only formula. By comparing the measured magnetic moment with the value calculated using the spin-only formula it can determine whether an octahedral complex is high spin or low spin and whether a 4-coordinate complex is tetrahedral or square planar.

1.2.9 Aqueous chemistry of the first row *d*-block ions

Ligand substitution reactions occur when one ligand replaces another. This happens stepwise, and each ligand replacement reaction has an equilibrium constant known as stability constant. The values of stepwise equilibrium constants decrease with increasing substitution for statistical reasons. Equilibrium constants are always higher for complexes of polydentate ligands than those of monodentate ligands. This is called the chelate effect and it is caused by greater changes in entropy. Redox reactions are common in aqueous solution, and the nature of the ligands affects the value of the reduction potential. Ions with a charge of +3 or more undergo hydrolysis, giving acidic solutions.

1.3 Introduction to ligand

1.3.1 Schiff Bases and their metal complexes

Compounds containing an azomethine group (-CH=N-), known as Schiff bases are formed by the condensation of a primary amine with a carbonyl compound. Schiff bases of aliphatic aldehydes are relatively unstable and are readily polymerizable while those of aromatic aldehydes, having an effective conjugation system, are more stable. Schiff bases have number of applications viz., preparative use, identification, detection and determination of aldehydes or ketones, purification of carbonyl or amino compounds, or protection of these groups during complex or sensitive reactions. They also form basic units in certain dyes.

Schiff bases are generally bi-or tri- dentate ligands capable of forming very stable complexes with transition metals. Some are used as liquid crystals. In organic synthesis, Schiff base reactions are useful in making carbon-nitrogen bonds. Schiff bases appear to be an important intermediate in a number of enzymatic reactions involving interaction of an enzyme with an amino or a carbonyl group of the substrate One of the most important types of catalytic mechanism is the biochemical process which involves the condensation of a primary amine in an enzyme usually that of a lysine residue, with a carbonyl group of the substrate to form an amine, or Schiff base.

Stereochemical investigation carried out with the aid of molecular model showed that schiff base formed between methylglyoxal and the amino group of the lysine side chains of proteins can bend back in such a way towards the N atom of peptide groups that a charge transfer can occur between these groups and oxygen atoms of the schiff bases. In this respect pyridoxal schiff bases derived from pyridoxal and amino acids have been prepared and studied from the biological point of view. Transition metal complexes of such ligands are important enzyme models. The rapid development of these ligands resulted in an enhance research activity in the field of coordination chemistry leading to very interesting conclusions.

1.3.2 Synthesis of schiff bases

It have reported the synthesis, complexation, antifungal and antibacterial activity studies of a new macro cyclic Schiff base (Ugras *et al.*,) as shown in Fig 3.

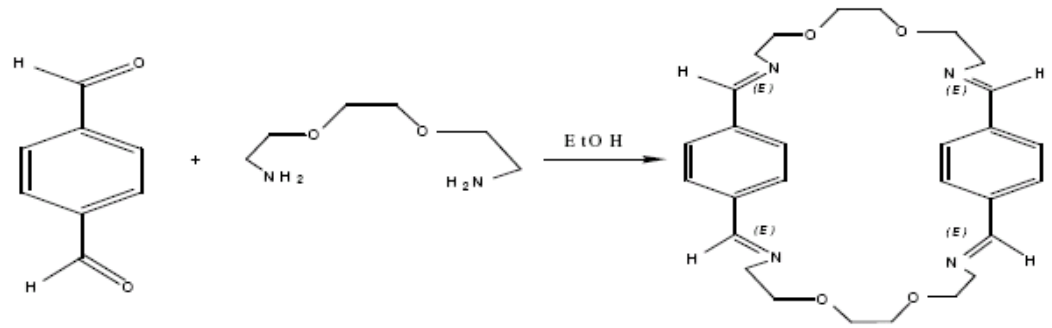

Fig 3: synthesis of schiff bases

Preparation, physical characterization and antibacterial activity of Ni (II) Schiff base complex was reported. (Morad *et. al.*,) (Fig 3 a).

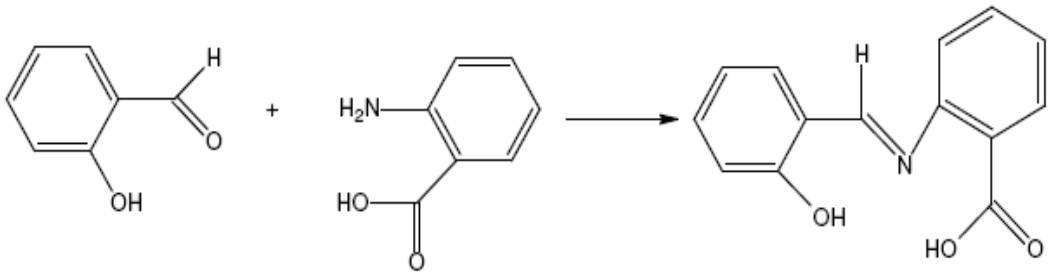

Figure 3a: Synthesis of schiff bases

Elzahany have synthesized some transition metal complexes with Schiff bases derived from 2- formylindole, salicylaldehyde and *N*-aminorhodanine as shown in Fig 3b.

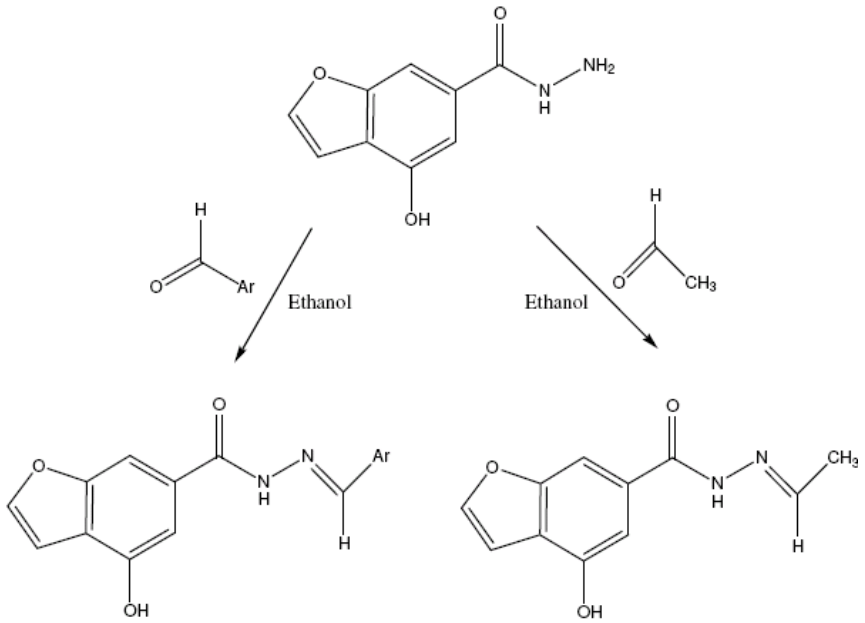

Fig 3 b: Synthesis of Schiff bases

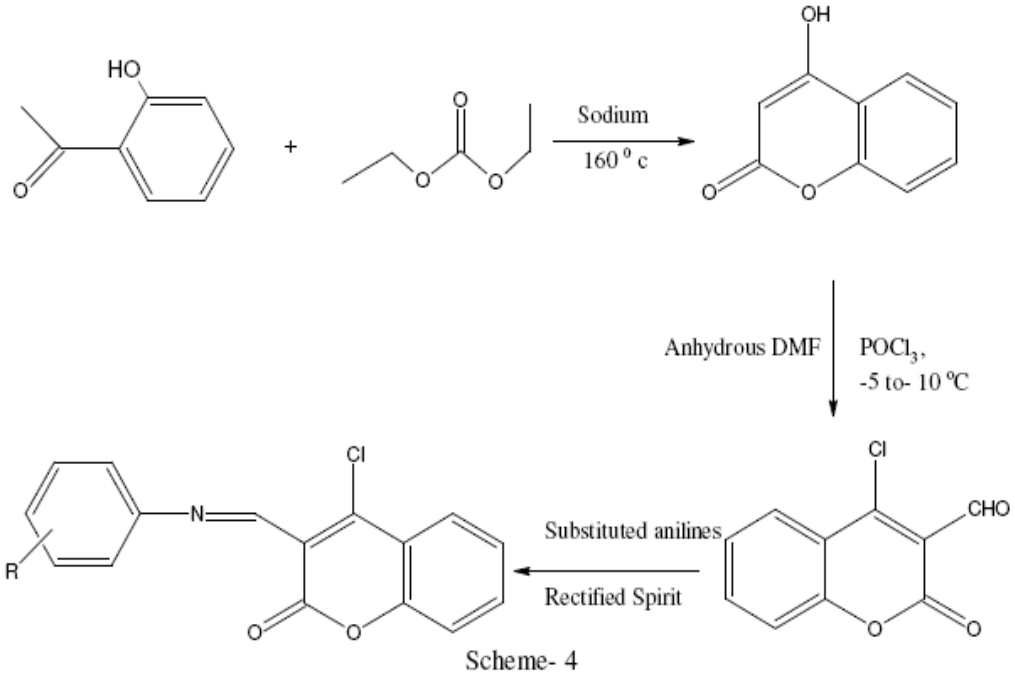

Figure 3 c: Synthesis of Schiff bases

1.3.3 Pyrazolines and their metal complexes

Pyrazoles and their reduced form pyrazolines are well known nitrogen containing heterocyclic compounds (Katritzky *et al.*, 1996 and 1984). They display a broad spectrum of biological activities (Elguero *et al.*, 2002; Gokhan *et al.*, 2003; Holla *et al.*, 2000; Plaska *et al.*, 2001 and Turan *et al.*, 2000). Pyrazolines and quinoxalines

have been developed as nonsteroidal anti-inflammatory drugs and block the formation of prostaglandins (Lombardino, 1985 and Faigon, 1994). Pyrazole metal complexes show extensive coordination chemistry as well as catalytic and biological properties (Monica, 1997 and Onoa *et al.*, 1999).

A set of 1-*N*-substituted pyrazoline analogues was synthesized by the cyclization of Mannich bases with substituted thiosemicarbazides in 9-28% yield (Abid and Azam, 2005). The Mannich bases were generated by the reaction of various ketones with formaldehyde and dimethylamine hydrochloride in 42-87% yield.

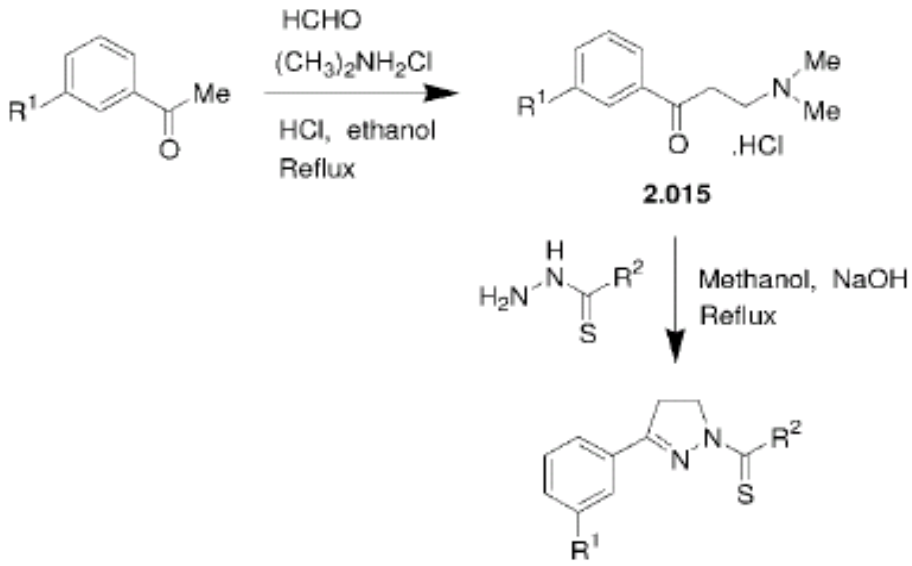

Figure 4: Synthesis of pyrazoline

Abid and co-workers synthesized a series of 1-*N*-thiocarboxamide- 3-phenyl-2-pyrazolines by cyclization of Mannich bases with unsubstituted thiosemicarbazides in 35-51% yield (Abid and Azam 2006).

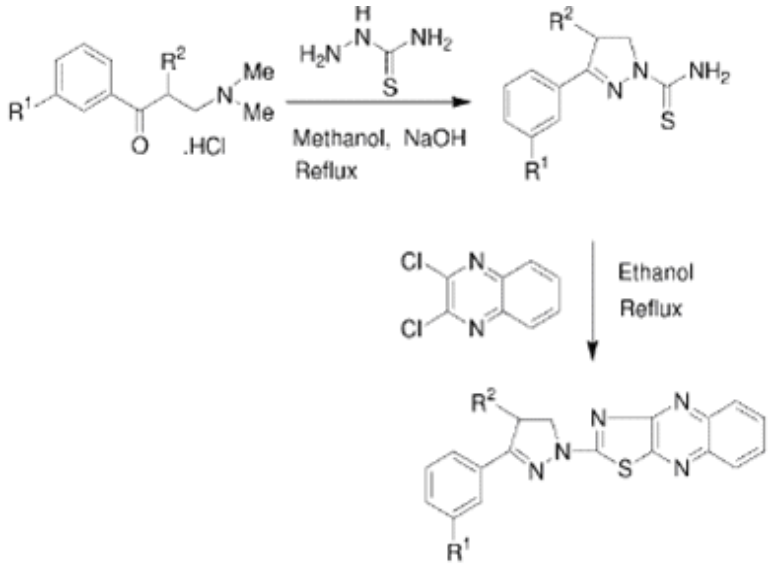

Figure 4 a : Synthesis of pyrazoline

It was concluded once again that the presence of a halogen substitutent on the phenyl ring and a 4-methyl group on the pyrazoline ring greatly affects the in vitro antiamoebic activity.

Recently, a series of 1-*N*-substituted thiocarbamoyl-3, 5-diphenyl-2-pyrazoline derivatives were reported (Budakoti *et al.,* 2007). First, a base-catalyzed Claisen-Schmidt condensation of benzaldehyde with acetophenone produced the chalcone (93% yields). Cyclization with various N-4 substituted thiosemi-carbazides gave the desired pyrazoline derivatives in 8-24% yield with a wide variety of aliphatic and aromatic amines. The palladium (II) complexes were also prepared by mixing an equimolar ratio of pyrazoline with $[Pd(DMSO)_2Cl_2]$ in 76-92% yield.

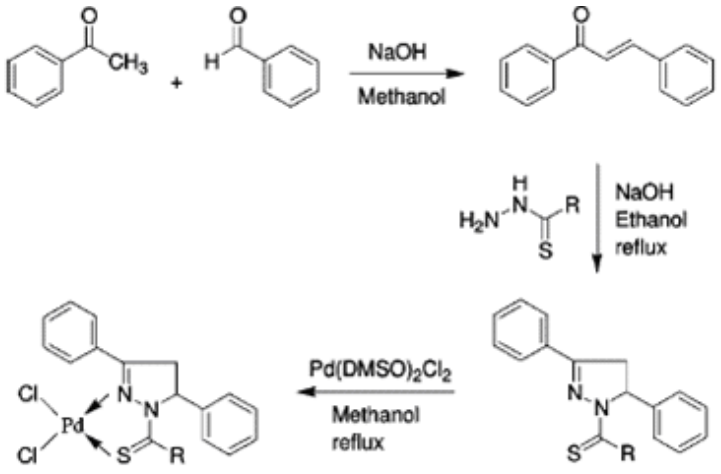

Figure 4 b: Synthesis of pyrazoline

1.3.4 Benzimidazoles and their metal complexes

Discovery of 5,6-dimethyl-1-(R-D-ribofuranosyl)benzimidazole, an integral part of the chemical structure of vitamin B_{12}, has generated considerable interest in the area of benzimidazole nucleosides and nucleotides (Bonnett, 1963 and Hill *et al.*,1969). Benzimidazole and its derivatives are widely used in searches for new drugs (Craigo *et al.*,1999; Gudmundsson *et al.*, 2000; Trivedi *et al.*, 2006; Townsend and Revankav, 1970; Kim *et al.*,1996 and Khalafi *et al.*, 2005). Recently, interest in the synthesis and characterization of transition metal complexes of the benzimidazole ligands has been stimulated as a result of their biological and pharmacological activity (Rajan *et al.*, 1996; Garcia, 1996, Cardwell *et al.*, 1997; Gable *et al.*, 1996; Piguet *et al.*,1989 and Aminabhavi *et al.*,1986). Benzimidazoles are commonly synthesized by coupling *o*-phenylenediamine with carboxylic acids (Sluka *et al.*, 1981). Alternatively *o*-phenylenediamine can be treated with benzaldehydes, followed by cyclization of the intermediate Schiff base in the presence of various oxidants such as nitrobenzene (Sluka *et al.*, 1981, Khairy and Hammad, 1978), 2,3-dichloro-5,6-dicyano-1,4-benzoquinone (Eynde *et al.*,1995), benzofuroxan (Patzold *et al.*,1992) and MnO_2(Khairy and Hammad 1978). Sondhi et al. described one-step synthesis of pyrimidobenzimidazoles in which isothiocyanatobutanal was condensed with *o*-phenylenediamine in refluxing methanol at pH ≈ 5 to give pyrimidobenzimidazole derivatives in 18-46% yield (Sondhi *et al.*, 2002).

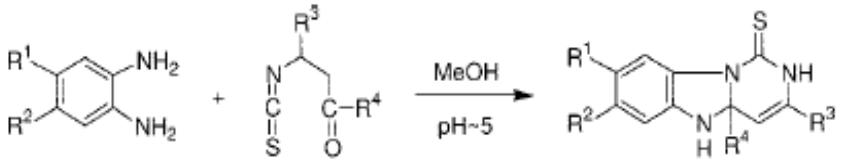

Figure 5: Synthesis of Benzimidazole

Another series of benzimidazoles was reported, as shown in Fig 6 along with their vanadium, molybdenum, and tungsten metal complexes (Bharti *et al.*, 2002; Maurya and Bharti,1999) 2-(Salicylideneimine)benzimidazole was synthesized by mixing equimolar amounts of salicylaldehyde and 2-aminobenzimidazole in refluxing methanol, whereas 2-(R-hydroxyalkyl/aryl)benzimidazoles were prepared by refluxing *o*phenylenediamine and substituted carboxylic acids in 4N HCl followed by neutralization with ammonium hydroxide. Dioxovanadium and dioxomolybdenum complexes were prepared by the reaction of aqueous KVO_3/MoO_3 solution with the

potassium salt of 2-(salicylideneimine)benzimidazole in refluxing methanol, respectively. Reaction of 2-(R-hydroxyalkyl/aryl)benzimidazole with peroxovanadium(V) generated peroxovanadium complexes, whereas similar peroxo complexes of molybdenum and tungsten were prepared by stirring MoO_3 or $WO_3 \cdot H_2O$ in aqueous 30% H_2O_2 solution with 2-(R-hydroxyalkyl/aryl)benzimidazole in aqueous ethanol. The dioxomolybdenum and dioxotungsten complexes were also isolated by the reaction of $[MoO_2(acac)_2]$ or $[WO_2(acac)_2]$(acacH)acetylacetone)] with 2-(R-hydroxyalkyl/aryl)benzimidazole.

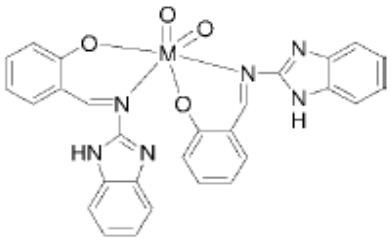

Figure 5a: Synthesis of benzimidazole

1.4 Nitroimidazole complexes

1.4.1 Nitroimidazole complexes as radiosensitizers

Nitroimidazoles (Segalas and Beauchem, 1992 and Chan *et al.,* 1989) and their complexes with metals like Pt, Ru and Rh are known to be effective radiosensitizers and chemotherapeutic agents. Ruthenium(II) compounds showing a promising potential as radiosensitizers have been prepared by James and coworkers (Keppler *et al.,*1987) with several 4-nitroimidazole derivatives. Among these compounds, the cis-$RuCl_4$,(DMSO), $(4(5)\text{-}NO_2Im)_2$ complex was identified as the best candidate. Several factors were proposed to explain its superior properties: greater reduction potential of the ligand, possible hydrolysis to a species capable of binding to DNA, presence of a pyrrolic proton to form hydrogen bonds that could stabilize the DNA-ruthenium interaction.

1.4.2 Nitroimidazole complexes as trypanocidal

In the search of new therapeutic tools for the treatment of American Trypanosomiasis, the largest parasitic disease burden in the American continent, three series of novel ruthenium complexes of the formula $[RuCl_2(HL)_2]$, $[RuCl_3(dmso)(HL)]$ and $[RuCl(PPh_3)(L)_2]$ with bioactive 5-nitrofuryl containing thiosemicarbazones as ligands (HL neutral, L monoanionic) were prepared. Their *in vitro* growth inhibition activity against *Trypanosoma cruzi* and the effect of co-ligands in related physicochemical properties i.e. nitro moiety redox potential, lipophilicity and free radical scavenger capacity show that although a loss of activity was observed as a consequence of ruthenium complexation, lipophilicity and free radical scavenger capacity of the obtained complexes could be correlated to their trypanocidal effect.

1.4.3 Nitroimidazole complexes as Anticancer

Nitroimidazoles are radiosensitizers and hypoxia detecting chemosensitizers. Intially nitroimidazoles were single dose antibiotic drugs. Recently nitroimidazole derivatives have emerged as multifunctional "drug-biomarker monitors" chemical compounds with importance in treatment of tumors, monitoring hypoxia and safer imaging contrast agents to monitor the therapeutic progress. Additionally, the number of nitroimidazole derivatives is growing and identified their importance as multifunctional nanoparticles. The nanoparticles synthesis scheme of nitroimidazole was proposed as nitroimidazole caged with metal oxide inside polymer coating and labeled with marker biomolecules. The multifunctional nitroimidazole nanoparticles were useful in detection and monitoring of hypoxia, cancer chemotherapy and soft tissue infections. In conclusion, nitroimidazoles are potential multifunctional molecules useful in chemotherapy, antiparasitic and monitoring hypoxia with greater possibility of simultaneous use of radiolabeled 2'nitroimidazoles as radiosensitizers, MRI-PET-US contrast imaging agents. 2'nitroimidazole compounds and analogs are becoming state of art radiosensitizers and chemosensitizers in cancer prevention and management. Apart from their newly discovered antitumor properties 2' nitroimidazoles had been proven antiparasitic drugs. However, their toxicity was remained a major issue as they showed strong DNA breaking properties by direct DNA binding and coupling with DNA strands and it caused skepticism of nitroimidazole acceptability as safe choice of non cancer therapeutic value. The binding of nitroimidazole with polymer depends on its hydrophilic bonds over its

molecules. The synthesis and properties of some nitroimidazole complexes of platinum and palladium starting from the MCl_4^{2-} salts are described metal complexes are now firmly established as clinically useful antitumour agents (Yang *et al.*, 1999).

A further relatively recent advance in this area is the demonstration that the original complex of this family cis$[PtCl_3(NH_3)_2]$ act as radiosensitizers in both bacterial and mammalian cells (Das *et al.,* 2003). Radiosensitization refers to the enhancement of radiation-induced damage by certain drugs, especially in hypoxic (oxygen-deficient) cells. This is critical because there are cases where tumour cure by radiotherapy is limited by the greater resistance of hypoxic cells, in comparison to normally oxygenated cells (Mallia *et al.,* 2005). The classic radiosensitizers are the nitroheterocycles as exemplified by nitrofurans (Li *et al.,*2005) and nitroimidazoles (Chu *et al.,* 2004); a general (but simplified) rationale being that the 'electron-affinic' nitro groups may interact with damage on DNA induced by radiation in a manner analogous to oxygen producing subsequently lethal hits (Jurrison and Lydon, 1999). The identification of DNA as the ultimate target of radiation damage naturally prompts the question as to how new species may be designed with potential radiosensitizing and DNA binding properties. In this respect, the strong binding of platinum, in its complexes, to purine and pyrimidine bases suggested that platinum complexes of known radiosensitizers could have interesting biological properties.

1.4.4 Nitroimidazole complex as diagnostic agents

Delineation of viable ischemic myocardium is an important problem in nuclear cardiology. To determine the feasibility of using a technetium-labeled nitroimidazole as an indicator of ischemic myocardium at risk of infarction, The distribution of a 2-nitroimidazole-derivatized PnAO ligand and its ^{99m}Tc complex, ^{99m}TcO(PnAO)-1-CH,-(2NI)(BMS-181321) was characterized in the ischemic territory of the left anterior descending (LAD) coronary artery of the rabbit. In preliminary experiments, the performance of ^{14}Cdeoxyglucose (^{14}C-2DG) and ^{14}C-misonidazole was assessed relative to apparent regional relative myocardial blood flow (rMBF) indicated by ^{99m}Tc-teboroxime using double-label autoradiography in the rabbit LAD occlusion model. After demonstrating that ^{14}C-2DG and ^{14}Cmisonidazole are selectively retained in the lateral border of the ischemic territory, BMS-181321 was co-injected intravenously, with either ^{14}C-2DG or ^{14}C-misonidazole, 20 min after LAD occlusion.

In a separate experiment, ^{99m}TcO(PnAO)-6-CH_3, a complex with the same lipophilicity (log k' 0.26 vs. 0.31) as BMS-181321 but which lacks the 2NI moiety, was co-injected with ^{14}C-2DG. After 30 min, the rabbits were sacrificed and ^{14}C ^{99m}Tc autoradiograms were obtained from the same tissue sections. The autoradiograms revealed that BMS-181321 was retained with the same microregional distribution as both ^{14}C-2DG and ^{14}C-misonidazole in the border zone of the ischemic LAD territory. The selective retention of BMS-181321 depends on the presence of the nitroimidazole group, since ^{99m}TcO(PnAO)-6-CH_3 has a uniformly low myocardial distribution in contrast to the enhanced uptake of co injected ^{14}C-2DG. These data demonstrate that BMS-181321 is selectively retained in hypoxic myocardium and demarcates the ischemic border zone in a manner similar to ^{14}C-2DG and ^{14}C -misonidazole.

Differentiation of viable ischemic myocardium from ischemic infarct is a major goal of nuclear cardiology. While many agents are available for imaging regional myocardial blood flow (rMBF) (Dearling *et al.,* 2002; Maurer *et al.*,2002; Goldstein et al.1986; Roizen-Towle et.al.,1986; Seldin *et al.,* 1989 and Shelton *et al.*,1990) fewer methods exist for detecting viable ischemic myocardium by external imaging. "F-2-fluoro-deoxy-Dglucose positron emission tomography (^{18}FDG PET) reveals that viable ischemic myocardium, in which some residual flow is retained, has an accelerated regional myocardial metabolic rate of glucose (rMMR) (Neely et al.1975), particularly under fasting conditions (Gould et al.,1991). The increase in rMMR,, can be attributed to the acceleration of glycolysis in ischemic hypoxic myocardium, which leads to increased lactate production and substrate level phosphorylation of adenosine 5'-diphosphate (ADP) (Rumsey et al.1993). The enhanced generation of adenosine 5'-triphosphate (ATP), as a product of anaerobic glycolysis during ischemia, at least partially compensates for a decline in mitochondrial oxidative phosphorylation. ^{18}FDG PET alone does not distinguish between nonischemic and necrotic myocardium, however, since nonischemic myocardium preferentially oxidizes fatty acids to provide respiratory substrate (Schelbert *et al*., 1982) and has a low rMMR that can approximate the rMMR, of necrotic tissue (Neely et al.,1975). On the other hand, sequential ^{13}N-ammonia and ^{18}FDG PET studies show that regions of ischemic myocardium that have low rMMR,, represent nonviable or infarcted myocardium (Neely *et al*.,1975). As pointed out previously (Janse et al., 1979), for patients with stable coronary artery disease, improvement in function was observed for 75-85% of

dysfunctional segments designated as "viable" by ^{18}FDG PET, whereas 78-95% of "nonviable" segments showed no improvement after revascularization (Bergmann et al.1984, Shelton et al.1990). On the other hand, problems with the interpretation of increased ^{18}FDG uptake have been described (Janse *et al*., 1979). Foremost among these is the inability of ^{18}FDG PET to indicate whether glucose metabolism is anaerobic or oxidative. This is an important point in light of studies that show that glucose metabolism and oxygen consumption, as well as mechanical work, increase in non ischemic myocardium proximal to the edge of the ischemic territory (Nunn *et al*., 1995). Thus, the suggestion has been made that indicators more directly associated with tissue hypoxia, such as ^{18}F-fluoromisonidazole, may detect viable ischemic myocardium with greater accuracy than ^{18}FDG (Janse *et al*., 1979). It is believed that intracellular misonidazole trapping is enhanced in hypoxic tissue due to diminished reoxidation of the reduced species by oxygen (Moulder and Rockwell, 1987). Studies of ^{14}C-misonidazole binding to V79 hamster cells show that increased binding occurs below oxygen concentrations of 2 mM or 1.4 mm Hg (Brown *et al*., 1984).

1.5 References

Abid M, Azam A. Synthesis and antiamoebic activities of 1-*N*-substituted cyclized pyrazoline analogues of thiosemicarbazones. Bioorg Med Chem 2005;13:2213-2215.

Abid M, Azam A. Synthesis and antiamoebic activity of new 1-*N*-substituted thiocarbamoyl-3,5-diphenyl-2-pyrazoline derivatives and their Pd(II) complexes. Eur J Med Chem 2005;40:935-938.

Abid M, Azam A. Synthesis, characterization and antiamoebic activity of 1-(thiazolo[4,5-b]quinoxaline-2-yl)-3-phenyl-2-pyrazoline derivatives. Bioorg Med Chem Lett 2006;16:2812-2814.

Ahmad G, Mishra PK, Gupta P, Yadav PP. Stereoselective synthesis and antimicrobial activity of benzofuran-based (1*E*)-1-(piperidin-1-yl)-N^2arylamidrazones. Eur J of Med Chem 2009;44:4985-4997.

Aminabhavi TM, Biradar NS, Patil SB, Hoffman DE. Structural and biological studies on benzimidazolyl amino acid complexes of dimethyldichlorosilane. Inorg Chim Acta 1986;125:125-128.

Banerji D, "Coordination Chemistry", Tata Mc-Graw Hill Publishing CO. Ltd. 1993.

Bergmann SR, Fox KAA, Rand AL, McElvany KD, Welch MJ, Markham J, Sobel BE. Quantification of regional myocardial blood flow in vivo with Hi50. Circulation 1984;70:724-733.

Berzelius JJ. Johreshbericht 1841;21:108-110.

Bethe H, Theoretical Investigation of the Electronic Energy Band Structure of SolidsAnn. Physik 1929;3:133-139.

Bharti N, Shailendra, Gonzalez Garza MT, Cruz-Vega DE, Castro-Garza J, Saleem K, Naqvi F, Maurya MR, Azam A. Synthesis, characterization and antiamoebic activity of benzimidazole derivatives and their vanadium and molybdenum complexes. Bioorg Med Chem Lett 2002;12:869-870.

Bonnett R. Chem Rev 1963;63:573-574.

Brown M, Yu NY, Brown DM, Lee WW. a 2-nitroimidazole amide which should be superior to misonidazole as a radiosensitizer for clinical use. Rad Oncol Biol Phys 1984;7:695-696.

Budakoti A, Abid M, Azam A. Syntheses, characterization and in vitro antiamoebic activity of new Pd(II) complexes with 1-*N*-substituted thiocarbamoyl-3,5-diphenyl-2-pyrazoline derivatives. Eur J Med Chem 2007;42:544-546.

Budakoti A, Abid M, Azam A. Synthesis and Characterization of a Novel 2-Pyrazoline. Eur J Med Chem. 2006;41:63-65.

Cardwell TJ, Edwards AJ, Hartshorn RM, Holmes RJ,McFadyan WD. Synthesis, crystal structures and properties of two copper(II) 2-aminomethylbenzimidazole complexes. Aust J Chem 1997;50:1009-1011.

Chan PKL, Chan PKH, Frost DC, James BR Skov KA. Can J Chem 1988;66:177-179.

Chan PKL, James BR, Frost DC, Chan PKH, Hu HL and Skov KA. Can J Chem 1989;67:508-510.

Chu T, Hu S, Wei B, Wang Yi, Liu X, Wang X. Synthesis and biological results of the technetium-99m-labeled 4-nitroimidazole for imaging tumor hypoxia. Bioorg Med Chem Lett 2004;14:747-749.

Claus C. Ann Chem 1856;98:317.

Cosar C, Criman R, Horclois RM, Jacob J, Robert S, Tehelitcheff R, Vaupre Nitroimidazoles-preparation et activity chimiotherapeutique. Arzneim Forsch 1966;16:23-29.

Craigo WA, LeSueur BW,Skibo EB. J Med Chem 1999;42:3324-3326.

Das T, Banerjee S, Samuel G, Sarma HD, Korde A, Venkatesh M, Pillai MRA. Nucl Med Biol 2003;30:127.

Dearling JLJ, Lewis JS, Mullen GED, Welch MJ, Blower PJ. Copper bis(thiosemicarbazone) complexes as hypoxia imaging agents: structure-activity relationships. J Biol Inorg Chem 2002;7:249-259.

Elguero J,Goya P, Jagerovic N,Silva AM. S. Pyrazoles as Drugs, Facts and Fantasies, Targets in Heterocyclic Systems. Italian Society of Chemistry. Rome, Italy. 2002; Vol.6:p 52.

Eynde JJV, Delfosse F, Lor P, Haverbeke YV. $H_2O_2/Fe(NO_3)_3$-Promoted Synthesis of 2-Arylbenzimidazoles and 2-Arylbenzothiazoles. Tetrahedron 1995;51:5813-5816.

Gable RW, Hartshorn RM, McFadyen WD, Nunno L. Synthesis, X-ray and NMR characterisation of cobalt(III) coordination compounds with 2-guanidinobenzimidazole. Aust J Chem 1996;49:625-630.

Garcia-Lozano J, Server-Carrio J, Coret E, Folgado JV, Escriva E, Ballesteros R. Synthesis and magnetic properties of the copper (II) complex derived from dimethyl aminomethylphosphine oxide ligand. X-ray crystal structure of DMAO and $[Cu(NO_3)_2(POC_3H_{10}N)_2]$. Inorg Chim Acta 1996;245:75-79.

Gerhardt G. Johreshbericht.1850;3:335.

Gmelin L. Handbounch der therorelischen chemie. J Cjem Phys1822;36:230-235.

Gokhan N, Yesilada A, Ucar G, Erol K Bilgin. 1-*N*-substituted thiocarbamoyl-3-phenyl-5-thienyl-2-pyrazolines: synthesis and evaluation as MAO inhibitors. Arch Pharm Med Chem 2003;336:362-370.

Goldstein RA, Mullani NA, Wong WH, Hartz RK, Hicks CH, Fuentes F, Smalling RW, Gould KL. Positron imaging of myocardial infarction with Rubidium-82. J Nucl Med 1986;27:1824-1829.

Gudmundsson KS, Tidwell J, Lippa N, Koszalka GW, van Draanen N, Ptak RG,Drach JC, Townsend LB. Synthesis of Fluorosugar Analogues of 2,5,6-Trichloro-1-(β-D-ribofuranosyl)benzimidazole as Antivirals with Potentially Increased Glycosidic Bond Stability. J Med Chem 2000;43:2464-2468.

Hill HA, Pratt JM,Williams RJ P, Hill HA,Pratt JM, Williams RJP. Chem Br 1969;5:156-158.

Holla BS, Akbarali PM, Shivanada, MK. IL Farmaco 2000;55:256-259.

Howerd HL, lynch JE, Kirlin JL. Antimicrob Agent chemeother 1969; 261-266.

Janse MJ, Cinca J, Morena H, Fiolet JWT, Kleber AG, De Vries GP, Becker AE, Durrer D. The "border zone" in myocardial ischemia. An electrophysiological, metabolic, and histochemical correlation in the pig heart. Circ Res 1979; 44:576-588.

Jurrison S, Lydon JD. Potential Technetium Small Molecule Radiopharmaceuticals.Chem Rev 1999;2205-2209.

Katritzky AR, Rees CW, Elguero. The structure of N-aminopyrazole in the solid state and in solution: an experimental and computational study. J Comprehensive Heterocyclic Chemistry II. Volume 5; Pergamon Press: Oxford, U.K. 1984; p 167.

Katritzky AR,Rees CW,Scriven EF, Elguero. Synthesis of chlorinated 3,5-diaryl-2-pyrazolines by the reaction of chlorochalcones with hydrazines. J. Comprehensive Heterocyclic Chemistry II. Volume 3; Pergamon Press:Oxford, U.K., 1984; p 1.

Kauffman GB. Dictionary of Scientific Biography.1972;4:92-95.

Keppler BK, Wehe D, Endres H and Rupp W. Synthesis and properties of molybdenum(VI)peroxo compounds with imidazole and the X-ray structure of $(C_3H_5N_2)_2[O\{MoO(O_2)_2H_2O\}_2]$, a novel imidazolium peroxo complex containing a μ-oxo bridged dimer. Inorg Chem 1987:26:844-849.

Khairy El-B,Hammad M. Egypt J Chem 1978;21:171-175.

Khalafi-Nezhad A,Rad MNS, Mohabatkar H, Asrari Z,Hemmateenejad B. Design, synthesis, antibacterial and QSAR studies of benzimidazole and imidazole chloroaryloxyalkyl derivatives. Bioorg Med Chem 2005;13:1931-1935.

Kim JS, Gatto B,Yu C, Liu A, Liu LF, LaVoie EJ. Substituted 2,5'-Bi-1H-benzimidazoles: topoisomerase I inhibition and cytotoxicity. J Med Chem 1996;39:992-994.

La Monica G, Ardizzoia GA. Synthesis, Structural Characterization and Spectroscopic Properties of 1,2-bis[4-(3,5-dimethyl-1H-pyrazol-1-yl)-2-oxobutyl]benzene. Prog Inorg Chem 1997;46:151-154.

Li T, Chu T, Liu X, Wang X. Preparation and biodistribution of technetium-99m-labeled 1-(2-nitroimidazole-1-yl)-propanhydroxyiminoamide (N2IPA) as a tumor hypoxia marker. Nucl Med Biol 2005;32:225-227.

Libavious. Commentationum Matlalicarum libri quotour de Nature Metallorum Frank furt, vi p II C9. Annonymous, Miscellaneous Berolinensia, 1710;1:377-379.

Lombardino G. Nonsteroidal Anti-inflammatory Drugs.John Wiley & Sons: New York. 1985.

Mallia MB, Mathur A, Subramanian S, Banerjee S, Sarma HD, Venkatesh M. Synthesis and evaluation of 2-, 4-, 5-substituted nitroimidazole-iminodiacetic acid-$^{99m}Tc(CO)_3$ complexes to target hypoxic tumors. Bioorg Med Chem Lett 2005;15:3398-3403.

Martin D.F. and Martin B.B., Coordination Compounds Mc Graw Hill New York 1964, 25-26.

Maurer RI, Blower PJ, Dilworth JR, Reynolds CA, Zheng Y, Mullen GED. Hypoxia-Targeting Copper Bis(selenosemicarbazone) Complexes: Comparison with Their Sulfur Analogues. J Med Chem 2002;45:1420-1431.

Maurya MR, Bharti N. Synthesis, Characterization and Antiamoebic Activity of Benzimidazole Derivatives and Their Vanadium and Molybdenum Complexes. Transition Met Chem 1999;24:389-392.

Miller MW, Jr. Howerd HL, English AR, Organophosphorus drugs (Review). Antimicrob Agent chemeother 1970;256-260.

Ming J. structure and functions of metalloantibiotic. Med Res Rev 2003;23:697-699.

Moulder JE, Rockwell S. Tumor hypoxia: its impact on cancer therapy. Cancer Metastasis Rev 1987;5:313-321.

Neely JR, Whitmer JT, Rovetto M J. Effect of coronary blood flow on glycolytic flux and intracellular pH in isolated rat hearts. Circ Res 1975;37:733-741.

Nielends JB. Struct Bonding. Berlin 1966;1:59-60.

Nunn A, Linder K, Strauss H W. Nitroimidazoles and imaging hypoxia. Eur J Nucl Med 1995;22:265-267.

Onoa GB, Moreno V, Font-Bardia M, Solans X, Pe'rez JM, Alonso C. New complexes with pyrazole-containing ligands and different metallic centres. Comparative study of their fluxional behaviour involving M–N bond rupture. J Inorg Chem 1999;75: 205-209.

Patzold F, Zeuner F, Heyen T, Niclas H. Synthesis of Fused Imidazoles and Benzothiazoles from (Hetero)Aromatic *ortho*-Diamines or *ortho*-Aminothiophenol and Aldehydes Promoted by Chlorotrimethylsilane. J Synth Commun1992;22:281-284.

Pauling LJ. J Am Chem Soc.1937;53:1376-1379.

Pauling LJ. Contribution to the study of molecular structure J Chem Soc (London) 1948;1461-1466.

Piguet C, Bocquet B,Mueller E, Williams AF. Structure of [2,6-bis(2-benzimidazolyl)pyridine]dichlorocopper(II) dimethylformamide. Helv Chim Acta .1989;72:323-325.

Plaska E, Aytemir M, Uzbay T, Erol D. Synthesis, Structure, Protolytic Properties, Alkylating and Cytotoxic Activity of Novel Platinum(II) and Palladium(II) Complexes with Pyrazole-Derived Ligands. Eur J Med Chem 2001;36:539-370.

Rajan R, Rajaram R, Nair BU, Ramasami T, Mandal SK. Chromium(III), manganese(II), cobalt(II), nickel(II), copper(II) and palladium(II) complexes of a 12-membered tetraaza [N_4] macrocyclic ligand. J Chem Soc. Dalton Trans. 1996;9:2019-2025.

Reiset J, Conpt Rend. 1855;9:219.

Roizen-Towle L, Hall EJ, Pirro JP. Oxygen dependence for chemosensitization by misonidazole. Br J Cancer1986;54:919-924.

Rumsey WL, Cyr JE, Raju N, Nana RK. A novel[99m]cechnetium-labeled nitroheterocycle capable of identification of hypoxia in the heart. Biochm Biophys Res Comm.1993;193:1239-1246.

Schelbert HR, Weisenberg G, Phelps ME, Gould KL, Eberhard H, Hoffman EJ, Gormesm A, Kuhi DE. Noninvasive assessment of coronary stenosis by myocardial imaging during pharmacological vasodilation. VI. Detection of coronary artery disease in man with intravenous N-13 ammonia and positron computed tomography. Am J Cardiol 1982;49:1197-1207.

Segalas I. Beauchamp AL. Transition Metal Complexes as Drugs and Chemotherapeutic Agents. Can J Chem 1992;70:943.

Seldin DW, Johnson LL, Blood DK, Muschel MJ, Smith KF, Wall R M, Cannon PJ. My ocardial perfusion imaging with technetium-99m SQ 30217: Comparison with thallium-201 and coronary anatomy. J Nucl Med1989;30:312-319.

Shelton ME, Dence CS, Hwang DR, Herrero P, Welch MJ, Bergmann, SR. In viva delineation of myocardial hypoxia during coronary occlusion using fluorine-18 fluoromisonidazole and positron emission tomography: A potential approach for identification of jeopardized myocardium. J Am CoII Cnrdiol 1990;16:477-485.

Sidgwick NV. Theoretical models of charge-transfer complexes. J Chem Soc (London) 1923;123:725-729.

Sluka J, Danek J, Bedrnik P, Budesinsky Z. (Thio)Amidoindoles and (Thio)Amidobenzimidazoles: An Investigation of Their Hydrogen-Bonding and Organocatalytic Properties in the Ring-Opening Polymerization of Lactide. Collect Czech Chem Commun 1981;46:2703-2706.

Sondhi SM, Rajvanshi S, Johar M, Bharti N, Azam A, Singh AK. Synthesis and Spectral Studies of Mannich Bases Derived from 2- Substituted Benzimidazoles. Eur J Med Chem 2002;37:835-840.

Sondhi SM,Johar M, Shukla R, Raghubir R, Bharti N,Azam A. ß-Isothiocyanatoketones: A Convenient Source of Heterocyclic Compounds. Aust J Chem 2001;54:461-471.

Tassaert, Ann Chim (Paris), 1798, 28, 94A.

Tiwari P,Tamrakar AK, SrivastavaAK, Maurya R. Synthesis of Novel Benzofuran Isoxazolines as Protein Tyrosine Phosphatase 1B Inhibitors. Bioorg Med Chem Lett 2006;16:2139-2143.

Townsend LB,Revankav GR. . 2-(2-Benzyloxy-3-methoxyphenyl)-1*H*-benzimidazole. Chem Rev 1970;70:389-395.

Trivedi R, De SK, Gibbs RA. Synthesis, characterization and crystal structure of 2-(4-(methylthio)phenyl)-1H-benzo[d]imidazole. J Mol Catal 2006;245:8-10.

Turan-Zitouni G, Chevallet P, Killic FS, Erol K. Synthesis of some thiazolyl-pyrazoline derivatives and preliminary investigation of their hypotensive activity. Eur J Med Chem. 2000;35:635-639.

Van vleck JH. The distribution of transition metal cations in spinels. J Chem Phys 1935;3:803-809.

Vaquelin LN. Ann chim (paris).1813;88:188.

Von Hoffman AW. Ann Chem.1851;78:253.

Weltzein K. Ann Chem.1856;97:19.

Werner A. The structure of platinum complexes Anorg Chem, 1893;3:267.

Wertz CA. Ann Chem Phys.1850;30:488.

Yang DJ, Ilgan S, Higuchi T, Zareneyrizi F, Oh CS, Liu CW, Kim EE, Podoloff DA. Hypoxia and oxidative stress in breast cancer: Tumour hypoxia – therapeutic considerations. Pharm Res.1999;16:743.

CHAPTER II
REVIEW OF LITERATURE

2.1 Metal ions in medicine

A number of drugs and potential pharmaceutical agents contain metal-binding or metal-recognition sites, which can bind or interact with metal ions and potentially influence their bioactivities and might also cause damage to the target biomolecules. Numerous examples of these ‘‘metallodrugs’’ and ‘‘metallopharmaceuticals’’ are reported, for instance: (a) a number of anti-inflammatory drugs, such as aspirin and its metabolite salicylglycine, ibuprofen (Abuhijleh *et al*., 1994), the indole derivative indomethacin,bioflavonoid rutin (Afanaseva *et al*., 2001), diclofenac, suprofen (Underhill 1993), and others (Underhill 1989) are known to bind to metal ions that affect their antioxidant and anti-inflammatory activities; (b) the potent histamine-H_2-receptor antagonist cimetidine and famotidine can form stable complexes with Cu^{2+} and Fe^{3+} (Kirkova 1999, Duda 1995); (c) the anthelmintic and fungistatic agent thiabendazole, used for the treatment of several parasitic diseases, forms a Co^{2+} complex with a metal to drug ratio of 1:2 (Umadevi *et al*., 1995); (d) the Ru^{2+} complex of the anti-malarial agent chloroquine exhibits an activity two to five times higher than the parent drug against drug-resistant strains of *Plasmodium falciparum* (Sanchez *et al*.,1996); (e) the antipsychotic drug trifluoperazine forms complexes with VO^{2+}, Ni^{2+}, Cu^{2+}, Pd^{2+}, and Sn^{4+} which exhibit higher activities than the metal free drug when tested in Moloney murine leukemia virus reverse transcriptase (Nacsa 1998); (f) the clinically useful β-lactamase inhibitor sulbactam can form complexes with Ni^{2+}, Cu^{2+}, and Fe^{3+}; (g) a few hormone-anchored metallodrugs have been prepared which show enhanced receptor binding and higher activities against cancer cells; (h) the thiosemicarbazone conjugated isatin (which shows a broad-spectrum bioactivity can bind late first-row transition metal ions and exhibit activity toward human leukemia cell lines, without inducing cell apoptosis; and (i) metal complexes (Be^{2+}, Mg^{2+}, Mn^{2+}, Co^{2+}, Ni^{2+}, Cu^{2+}, Zn^{2+}, Cd^{2+}, Pb^{2+}, Fe^{3+}, and Al^{3+}) of several carbonic anhydrase inhibiting sulfonamides (Supuran 1998) have been investigated for their topical intraocular pressure lowering properties and as potential agents against gastric acid imbalances.

There are a number of metallodrugs and metallopharmaceuticals which have been utilized for the treatment of diseases and disorders or as diagnostic agents (Orvig *et al*., 1999 and Sadler, 1991) such as gold as antiarthritic drug, bismuth as antiulcer drug, gadolinium as MRI contrast agents, technetium as radiopharmaceutical, metal-based X-ray contrast agents and photo- and radiosensitizers, vanadium as insulin mimetic, and lithium as antipsychotic drug. Li^+ can be considered the smallest effective metallodrug whose carbonate and citrate salts exhibit significant therapeutic benefit in the treatment of manic depression (bipolar mood disorder) (Birch *et al*., 1988). The status of Li^+ in cells have been extensively studied and recently reviewed (Mota de Freitas, 1993). It is also interesting to point out that the metal ion Sb^{3+} may be regarded as the simplest ‘‘metalloantibiotic’’ from a broader viewpoint of the term, whose salts (including N-methylglucamine antimonite and Nastibogluconate or Meglumine antimonate) have been utilized for the treatment of leishmaniasis against the protozoan parasite Leishmania (Yan *et al*., 2000). The antiprotozoal mechanism of Sb^{3+} is thought to be attributed to its binding to trypanothione which is essential for the growth of the parasite.

2.2 Metalloantibiotics: structure and function

Antibiotics can interact with a variety of biomolecules, which may result in inhibition of the biochemical or biophysical processes associated with the biomolecules. This can be illustrated through the interactions of the peptide antibiotic polymyxin with glycolipids, which affect membrane function (David *et al*., 1992), the anthracyclines (ACs) with DNA base pairs, which stops gene replication, the imbedding of the lipophilic antibiotic gramicidin (Hinton *et al*., 1985) and the insertion of the amphiphilic antibiotic protein colicin A into cell membrane (Parker *et al*., 1989), which disturbs normal ion transport and transmembrane otential of cells, the inhibition of transpeptidase by penicillins, which affects cell wall synthesis (Oka *et al*., 1980), and the inhibition of aminopeptidase by bestatin, amastatin, and puromycin, which impair many significant biochemical processes (Oka *et al*., 1980). Although most antibiotics do not need metal ions for their biological activity, there are several families of antibiotics that require metal ions to exhibit biological activities. In some cases, metal ions are bound tightly and are integral part of the structure and function of the antibiotics. Removal of the metal ions thus results in deactivation and/or change in structure of these antibiotics, such as bacitracin, bleomycin (BLM), streptonigrin (SN), and albomycin. In other cases, the binding of metal ions to the antibiotic molecules may engender profound chemical and biochemical consequences, which may not significantly affect the structure of the drugs, such as tetracyclines (TCs), actinomycins (ACs), aureolic acids, and quinolones. Similar to the case of ‘‘metalloproteins,’’ these families of antibiotics are thus dubbed ‘‘metalloantibiotics’’.

Metal ions play a key role in the actions of synthetic and natural metalloantibiotics, and are involved in specific interactions of these antibiotics with proteins, membranes, nucleic acids, and other biomolecules. For example, the binding of Fe/Co–BLM, Fe/Cu–SN, Mg–quinolone, Mg-quinobenzoxazine, Mg–aureolic acid, and platinum in cisplatin, impair DNA functions or result in DNA cleavage; the binding of metallobacitracin to undecaisoprenyl pyrophosphate which in turn, prohibits the recycling of the pyrophosphate to phosphate and thus results in inhibition of cell wall synthesis. The structural and functional roles of metal ions in metalloantibiotics have been further advanced in recent years through extensive biological, biochemical and physical studies (Guschlbauer *et al*., 1987).

2.2.1 Classes of metalloantibiotics

2.2.1.1 Aminoglycosides

Aminoglycosides form a unique and structurally diverse family of antibiotics, which include the famous Waksman's streptomycin and the widely used neomycin (an ingredient in''triple antibiotic''ointment along with bacitracin and polymyxin B). Antibiotic aminoglycosides work by inhibiting protein synthesis in bacteria and compromise the structure of the bacterial cell wall. The mode of action involves binding to the bacterial 30s ribosomal subunit (some work by binding to the 50s subunit) and inhibit the translocation of the peptidyl-tRNA. (e.g. Amikacin, gentamicin, kanamycin, neomycin, netilmycin, tobramycin, paromomycin, streptomycin).

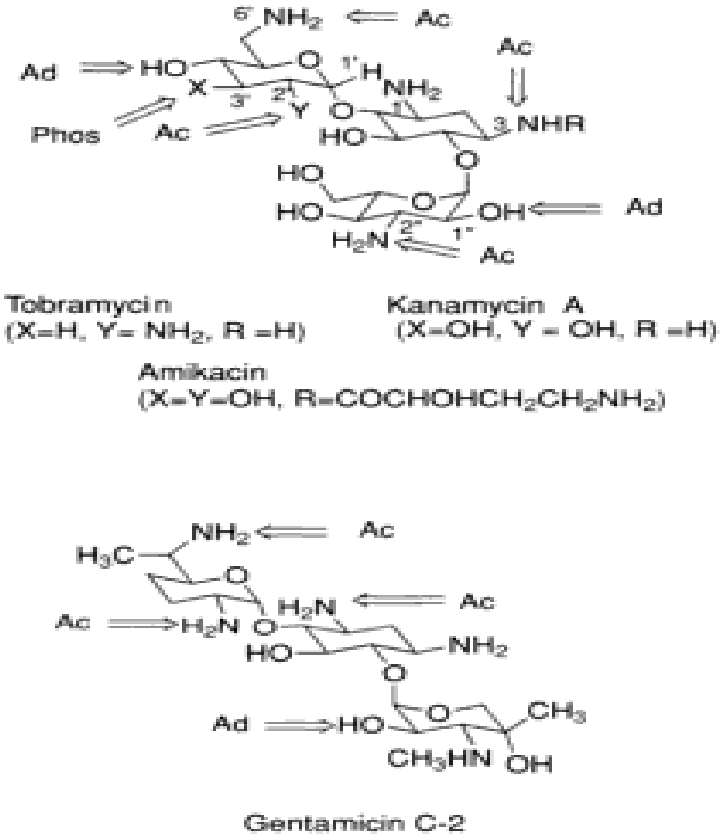

Fig 6: Structure of aminoglycosides

Neomycin has also been determined to inhibit the selfcleavage of the ribozyme from human hepatitis virus by direct replacement of the active divalent metal ions. Aminoglycosides work against infections caused by Gram negative bacteria, such as *Escherichia coli* and *Klebsiella* specialy *Pseudomonas aeruginosa* and are effective against aerobic bacteria. The ability of aminoglycosides to bind metal ions is

primarily governed by sugar ring substitution on the 2-deoxy streptamine ring (Ring B). Vicinal amine and hydroxyl groups can form a potential metal chelating motif, as found within the 2-deoxy streptamine ring (1-amine and 6-hydroxyl) (Gokhale et al.2007). Gentamicinsalso possess metal chelate donor atoms in ring C (Petrukhin et al.2009, Arya 2007). Aminoglycoside phosphotransferase (3')-IIIa (APH) has broadest substrate range among the phosphotransferases that cause resistance to aminoglycoside antibiotics. The presence of metalnucleotide increased the binding affinity of aminoglycosides to APH. In addition, the replacement of magnesium (II) with manganese (II) lowered the catalytic rates significantly while affecting the substrate selectivity of the enzyme such that the aminoglycosides with 2'-NH(2) become better substrates (higher Vmax) than those with 2'- OH (Wu and Serpersu, 2009). Aminoglycosides can be considered as "metal mimics" (Mikkelsen *et al*., 2001) because they bind to metal-ion binding sites of RNA molecules and interfere with the function of RNA by displacing functionally/structurally important metal (II) ions. Aminoglycosides promoted biochemical activities of a large ribozyme by acting as a Mg^{2+} mimic (Bao and Herrin, 2006).

Scientists showed that aminoglycosides also interfere with metal ion binding sites of protein enzymes, showing that the "metal mimics" property of aminoglycosides is not only restricted to the interaction between aminoglycosides and RNA (Yan *et al*., 2002). Thus, aminoglycosides as "metal mimics" have the potential to be used as functional probes to perturb the catalytic activity of both ribozymes and metalloenzymes as functional or structural probes, to map and characterize the active sites of such catalytic activities.

2.2.1.2 Ansamycins

Ansamycins prevents bacterial cell division by inhibiting cell wall synthesis. 17-(allylamino)-17-demethoxygeldanamycin (17AAG), a benzoquinone ansamycin Hsp_{90} inhibitor, has promising anticancer activity *in vitro*, in animal models and in clinical trials. It was demonstrated that $17AAGH_2$ was a more potent Hsp90 inhibitor than its parent quinine; however, $17AAGH_2$ can be oxidized back to 17AAG under aerobic conditions. Results suggested that human serum albumin prevented $17AAGH_2$ oxidation via a copper chelation mechanism (Guo *et al*., 2008).

2.2.1.3 Carbacephems

Carbacephems inhibit cell wall synthesis. Iron-dependent pathogen control is a promising field and offers a broad array of possible therapeutic applications. While the siderophore-antibiotic strategy uses Fe-siderophore uptake systems as gateways for cellular infiltration with established antibiotics, the siderophore pathway inhibition strategy tries to abolish siderophore utilization in order to starve the pathogens out for iron. Both concepts proved to be successful with *in vitro* and *ex vivo* culture model systems. However, most of these compounds have to be evaluated in appropriate *in vivo* systems. The crystal structure of the Fe-enterobactin binding protein CeuE was found in a status of ligand dependent dimerization, which was observed upon co-crystallization with the synthetic enterobactin analogue 1,3,5-N,N',N''-tris-(2,3-dihydroxybenzoyl) triaminomethylbenzene (MECAM), possessing an aromatic backbone. The ligand dimerization that led to face-to-face joining of two periplasmic binding proteins was dependent on the iron bound to the ligand complex and the stacking interactions between the aromatic backbones of the ligand molecules (Miethke and Marahiel, 2007).

2.2.1.4 Carbapenems

They inhibit cell wall synthesis. Metal analyses demonstrated that recombinant metallo-β-lactamase Bla_2 from *Bacillus anthracis* tightly binds one equiv of Zn (II). Results showed that mono-Zn (II) Bla_2 (1Zn-Bla_2) was active, while di-Zn (II) Bla_2 (ZnZn-Bla2) was unstable. However, di-Co (II) Bla_2 (CoCo-Bla_2) was substantially more active than the mono-Co (II) analogue. Further, Co (II) binding to Bla_2 was found distributed, while Zn (II) binding sequential. These results demonstrated that Zn enzyme binds Co (II) and Zn (II) via distinct mechanisms, underscoring the need to demonstrate transferability when extrapolating results on Co (II) substituted proteins to the native Zn (II) containing forms (Hawk *et al*., 2009). Metallo-beta-lactamases are bacterial Zn (II) dependent hydrolases capable of hydrolyzing all known classes of beta-lactam antibiotics, rendering them ineffective. These enzymes can be subdivided into three subclasses (B_1, B_2 and B_3) that differ in their metal binding sites and their characteristic tertiary structure. BcII is a B_1 metallo-beta-lactamase which is found in both mononuclear and dinuclear forms. The position of Zn (II) has been reported as essential for a productive substrate binding and hydrolysis (González *et al*., 2007). Co (II) BcII hydrolyzed α-lactam imipenem (both

the mono- and dinuclear forms) and the intermediate formed was a metal-bound anionic species with a novel resonant structure that was stabilized by the metal ion at the DCH or Zn (II) site (Tioni *et al*., 2008).

2.2.1.5 Cephalosporins

Cephalosporins inhibits the synthesis of the peptidoglycan layer of bacterial cell walls e.g. lactams. Many drugs possess modified toxicological and pharmacological properties when in the form of metal complexes. Sultana and Arayne reported that interaction of cefadroxil, cephalexin, cefatrizine and cefpirome with essential and trace elements caused antagonistic effect in many cases which was shown by decrease in antimicrobial activity of cephalosporins and MIC values were increased (Sultana and Arayne, 2007). The complex [Cu(cefotaxime)Cl] was found to have higher activity than that of cefotaxime against the bacteria strains studied under the test conditions, showing that it has a good activity as bactericide (Anacona and Da Silva, 2005).

2.2.1.6 Glycopeptides

These are peptidoglycan synthesis inhibitors. The monomeric complexes of Fe (III) with small molecules (glycopeptides) related to peptidoglycan monomer structure were prepared and characterized by chemical and physicochemical methods (Ladesiæ *et al*., 1992). Complexes of antibiotics with metals are useful in detecting microorganisms, including gram-positive bacteria. The complexes are preferably chelated complexes between a glycopeptide antibiotic and a detectable label comprising a transition or lanthanide metal (Olstein and Feirtag, 2005).

2.2.1.7 Aurecolic acids

The glycoantibiotic aureolic acid family produced by *Streptomyces species* is comprised of several members with similar structures, including chromomycin A3 (ChrA3), mithramycin, olivomycin, and variamycin, which exhibit activities toward Gram-positive bacteria, DNA viruses, and tumors. A divalent metal ion, such as Mg, Co, Zn, or Mn is required for aureolic acid to bind to a double helical DNA to form a drug-metal-(DNA) ternary complex which is bound to DNA in the minor groove. One of the major attributes for the biological action of the aureolic acid anticancer antibiotics chromomycin A3 and mithramycin is their ability to bind bivalent cations

such as Mg(II) and Zn(II) ions and form high affinity 2:1 complexes in terms of the antibiotic and the metal ion, respectively.

Chromomycin A_3 and mithramycin inhibited enzyme activity of alcohol dehydrogenase with inhibitory constants of micromolar order. The natures of the enzyme inhibition, the binding stoichiometry of two antibiotics per monomer, and comparable dissociation constants for the antibiotic and free (or substrate-bound) ADH imply that the association occurs as a consequence of the binding of the antibiotics to Zn (II) ion present at the structural center. Confocal microscopy showed the colocalization of the antibiotic and the metalloenzyme in $HepG_2$ cells, thereby supporting the proposition of physical association between the antibiotic(s) and the enzyme inside the cell (Devi *et al*., 2009).

The anticancer antibiotic chromomycin A3 (Chro) is a DNA minor groove binding drug belonging to the aureolic family. The effects of spermine on the interaction of 2:1 Chromomycin (Chro)-metal (Fe (II), Co (II), or Cu (II) ion) complexes revealed that spermine strongly competed for the Fe(II) and Cu(II) cations in dimeric Chro-DNA complexes, and disrupted the structures of these complexes. However, the DNA-Co(II)(Chro)(2) complex showed extreme resistance to spermine-mediated competition for the Co(II) cation. Further, a 6mM concentration of spermine completely abolished the DNAbinding activity of Fe (II) (Chro) (2) and Cu(II)(Chro)(2) and interfered with the associative binding of Co(II)(Chro)(2) complexes to DNA duplexes, but only slightly affected dissociation. Additionally, DNA condensation was observed in the reactions of DNA, spermine, and Fe(II)(Chro)(2). Despite the fact that Cu(II)(Chro)(2) and Fe(II)(Chro)(2) demonstrated lower DNA-binding activity than Co(II)(Chro)(2) in the absence of spermine, while Cu(II)(Chro)(2) and Fe(II)(Chro)(2) exhibited greater cytoxicity against HepG2 cells than Co(II)(Chro)(2), possibly due to competition of spermine for Fe(II) or Cu(II) in the dimeric Chro complex in the nucleus of the cancer cells. Such results should have significant relevance to future developments in metalloantibiotics for cancer therapy (Lu *et al*., 2009). The [(Mithramycin)2-Fe(II)] complex exhibited higher cytotoxicity than the drug alone in some cancer cell lines, probably related to its higher DNA-binding and cleavage activity (Hou and Wang, 2005)**.**

2.2.1.8 Macrolides

These irreversibly block 50s microbial ribosome, inhibit translation of tRNA as well as protien synthesis. Erythrocin has been the only macrolide antibiotic in general clinical use for about 40 years. Recently, a host of new macrolides and related antibiotics have become available, e.g. tylosin, spiromycin, leucomycin, oleandomycin, medemycin, josamycin, androxithromycin, larithromycin, azithromycin are the most important among them. The animal specific breeds include tylosin and tilmicosin. Macrolides inhibited bacterial protein synthesis by an effect on translocation and their action may be bactericidal or bacteriostatic. The macrolide antibiotic erythromycin contains two sugar moieties and a hydroxyl groups which potentially can serve as metal binding groups. Iron-erythromycin complex exhibit superoxide scavenging activity (Muranaka *et al*., 1997).

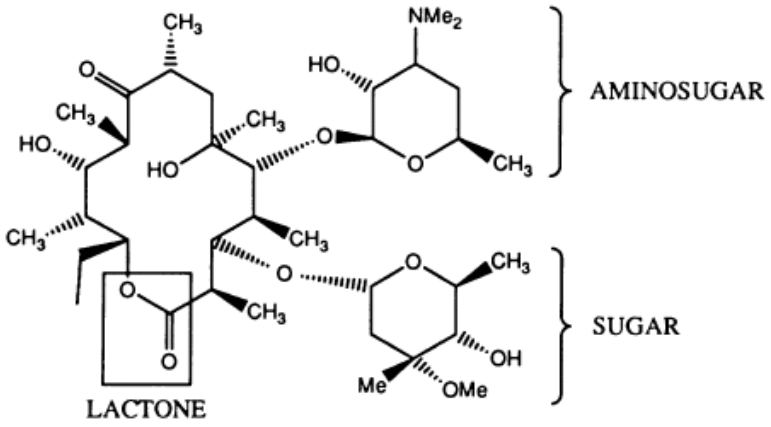

Figure 7: Sturucture of macrolide

2.2.1.9 Lincosamides

These are active against Grampositive cocci, e.g. *staphylococci*, hemolytic *streptococcus* and *pneumococcus*, and also against *clostridium tetani* and *mycoplasma*, but not against Gram-negative organisms. The mechanism of action involves the inhibition of protein synthesis. For example, Lincomycin is a broad spectrum antibiotic synthesized by *Streptomyces lincolnensis* that is particularly active against Grampositive bacteria. It is widely used in human and veterinary applications. Manganese dioxides in soils and sediments could contribute to the decomposition of lincosamide antibiotics released into the environment (Chen *et al*., 2010).

2.2.1.10 Penicillins

These inhibit synthesis of peptidoglycan and cell wall. Amoxicillin and silver nanoparticles combination resulted in greater bactericidal efficiency on *Escherichia coli* cells when they were applied separately. Moreover, the bactericidal action of silver nanoparticles and amoxicillin on *Escherichia coli* showed a higher antibacterial effect in Luria–Bertani medium with increasing concentration of both amoxicillin (0–0.525 $mgml^{-1}$) and silver nanoparticles (0–40 μgml^{-1}). Dynamic tests on bacterial growth indicated that exponential and stationary phases were greatly decreased and delayed in the synergistic effect of amoxicillin and silver nanoparticles. In addition, the effect induced by a preincubation with silver nanoparticles results showed that solutions with more silver nanoparticles have better antimicrobial effects (Li *et al*., 2005).

2.2.1.11 Quinolones

Quinolones are comprised of a large family of antibacterial agents such as nalidixic acid, pefloxacin, norfloxacin, ofloxacin, and ciprofloxacin (Smith 1984, Wolfson 1993). The first-generation nalidixic acid is active only against Gram-negative bacteria, whereas the later generations, such as the fluoroquinolones with a fluorine atom on the number 6 carbon, have been modified to provide effective antibacterial agents which exhibit a broad spectrum of activity, highly active against Gram-negative bacteria and less active against Gram-positive bacteria and also show significant activity against anaerobic bacteria. Fluoroquinolones have been further modified to produce quinobenzoxazines, which are found to show anti-tumor activities which is attributed to their interaction with topoisomerase II (whereas the parent quinolones lack such activities (Chu, 1992).

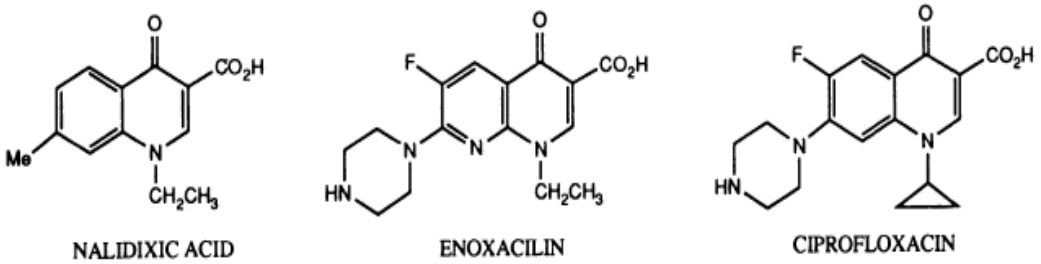

Fig 8: structures of quinolone

A few metal complexes (Fe^{3+}, Cu^{2+}, and Bi^{3+}) of quinolones were prepared in acidic solutions, from which crystals were obtained and their structures solved (Turel *et al*., 1997). A recent theoretical study suggested that metal binding to quinolones was associated with their activity. Fluorescence quenching measurements indicate the presence of a π–π stacking which has been suggested to be associated with the DNA intercalation capability of the drugs and their Cu^{2+} complexes (Roberts *et al*., 2000).

Metal complexes of quinolones

Quinolones can bind with several divalent and trivalent metal ions, including Mg^{2+}, Ca^{2+}, Co^{2+}, Ni^{2+}, Cu^{2+}, Cd^{2+} and Al^{3+} (Mendoza *et al*., 1996 and Turel, 1996),which may result in changes in their activity. Mg^{2+} and Al^{3+} were found to decrease the activity of the drugs (Hoffken 1985). The crystal structures of the Ni^{2+} and Cu^{2+} complexes of cinoxacin have been solved, in which the metals are found to bind to the α-carboxylketo moiety to form 1:2 metal-to-drug complexes (Turel, 1994).

Mechanism of quinolone action

The binding of quinolones to DNA-gyrase or topoisomerase IV has been considered to be the key step in the action of these drugs, which prohibits DNA religation activity and distorts DNA in the complex (Levine *et al*., 1998). Recent studies on the mapping of the functional interaction domain of topoisomerase II revealed that the quinolone-action site on the enzyme overlaps with the sites for the DNA cleavage-enhancing drugs, including etoposide, amsacrine, and genistein (Elsea *et al*., 1997). Norfloxacin exhibits Mg^{2+}dependent binding to plasmid DNA in the absence of the enzymes (Palu *et al*., 1992), wherein metal–drug, metal-DNA, and drug-metal-DNA complexes are detected. The drug does not bind to DNA in the absence or in the presence of an access amount of Mg^{2+}. Intercalation of norfloxacin into DNA is proposed in the study, and Mg^{2+} is proposed to serve as a ‘‘bridge’’ for the carboxylate of the drug to interact with DNA. However, DNA unwinding efficiency of ~10° by this drug is only marginal for weak intercalation (Tornaletti *et al*., 1988). Fluorine-19 NMR study of the binding of pefloxacin with double stranded DNA also revealed the participation of Mg^{2+} in the binding process (Lecomte *et al*., 1998). Moreover, the Mg^{2+}dependent single-stranded DNA binding affinities of several 6-substituted quinolones are found to correlate with the gyrase poisoning activity of these drugs (Sissi *et al*., 1998). This confirms the involvement of Mg^{2+} in such interactions and the significance of the

substitution at position-6. Quinobenzoxazines have been proposed to bind DNA duplex in the presence of Mg^{2+} to form a ternary complex in the form of 2drug-2Mg^{2+}-DNA, in which one drug molecule is proposed to intercalate into the DNA base pairs while the other is ‘‘externally bound.’’ (Fan *et al*., 1995). The two Mg^{2+} ions serve as salt bridges which interact with both molecules of the drug and the phosphoester backbone of DNA. The metal-quinobenzoxazine complex interacts with DNA in a cooperative manner,i.e., a 4:4 metal–drug complex is proposed to interact with DNA as a unit, in which two drug molecules intercalate into DNA base pairs while the two ‘‘external’’ molecules have π–π interactions and are expected to interact with the enzyme topoisomerase II or gyrase. The 2:2 metal–drug complexes is also suggested to be assembled in the presence of topoisomerase II based on the results from photocleavage assays, the use of mismatch sequences and competition experiments (Kwok, 1999). The formation of the 2:2 metal–drug complexes suggests that different quinobenzoxazine or quinolone drug molecules should be utilized to form ‘‘hybrids’’ for the pursuit of optimal structure–activity relationship.Because of increase in incidences of bacterial resistance towards many currently used antibiotics in recent years, further development of new antibiotics has become an urgent mission. Better understanding of the structures, functions, and mechanisms of existing metalloantibiotics and the mechanisms of antibiotic resistance would lead to better design of metal complexes. As the chemical properties of metal ions can vary significantly and can also be further fine-tuned by proper design of drug ligands for targeting different biomolecules and biocomponents, new generations of various ‘‘metalloantibiotics’’ isolated from natural resources or obtained via chemical syntheses and/or modifications that exhibit more effective antiparasitic, antibacterial, antiviral, and anti-tumor activities are under investigation.

2.2.1.12 Sulfonamides

They are competitive inhibitiors of bacterial enzyme dihydropteroate synthetase, and microbial nuclic acids synthesis was also inhibited along with microbial folic acid synthesis. Quinolinyl sulfonamides, such as *N*-(quinolin-8-yl) methanesulfonamide and *N*-(5-chloroquinolin-8-yl) methanesulfonamide [potent methionine aminopeptidase (MetAP)] inhibitors showed different inhibitory potencies of Co(II)-, Ni(II)-, Fe(II)-, Mn(II)-, and Zn(II)-forms on *Escherichia coli* MetAP, and their inhibition was dependent on metal concentration. X-ray structures of *E.coli* MetAP

complex with *N*-(quinolin-8-yl) methanesulfonamide revealed that the inhibitor formed a metal complex with the residue H79 at the enzyme active site; the complex was further stabilized by an extended H-bond and metal interaction network. Analysis of the inhibition of MetAP by these inhibitors indicated that this as a typical mechanism of inhibition for many non-peptidic MetAP inhibitors and emphasized the importance of defining *in vitro* conditions for identifying and evaluating MetAP inhibitors that will be capable of giving information relevant to the in vivo situation (Huang et al.2006). Markus et al reported that significant degree of selectivity can be attained with metal-dependent MetAP inhibitors (Altmeyer *et al*., 2010).

2.2.1.13 Tetracyclines (TCs)

They inhibit binding of aminoacyl-tRNA to the mRNA-ribosome thereby inhibiting translation process which is an important step in protein synthesis. Their usage has been limited in recent years because of side effects. The acidicoxy-groups at positions 1, 3, 10, 11, and 12 of TC are the potential metal binding or chelating site. Recent studies of the mechanism for bacterial resistance of this drug has afforded new insight into rational design of analogues and searching for new analogues of this broad-spectrum antibiotic family, such as the novel 9-glycylamido derivatives the‘‘glycylcyclines,’’ for defending bacterial infections.One of the glycylcyclines 9-t-butylglycylamidominocycline (GAR - 936, tigilcycline) is currently under phase II clinical trials. Antibiotics drugs of the tetracycline family are chelators of Ca^{2+} and Mg^{2+} ions. Tetracyclines coordinate metal (II) ions including Ca^{2+} and Mg^{2+} ions under physiological conditions forming chelate complexes with their ketoenolate moiety at rings B and C. These metal (II) complexes were the biologically relevant molecules conferring the antibiotic character of the drug by inhibiting ribosomal protein biosynthesis in prokaryotes. Evidece suggested that no other metal ion can compete with Mg2+ for TetR/[MeTc](+) complex formation (Palm *et al*., 2008).

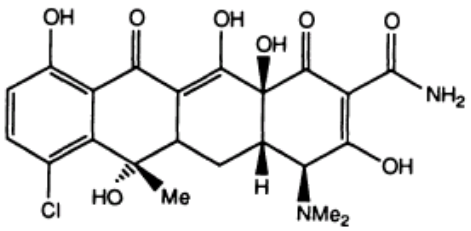

Fig 9: Sturucture of tetracycline

The beneficial effects of tetracyclines are attributed to their metal complex. Tetracyclines complex with copper acts as antioxidants and anti-inflammatory agents (electron scavengers) by neutralizing the damaging oxygen free radicals produced by the activated leucocytes**.** By combining with the copper, zinc, iron and other trace metal elements in enzymes such as collagenase, tetracyclines inhibited the enzymatic destruction of tissues. On the other hand tetracycline's greater affinity for nucleic acids and lipids than most chelates resulted in a greater inhibition of protein synthesis and microbial growth. Preformed copper-aspirinate would be more effective in the control of inflamation and the preformed copper-tetracyclinate would control the collagen vascular disorders of microbial origin.

Administration of certain dietary items (milk, containing calcium) or drugs (antacids, iron preparations, products containing calcium salts) to patients on tetracycline therapy could cause a significant decrease in the amount of tetracycline absorbed. TCs are highly susceptible to oxidative transformation mediated by dissolved Mn (II) and Cu (II) ions and manganese dioxide under environmentally relevant conditions. The oxidative transformation occurred via different TC structural moieties and reaction pathways when different metal species were involved, leading to complicated product formation patterns. It was also found that Al oxide surfaces promoted the acid-catalyzed isomeration and dehydration of TCs.

These findings significantly advances the fundamental understanding of the reaction mechanisms of TC compounds and provided the knowledge basis for better risk assessment of these compounds in the environment (Chen, 2008). The fundamental understanding of the reaction mechanisms of TC antibiotics with important metal species in the aquatic environment provides the knowledge basis for better environmental fate prediction and risk assessment for these biologically active contaminants (Artsimovitch, 2005).Tetracyclines coordinate metal (II) ions under physiological conditions forming chelate complexes with their ketoenolate moiety at rings B and C are the biologically relevant molecules conferring the antibiotic character of the drug by inhibiting ribosomal protein biosynthesis in prokaryotes.

The Tet repressor, TetR, is the molecular switch for tetracycline resistance determinants in gram-negative bacteria and controls transcription of a gene encoding the integral membrane protein TetA, which mediated active efflux of a tetracycline-

metal(II) cation, [MeTc](+), by equimolar antiport with a proton. Researchers evaluated distinct characteristics of the metal binding by crystal structure determination of TetR/[MeTc](+) complexes and of association equilibrium constants of [MeTc](+) and TetR/[MeTc](+) complexes. Various divalent metal ions bind to the same octahedral coordination site, defined by a histidine side chain of TetR, the tetracycline, and three water molecules. Whereas association constants for [MeTc](+) vary within 3 orders of magnitude, association of the [MeTc](+) cation to TetR is very similar for all measured divalent metals. Taking intracellular cation concentrations into account, it was shown that no other metal ion can compete with $Mg^{(2+)}$ for TetR/$[MeTc]^{(+)}$complex formation (Palm *et al*., 2008).

2.2.1.14 Rifamycin

Rifamycin antibacterial agents inhibited bacterial RNA polymerase (RNAP) by binding to a site adjacent to the RNAP active center and prevented synthesis of RNA products. Artsimovitch et al. proposed that rifamycins function by allosteric modulation of binding of Mg^{2+} to the RNAP active center. It was also concluded that rifamycins do not function by allosteric modulation of binding of Mg^{2+} to the RNAP active center (Feklistov, 2008).

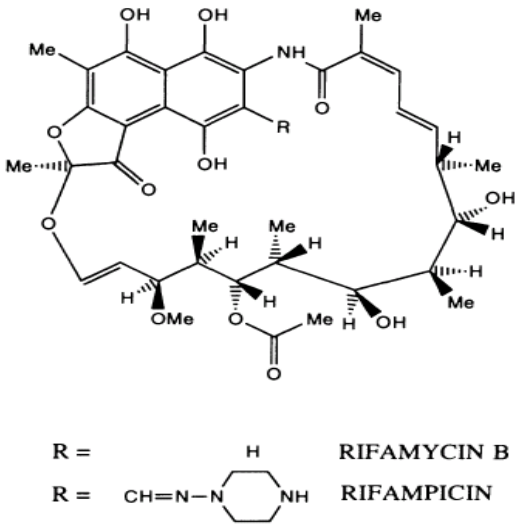

Fig 10: Structures of rifamycin analogues

2.2.1.15 Anthracycline

Anthracycline (AC) antibiotics are produced by *Streptomyces species* and exhibit wide spectrum of antineoplastic activity toward both solid and hematologic tumors

and cancers. The redox activity of the AC ring plays a key role in the action of these drugs. In addition, the metal ion bound to the 11, 12-b ketophenolate site is also thought to be involved in some actions of these antibiotics. Doxorubicin 50 is powerful chelators of other metal ions, including Cu^{2+} and Al^{3+}.Copper-complexation had no affect on the cytotoxicity of the doxorubicin drug suggesting thereby that extracellular as well as intracellular mechanisms may be involved in the development of its antitumor activity (Monti *et al*.,1990).

2.2.1.16 Streptonigrin

Streptonigrin is a metal-binding quinone-containing antibiotic produced by *Streptomyces flocculus.* Redox active metal ions such as Fe and Cu are required for this antibiotic to exhibit full antibiotic and anti-tumor activities. The implication for the formation of metal complexes of the antitumor antibiotic streptonigrin, which cleaves DNA in the presence of metal ions, has been reported (Anderberg *et al*., 2002). *In vivo*, metal ions such as Zn (II), Cu (II) and Mn(II) facilitated the initial reduction of streptonigrin to the semiquinone by capturing the semiquinone after streptonigrin reduction by biological reductants.

2.2.1.17 Bleomycin (BLM)

Bleomycin (BLM, also known as Blenoxane) was first isolated as a Cu^{2+}-containing glycooligopeptide antibiotic from the culture medium of *Streptomyces verticullus* (Umezawa*et al*., 1966), and was later found to be an antiviral agent (Takeshita*et al*., 1974). It was soon found to be an anticancer agent and has ever since become one of the most widely used anticancer drugs (Lazo *et al*., 1996), for the treatment of testis cancer, lymphomas, and head and neck cancer, as well as the AIDS-related Kaposi's sarcoma in combination with cisplatin and adriamycin. However, it can cause life-threatening side effects, including lung fibrosis. BLM contains a few uncommon amino acids, such as β-aminoalanine, β-hydroxyhistidine, and methylvalerate, two sugars (gulose and mannose), a few potential metal-binding functionalities such as imidazole, pyrimidine, amido, and amino groups, and a peptidyl bithiazole chain considered to be the DNA recognition site. Similar to many other natural products, BLM is produced as a mixture of several analogs with BLM A2 and B2 being the most abundant ones (Umezawa *et al*., 1966).

BLM is the most extensively studied metalloantibiotic from several view points, such as its metal binding property, structural studies using a variety of spectroscopic methods, mechanistic study of its oxidative DNA cleavage, investigation of its structure–function relationship, and its use as a non-heme model for investigation of dioxygen activation and DNA recognition/cleavage (Burger *et al*., 2000). There are a few BLM-like antibiotics which exhibit similar physical, structural, and biochemical characteristics as BLM, which have been previously reviewed (Umezawa *et al*., 1980) Bleomycin is a glycosylated linear nonribosomal peptide antibiotic produced by the bacterium *Streptomyces verticillus*. Bleomycin when used as an anti-cancer agent, the chemotherapeutical forms are primarily bleomycin A2 and B2. Bleomycin A2 is used in the treatment of Hodgkin lymphoma (as a component of the ABVD regimen), squamous cell carcinomas, and testicular cancer, pleurodesis as well as plantar warts. [62Zn] BLM can be used in PET oncology studies due to its suitable physicochemical properties as a diagnostic complex *invitro* and *in vivo* (Jalilianet *et al*., 2003 and Bahrami-Samani *et al*., 2010). DNA cleavage by bleomycin depends on oxygen and metal ions, at least in *in vitro*. It is believed that bleomycin chelates metal ions (primarily iron) producing a pseudoenzyme that reacts with oxygen to produce superoxide and hydroxide free radicals that cleave DNA.

The bleomycin-iron complex was the well-studied example of site-specific, metal-mediated damage to DNA (Grollman *et al*., 1985). The bleomycin- mediated cleavage of DNA occurred *via* formation of a ternary complex, DNA-bleomycin-iron. Further, oxidation of the complexed Fe (II) resulted in a site-specific oxidation of DNA, most probably by the hydroxyl radical (Sausville *et al*., 1978). Antitumor properties of bleomycin and several of its metal complexes as well as nucleic acid recognition by metal complexes of bleomycin has been reported (Claussen and Long 1997, Rao *et al*., 1980). Bleomycin (BLM) effectively carries out single-and double-stranded DNA cleavage. Activated BLM (ABLM), a low-spin ferric-hydroperoxide, BLM–FeIII–OOH, is the last intermediate detected before DNA cleavage. The DNA dependence of the ABLM reaction indicated that the involvement of DNA in the transition state for ABLM decay and thus reacted directly with BLM–Fe III–OOH instead of its decay product (Marina *et al*., 2008).

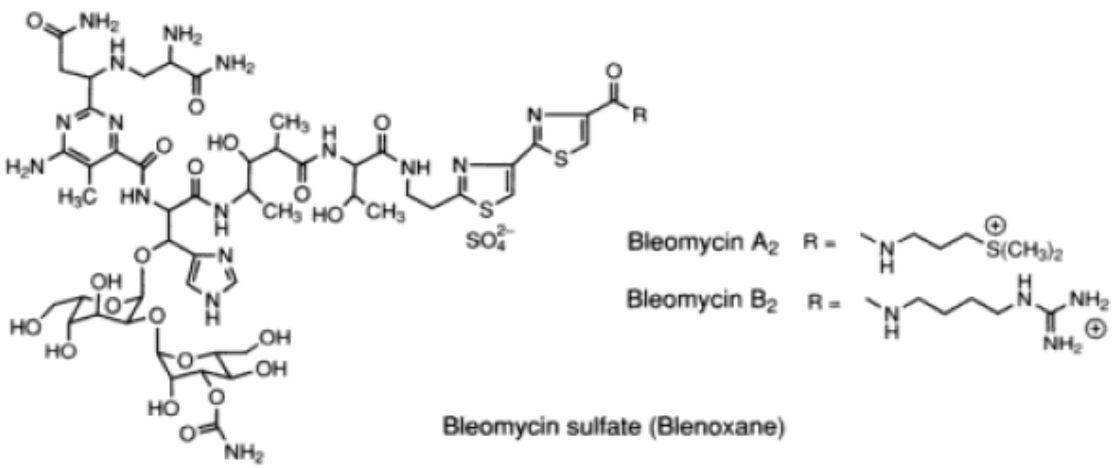

Fig 11: Anticancer agent bleomycin

2.2.1.18 Polyether ionophores

The polyether ionophores (monensin, salinomycin, ionomycin, maduramycin etc.) are naturally occurring antibiotics produced by the soil bacteria strains of *Streptomyces spp*. and are widely applied in veterinary medicine. Besides their well known anticoccidiosis activity against *Eimeriya spp*., this class of compounds possesses well studied antibacterial, antifungal, antimucosal and especially in case of salinomycin – anticancer properties. Scientists have shown that monensins (MonH / MonNa /MonK) formed three types of complex species: $[M(Mon)_2(H_2O)_2]$ (M = Mg, Ca, Ni, Zn, Co, Mn (1)), $[M(Mon)(H_2O)]$ (M = Hg (2)), $[M(MonNa)_2Cl_2]$ (M =Co, Mn,Cu (3). Sodium salinomycin (SalNa) produces two different complex types of composition [M(Sal)2(H2O)2] (M = Co, Ni, Cu, Zn (4)) and $[M(Sal)_2(H_2O)]$ (M = Pb (5)), while the known divalent metal compounds of maduramycins (NH 4Mad / MadH) consisted of [M(Mad)Cl] (M = Mn, Co (6)) as a main complex unit (Pantcheva *et al*., 2010 and Dorkov *et al*., 2008).

2.2.1.19 Platinum compounds

The antibiotic activities of Platinum (II) complexes such as Cisplatin have been used as anticancer agents since long (Jamieson and Lippard 1999, Hannon 2007). Inside the cell, cisplatin causes platination of DNA, which involves interstrand and intrastrand crosslinking as well as formation of adducts, usually through guanine. Formation of cisplatin DNA adducts causes distortion and results in inhibition of DNA replication (Lee *et al*., 2002). DNA is considered the main biological target of cisplatin. Different strategies have been used to improve efficacy of cisplatin like use

of nanotechnology to specify the effect of the drug in the target cells (Liang *et al*., 2010). Platinum complexes with distinctively different DNA binding modes from cisplatin may provide higher antitumor activity against cisplatin resistant cells. The *trans* isomer of diamminedichloro Pt (II) has also been studied, trans DDP offers a different attachment mode with DNA and is used as anticancer drug for cisplatin resistant cancer cells. A series of *trans* piperazine compounds were reported to have significant cytotoxicity against cisplatin resistant cells (Najajreh and Perez2002). Irradiation of cis-platin modified DNA with UV light induced cross-links with the protein HMG, which inhibited RNA transcription (Bartkowiak *et al*., 2009). The molecular mechanism of action of an antitumor platinum complex [PtCl2(*cis*-1,4-DACH)] (DACH = diaminocyclohexane) has been reported. The inhibition of DNA polymerization by Pt–DNA adducts could be responsible for markedly different effects of DNA adducts of [$PtCl_2$(*cis*-1,4-DACH)] and conventional cisplatin (Kasparkova *et al*., 2010).

2.2.1.20 Ruthenium compounds

In recent years, ruthenium-based molecules have emerged as promising antitumor and antimetastatic agents with potential uses in platinum-resistant tumors or as alternatives to platinum. Ruthenium compounds theoretically possess unique biochemical features allowing them to accumulate preferentially in neoplastic tissues and to convert to their active state only after entering tumor cells. Ruthenium complexes with oxidation state +2 or +3 show antitumor activity against metastasis cancers but have minimal effects on primary tumors. Two ruthenium based drugs, NAMI-A and KP1019, have reached human clinical testing. Some developments in the ruthenium-based antitumor drugs field on mixed diruthenium-organic drugs as metallopharmaceuticals in cancer therapy were described. Novel organic pharmaceuticals-containing diruthenium (II, III) complexes have shown promising antitumor activity for C6 rat glioma - a model for glioblastoma multiforme (GBA) (Silva *et al*., 2010). Other promising ruthenium agents include novel ruthenium compound ONCO4417 and DW1/2 that has demonstrated Pim-1 kinase inhibition in preclinical systems. Further development of these and other ruthenium agents may rely on novel approaches including rational combination strategies as well as identification of potential pharmacodynamic biomarkers of drug activity aiding early phase clinical studies (Antonarakis and Emadi, 2010). Imidazolium trans-

imidazoledimethyl sulfoxide tetrachlororuthenate (NAMI-A), [ImH][trans-$RuCl_4$ (DMSO-S)(Im)], (Im=imidazole; ImH=imidazolium) remains one of the leading ruthenium complexes with the best chances of becoming an anticancer drug (McGowan 2005). The relative binding of ruthenocene derivatives were very high and even better than hydroxyl tamoxifen which is novel antagonist for estrogen (Clarke 2003). Galanski and his co-workers studied the anticancer properties of Ru (III) arene complexes (Galanski *et al*., 2003). Ruthenocene-cymene complexes have shown to damage DNA by forming monofunctional adducts selectively with guanine bases (Allardyce *et al*., 2001).

Ruthenocene complexes showed antiproliferative effect on the MCF-7 (ER-positive) breast cancer cell lines. Many of Ru complexes exhibit anti-estrogen properties similar to that observed for novel anti-estrogen Tamoxifen (Anne *et al*., 2005). The electrochemistry of $RuL_2(CO)_2Cl_2$ [L2 = 7-amino-6-methoxy-5,8-quinolinedione) and the implications for the formation of metal complexes of the antitumor antibiotic streptonigrin which cleaves DNA in the presence of metal ions were reported (Anderberg *et al*., 2002).

2.2.1.21 Organometallics

The first successful application of an organometallic compound as a drug was the anti-syphilis drug Salvarsan in 1910. Some successful examples of organometallic based drugs include the anti-tumor properties of the cisplatin, ferroquine for the treatment of malaria, and the use of radioactive 99m Tc compounds as radiopharmaceuticals. It is believed that proteins could be the biological target of organometallics and researchers have shown that compounds with thiosemicarbazone ligands can bind strongly to human serum albumin (Beckford *et al*., 2010). Several organometallic compounds have been found to exhibit antineoplastic activities. Organometallic compound like Iron (III)-salophene with selective cytotoxic and anti-proliferative properties have been used in platinum-resistant ovarian cancer cells (Lange *et al*., 2008). Complexes of transition metal like iron have shown remarkable antiproliferative properties (Ray *et al*., 2007 and Sun *et al*., 2007). Ferrocifenes exhibited anticancer activity against hormone dependent and hormone independent breast cancers (Top *et al*., 2003). Many organometallic analogues of tamoxifen were used as a vehicle for introducing other cytotoxic agents to the cancer cells (Kiat *et al*.,

2006). Newly emerging ruthenium (II) organometallic complexes not only bind to DNA coordinatively, but also by H-bonding and hydrophobic interactions triggered by the introduction of extended arene rings into their versatile structures. Intriguingly osmium (the heavier congener of ruthenium) reacted differently with DNA but also produce highly cytotoxic organometallic complexes (Pizarro and Sadler, 2009).

2.2.1.22 Antimicrobial implants

Antimicrobial implants represent a preventive method against infection. One of the inorganic antimicrobials Novaron (grade VZ 600) coated at 3.0 MPa to titanium alloy (Ti6Al4V) plates exhibited the antimicrobial activity against *Staphylococcus aureus, Pseudomonas aeruginosa*, and *Klebsiella pneumoniae*. These results indicated that there is a possibility of using them not only for clean operations but also for operations with suspected bacterial contamination, such as fixation of slight compound fractures (Tamai *et al*., 2009). Fusidic acid is a bacteriostatic antibiotic that is often used topically in creams and eyedrops, but may also be given systemically as tablets or injections. The global problem of advancing antimicrobial resistance has led to a renewed interest in its use recently (Falagas *et al*., 2008). Transition metal complexes or salts of fusidic acid, especially the silver and zinc salts were found particularly suitable for topical applicationas as anti-infective agents (Masterson 1991). The radical scavenging activity of various metallobacitracin complexes was shown to be higher than those of free transition metal ions and metal-free bacitracin. The superoxide dismutase activity of the complex was found to be in the order of Mn (II) > Cu (II) > Co (II) > Ni (II) (Piacham *et al*., 2006).

2.3 DNA Binding metalloantibiotics

DNA can bind with many different biomolecules and synthetic compounds, including proteins, antibiotics, polyamines, synthetic metal complexes and organometallic compounds (Chaires, 2001). In a case of very specific protein-DNA interaction, transcription is regulated to turn on or off a specific biological process. DNA is also a target for therapeutic treatment of disorders, such as cancer. The ligands can directly bind to DNA or DNA-regulating biomolecules. Several clinically used anti-cancer antibiotics, such as BLM and the ACs, are DNA-binding (and cleaving) agents. A better understanding of the structures of these antibiotics and their DNA complexes, and of the relationship of structure, function, and toxicity of these drugs can provide

information for the design of more effective but less toxic drugs for therapeutics. Investigations in the interaction between DNA and synthetic compounds or metal complexes can further our understanding of DNA–ligand binding specificity which could provide clues for rational design of DNAspecific drugs in future (Tullius *et al*., 1989).

2.4 DNA/RNA Binding and Cleavage

The antibiotic mechanism of BLM has been proposed on the basis of the results from the studies on its Fe and Co derivatives (Burger, 2000). In the presence of reducing agents, the metal ions in Fe^{2+} or Co^{2+}BLM bind dioxygen and convert it into an ‘‘activated form’’ HOO-Fe-BLM or HOO-Co-BLM via a superoxide-Fe-BLM intermediate. DNA cleavage by Fe–BLM is proposed to be carried out by oxidation at C4′ and C2′ proton abstraction from the deoxyribose of DNA following oxidation of 5′-GC and 5′-GT sequences (Kane, 1994 and Takeshita, 1978). The damaged deoxyribose then breaks down resulting into cleavage of DNA strand. The mechanism for DNA cleavage by Co–BLM has been suggested to follow a similar mechanism (Chang 1984). In the presence of H_2O_2, Fe^{3+}- BL M generates hydroxyl ($^{\cdot}OH$) free radical in the vicinity of DNA which is expected to cause DNA cleavage *in vivo* (Chakrabarti *et al*., 1996). Several studies indicate that Fe^{2+}–BLM can also bind and cleave RNA molecules, including tRNA and its precursors, and rRNA (Magliozzo *et al*., 1989). The cleavage occurs mainly at the junctions between double stranded and single-stranded regions in RNA molecules such as at C26 and A32 in E. coli (Carter *et al*., 1991).

2.5 Metal Complexes of SN

Zinc ions bind SN to afford complexes with varying metal to ligand ratios at various temperatures, in which 1:1 metal–drug complex is the predominant one (Long *et al*., 1997). The interaction of Zn^{2+}–SN with DNA and oligonucleotides has been investigated with 1H- and 31P-NMR spectroscopy. This study concluded the requirement of metal ions for SN binding to DNA (Long *et al*., 1997). SN can bind to several different paramagnetic metal ions, including Co^{2+} and Fe^{2+} with large formation constants to form 1:1 metal-SN complexes (Wei, 1998). The study of Fe^{2+}–SN complex is particularly important since it is considered an active form exhibiting

enhanced activity towards DNA destruction, both *in vitro* and *in vivo* (Merryfield *et al*., 1982).

2.6 Metal Binding and Bioactivities

Metal ions have been found to be involved in some unique activities of aminoglycosides. The binding of iron to gentamicin has been postulated to induce free radical formation which causes peroxidation of lipids (Priuska *et al*., 1995). The Fe^{2+}/Fe^{3+} complexes of gentamicin have recently been investigated. These redox-active iron complexes were implied for aminoglycoside toxicity. Several aminoglycoside antibiotics have been observed to bind Cu^{2+}, including lincomycin (Jezowska *et al*., 2001 a), kasugamycin (Jezowska *et al*., 2001b), kanamycin B (Jezowska *et al*., 1998 a), tobramycin (Jezowska *et al*., 1998b), genticin (Jezowska *et al*., 1998 c), and the semi-synthetic amikacin (Jezowska *et al*., 2001 b). In addition, a few simple aminosugars have also been reported to bind Cu^{2+}, which serve as simple model for binding of aminoglycoside antibiotics to metals (Jezowska *et al*., 1996). The Cu^{2+}-aminoglycoside complexes are observed to exhibit oxidative activity, which can catalyze oxidation of nucleotides in the presence of H_2O_2. Hydrolytic cleavage of DNA and RNA molecules including the RNA of the HIV-1 viral Rev response element, under physiological conditions, by Cu^{2+}-aminoglycoside complexes were also observed (Sreedhara *et al*., 1999). The metal ion in these complexes has been proposed to bind through a chelating vicinal aminohydroxyl binding moiety of the drugs. Although, the macrolide antibiotic erythromycin has a structure different from the streptomycin-like antibiotics, yet it contains two sugar moieties (one being a *t*-aminosugar), carbonyl and hydroxyl groups which can serve as potential metal binding ligands. An erythromycin–iron complex was observed to exhibit superoxide scavenging activity that was not observed for the antibiotic without the metal (Muranaka *et al*., 1997).

2.7 Metal complexes and bacterial resistance

An accepted definition of antibiotic resistance as presented in 1998 by the Institute of Medicine is "a property of bacteria that confers the capacity to inactivate or exclude antibiotics, or a mechanism that blocks the inhibitory or killing effects of antibiotics, leading to survival despite exposure to antimicrobials (Bahe *et al*., 2006). The presence and spread of antibiotic resistance in nonagricultural, non-clinical

environments has been reported (Allen *et al*., 2010). Studies have reported the occurrence of bacterial antibiotic resistance due to the use of the same antibiotics in both humans and animals (Wegener 2003). Further, production of ß lactamases is the most common mechanism of bacterial resistance (Samaha *et al*., 2003). Metal contamination represents a longstanding, widespread and recalcitrant selection pressure with both environmental and clinical importance that potentially contributes to the maintenance and spread of antibiotic resistance factors (Baker *et al*., 2006).

Although overuse of antibiotics in agriculture and medicine seems partially responsible, environmental exposure to heavy metals may also contribute to antibiotic resistance, even in the absence of antibiotics themselves. Data on a series of eight lab-scale activated-sludge reactors amended with Zn and/or a suite of three antibiotics (oxytetracycline, ciprofloxacin, and tylosin), in parallel with unamended control showed that sub-toxic levels of Zn caused increased antibiotic resistance in waste treatment microbial communities at comparatively low antibiotic levels, probably due to developed crossresistance resulting from pre-exposure to Zn (Peltier *et al*., 2010). Researchers have come up with a possible substitute that utilizes the metal gallium to mimic iron needed by bacteria to survive. Rather than a drug designed to attack the bacteria itself, gallium boosts of the body's own natural defenses by fooling bacteria into thinking they are well-nourished (Banin *et al*., 2008). The prevalence of antibiotic resistance may increase in populations via indirect or coselection from heavy metal contamination. Selection for metal tolerance among sediment bacteria may influence selection for antibiotic resistance differently in sediments than in the water column (Cary and Vaun, 2008). Colony forming heterotrophic metal resistant bacteria isolated from the sediments of Sunchon Bay, South Korea exhibited resistance to various heavy metals and also to wide spectrum of antibiotics. Plasmid curing results in loss of antibiotic and heavy metals resistance in some of the isolates confirmed a relationship between antibiotic and heavy metal resistance (Kamala and Lee, 2008). Heavy metal pollution contributed to increased antibiotic resistance through indirect selection also (Vaun and Cary, 2000). Metal pollution resulted in selective pressure that leads to the development of multiple metal/antibiotic resistance among bacterial populations, probably through horizontal gene transfer (Ming and Epperson, 2002). Researchers have obtained single-stranded DNA's (reversible, noncompetitive inhibitors of the metalloenzyme, with Ki and Ki' values in the

nanomolar range) that are potent inhibitors of the *Bacillus cereus* 5/B/6 metallo-ß-lactamase. The inhibition patterns and metal ion dependence of their inhibition suggested that the oligonucleotides alter the coordination of the active site metal ion(s) (Kim *et al*., 2009).

2.8 Siderophores and ionophores

Molecular receptors known as siderophores are also polydentate ligands that can selectively bind and transport alkali or alkaline earth metal ions and Fe^{3+}, respectively, across cell membranes and artifcial lipid bilayers (for example, enterobactins, ferrichromes, ferrioxamines). Ionophores are special carrier molecules that wrap around metal ions forming typically 1:1 complex, so they can pass through the membrane by diffusion. These molecules can serve as antibiotics by (a) disturbing the ionic balance across membrane via ion transport (particularly, the transport of alkali and alkaline earth metal ions), such ions through the pores, such as gramicidins, and (c) competing for essential iron in the environment, such as ferrichromes. Gramicidin represents ion channel-forming molecule [helical peptide dimer, hydrophobic outer surface interacts with membrane, carbonyls and nitrogens on inner surface can interact with cations as they pass through, potassium selective: *pore* size and ligands select for K+. Ionophore antibiotics can disrupt this ionic imbalance by allowing ions to penetrate the cell membrane as ion-ionophore complexes or via the formation of ion channels. Grampositive bacteria appear to be particularly sensitive to the effect of ionophores perturbing normal ion transport. Iron recognition and active transport relies on the biosyntheses and use of microbe-selective iron-chelating compounds called siderophores. Siderophores and analogs can be used for iron transport-mediated drug delivery ("Trojan Horse"antibiotics) and induction of iron limitation/starvation. Recent extensions of the use of siderophores for the development of novel potent and selective anticancer agents have been reported (Miller *et al*., 2009).

2.9 Metal complexes as antibiotic mimics/artificial metalloantibiotics

Artificial metalloantibiotics activity mimics antibiotics. Biological macromolecules present in living organisms, like proteins, DNA, have many metal-binding sites. As a consequence, coordination compounds can react with such cellular components, displaying possible toxic effects, or they also may have beneficial applications. A

number of reports on design and synthesis of metal compounds as potential antibacterial agents (metalloantibiotics) are available in literature. The results generally indicated that more potent complexes possessed better physical properties and are much more effective as chemotherapy agents than their parent antibiotics. However, the complexes may be toxic at the dose level used to the liver and kidney but can be consider as potential antibiotics drugs after reduction in the level of metal ion which is responsible for the toxicity (Ogunniran *et al*., 2008). Classical examples, like cisplatin, and new examples of Pt and Ru compounds are known to bind to several biomacromolecules in a specific way, and eventually bind at DNA (Rafique *et al*., 2010 and Reedijk 2008). The metal ions can be administered in polymeric microparticles, deformable films or microparticles embedded within deformable films. The metal ions exhibited microbiocidal action to the bacterial pathogens that are the causative agents of periodontal disease. Ternary complex seems worth pursuing as a possible antimicrobial agent candidate. Moreover, as the biological studies showed, both the synthesised complexes and the solutions prepared by mixing the components exhibited the same behavior, thereby, proposing a new, faster and accurate methodology to screen metalloantibiotics prior to synthesis of the complexes. (Saraiva *et al*., 2010). Metal-mediated inhibition is a viable approach for discovering methionine aminopeptidase inhibitors that are effective for therapeutic application (Chai and Ye 2009). Cu (hesperetin)$_2$(H_2O)$_2$]nH_2O exhibited growth inhibition of SGC-7901 and HepG2 cell lines with respect to hesperetin and was found to bind DNA in intercalation modes. Further, the binding affinity of complex was stronger than that of free hesperetin (Tan *et al*., 2009). Erythromycin and clarithromycin metal complexes resulted in synergistic effects whereas roxithromycin metal complexes resulted in antagonistic effect (Najma *et al*., 2005). Various factors influencing the stability of fluoroquinolone-metal complexes have been reported (Urbaniak and Kokot, 2009). Interaction of cholinesterases with other molecules in neuritic plaques and neurofibrillary tangles mediated by transition metal ions were known to be present in AD pathology lesions (Darvesh *et al*., 2010). The possibility of designing niobium-based antibiotics which block iron uptake by pathogenic bacteria was discussed (Shi *et al*., 2010).

A new synthetic ribonuclease [Tb(L1) (OTf) (OH_2)] $(OTf)_2$·MeCN {L1=2-[7-ethyl-4,10-*bis* (isopropylcarbamoylmethyl)-1,4,7,10-tetraazacyclododec-1-yl] -*N*isopropyl-

acetamide }in which the terbium(III) center is 9-coordinate, with a capped square-*anti*prism geometry effectively promoted RNA cleavage in footprinting experiments, in which binding of the Tat peptide and neomycin B to the bulge region of the TAR stem-loop was confirmed (Belousoff *et al*., 2009). Researchers suggested the possibility that the scavenging effect of the pirfenidone PFD–iron complex contributed to the anti-fibrotic action of pirfenidone used for treating idiopathic pulmonary fibrosis (Mitani *et al*., 2008). Quinolones activity decreased in the environment of certain metal ions by formation of sparingly soluble metal chelates. Fluoroquinolones metal complexes were also discussed in terms of their therapeutic application, in terms of the nuclease activity and antibacterial activity (Serafin and Stanczak, 2009). A method was reported for inhibiting microbial growth by administering an effective amount of a silver complex of a N-heterocyclic amine (Youngs *et al*., 2010). Some important contributions in the area of synthetic analogues of metallo-betalactamases, with major emphasis on the role of dinuclear Zn (II) complexes in the hydrolysis of beta-lactam antibiotics have been reported (Tamilselvi and Mugesh, 2008). Some furanyl-derived sulfonamides behave as bidentate ligands in complexation with cobalt(II), copper(II), nickel(II) and zinc(II) with an octahedral geometry and their *in vitro* cytotoxic properties were reported using brine shrimp bioassay (Chohan, 2009). Researchers have suggested the development of new anti-cancer drugs using chelators and chelator complexes with platinum and other metals, and also new protocols of combinations of chelators with known anti-cancer drugs (Kontoghiorghes *et al*., 2008). Collectively, lewis acidity, flexible coordination numbers and geometries, and fast ligand exchange rates make metal ions particularly, Zn^{2+} well suited to serve as cofactors for catalyzing hydrolytic reactions or enhancing the reactivity of the water nucleophile and stabilizing reaction intermediates (Hernick and Fierke 2010). Artificial metalloantibiotics might block iron uptake by pathogenic bacteria, in effect starving them to death. Within the body, iron is present in the form of iron ions with a threefold positive charge (Fe^{3+}) and must always be well "wrapped" to prevent it from reacting with proteins and causing damage. In blood plasma, iron is carried in the "pockets" of the iron transport protein transferrin. It only gets unwrapped once it is inside special cellular organelles. Further, researchers have shown that transferrin can clump together to form wormlike fibrils (Sadler *et al*., 2008). The researchers showed that most of the metal complexes Zn(II), Cu(II), Co(II) and Ni(II) with imidazole derivative were more active than the neat ligand,

against *Eschereschi coli*, *Pseudomonas aeruginosa, Klesbiella pneumonia and Staphylococcus aureus* pected (Rehman *et al*., 2010). Short oxo-titanium (IV) bond in bacterial transferring has been reported as a protein target for metalloantibiotics (Guo *et al*., 2006). Nickel and copper complexes of ethambutol having octahedral geometry showed anti-tubercular activity (Annapurna *et al*., 2006).

Researchers reported two qualitative methods for characterizing Au(I)–protein adducts and a photoreactive Au(I) complex that produced a covalent bond between the Au(I) complex and the biomolecule(Karver and Barrios 2008). The palladium(II) and platinum(II) complexes with fluoroquinolones (ciprofloxacin, levofloxacin, ofloxacin, sparfloxacin, and gatifloxacin) showed activity against *Mycobacterium tuberculosis* strain H37Rv (Vieira *et al*., 2009). Complexes of antibiotics (a polymyxin/colistin/aminoglycoside,) and metals were found useful in detecting bacteria and other biological analytes, particularly Gram-negative bacteria (Olstein and Feirtag, 2001). A solid dosage form of a doxycycline metal complex has been reported (deVries and Gold, 2009). Gentamicin known adverse side effects to the kidney and the inner ear resulted from complex formation of gentamicin with Co, Ni, and Cd with square planar arrangement around the metal ions (Mishra and Sharma, 2008).

The toxic side effects of synthetic drugs may, in part, be arising due to their interactions with essential metal ions, especially when the metal ions are administered along with the drug as mineral supplements. Researchers reported the interaction between ranitidine and calcium(II), magnesium(II), and iron(II) ions and between levothyroxine and copper(II) and iron(II) ions at the physiological pH values 1.5, 7.4, and 8.0 and the concentrations of the drugs and mineral supplements used were comparable to those in their usual doses (Sridevi and Mohammed, 2007). The possible binding modes between duplex oligonucleotides and metallocomplexes were reported (Anichina and Bohme, 2009). Scientists have reported the role of metal ions, especially iron, in the action of antibiotics employed in anticancer chemotherapy (Petering *et al*., 2004).

Advances in the screening for antiproliferative potential of organotins have been reported (Hadjikakou and Hadjiliadis, 2009). Vancomycin was conjugated to a

hydrolysis catalyst (or TACzyme). Targeted hydrolysis by such a conjugate was observed using membranes containing lipid II. MIC-values of targeted hydrolysis catalyst constructs could be modulated by Zn(II) (Bauke Albada, 2009).It has been reported that tungsten compounds mimic the action of insulin in intact cell systems. Low concentration (0.1 mM) of sodium tungstate, tungstophosphoric acid, and tungstophosphoric acid dissolved in 2% DMSO could be the good candidates for *in vivo* investigation of their antidiabetic properties (Topic *et al*., 2010).

Synthesis, characterization and cytotoxic activity of gallium(III) complexes anchored by tridentate pyrazole based ligands has been reported (Silva *et al*., 2010). Ga has been reported as a potentially promising new therapeutic for *P.aeruginosa* infections as it can substitute for Fe in many biologic systems and inhibit Fe-dependent processes (Kaneko *et al*., 2007). Periodontal disease can be treated by the administration of metal ions, preferably silver ions, to the site where the microorganisms that cause this disease residue.

Administration can be to periodontal pockets or adjacent to exposed tooth roots or alveolar bone during periodontal surgical procedures (Roberts *et al.,* 2000). The nuclease activity and antibacterial activity of fluoroquinolones metal complexes were compared to free fluoroquinolones (Serafin and Stanczak, 2009). Biomimetic systems containing one or two zinc(II) ions supported by phenolate ligands developed as functional mimics of metallo-beta-lactamase catalytically hydrolyzed beta-lactam substrates, such as oxacillin and penicillin G. (Tamilselvi *et al*., 2006). Bismuth-fluoroquinolone complexes have the potential to be developed as drugs against *H. pylori* related ailments (Shaikh *et al*., 2009). Copper(II) bis arginate [Cu(l-arg)$_2$](NO_3)$_2$(1) and [Cu(l-arg)(phen)Cl]Cl(2) as mimics of the minor-groove-binding natural antibiotic netropsin showed preferential binding to the ATrich region of double-stranded DNA. The complexes with a d-d band near 600 nm displayed oxidative DNA cleavage activity on photoirradiation at UV-A light of 365 nm and at red light of 647.1 nm (Ar”Kr laser) in a metal-assisted photoexcitation process forming singlet oxygen (1O2) species in a type-2 pathway (Patra *et al*., 2007). [Cu(arginine)$_2$](NO3)$_2$ mimics the minor groove binder netropsin by showing preferential binding to the AT-rich sequence of doublestrand (ds) DNA showed efficient DNA photocleavage activity (Patra *et al*., 2009).

The opportunistic pathogen *Pseudomonas aeruginosa* causes infections that are difficult to treat by antibiotic therapy. This bacterium can cause biofilm infections where it shows tolerance to antibiotics. The novel use of a metallo-complex, desferrioxamine-gallium (DFO-Ga) that targets *P. aeruginosa* iron metabolism has been reported. This complex kills free-living bacteria and blocks biofilm formation. A combination of DFO-Ga and the anti-*Pseudomonas* antibiotic gentamicin caused massive killing of *P. aeruginosa* cells in mature biofilms. In a *P.aeruginosa* rabbit corneal infection, topical administration of DFO-Ga together with gentamicin decreased both infiltrate and final scar size by about 50% compared to topical application of gentamicin alone. The use of DFO-Ga as a Trojan horse delivery system that interferes with iron metabolism showed promise as a treatment for *P.aeruginosa* infections (Banin *et al*., 2008). Iron (III) Schiff base complexes of arginine and lysine as netropsin mimics showed ATselective DNA binding and plasmid DNA cleavage activity in visible light (Ameerunisha *et al*., 2010).

Dimers of vancomycin linked by a rigid metal complex, $[Pt(en)(H_2O)_2]^{2+}$, exhibited potent activities (MIC 0.8 mcg/mL, 720 times more potent than that of vancomycin itself) against vancomycin-resistant enterococci ,thereby, suggesting that combining metal complexation and receptor/ligand interaction offers a useful method to construct multivalent inhibitors (Xing *et al*., 2003). A series of Co (II), Cu (II), Ni (II) and Zn (II) complexes of modified mercaptothiadiazole compared to the prepared un-complexed Schiff bases against four Gram-negative, *Escherichia coli*, *Pseudomonas aeruginosa*, *Salmonella typhi* and *Shigella flexneri*, and two Gram-positive *Bacillus subtilis* and *Staphylococcus aureous* bacterial strains were reported (Chohan et al.2006). Silver nanoparticles coated on common polyurethane foams can be used as a drinking water filter to control bacterial contamination of the surface water. Nanoparticles were found stable on the foam and were not washed away by water. Moreover, morphology of the foam was retained after coating. The nanoparticle bind with the nitrogen atom of the polyurethane foams. At a flow rate of 0.5 L/min, in which contact time was of the order of a second, the output count of *Escherichia coli* was nil when the input waterhad a bacterial load of 105 colony-forming units (CFU) per mL (Jain and Pradeep, 2005).Schiff base-derived sulfonamides metal [Co(II), Cu(II), Ni (II) and Zn (II)]complexes showed moderate to significant *in-vitro* antibacterial activity against six Gramnegative; *E. coli, K. pneumoniae,*

P. aeruginosa, *P.mirabilis*, *S. typhi* and *S. dysenteriae* and four Grampositive; *B. cereus*, *C. diphtheriae*, *S. aureus* and *S.pyogenes* bacterial strains and for *in-vitro* antifungal activity against *T. longifusus*, *C. albicans*, *A. flavus*, *M.canis*, *F. solani*, and *C. glaberata*. However, the zinc (II) complexes were found to be more active. Some of the compounds also showed significant antifungal activity,and cytotoxic activity against *Artemia salina*. The X-raystructure of 4-[(2-hydroxybenzylidene) amino] benzenesulfonamide was also reported (Chohan, 2008).

Several families of individual copper complexes have been studied as potential antitumor agents and these investigations, revealed the occurrence of mechanisms of action quite different from platinum drugs (Tisato *et al*., 2010). A method of administering cobalt (III) compound having the formula $CoR_1R_2R_3R_4R_5R_6$ or a salt thereof and an antibiotic compound.Each of R_1,R_2,R_3,R_4 and R_5 is the same or different and includes an N-based ligand donor atom selected from the group consisting of ammonia, primary amine, or secondary amine, or salt thereof. R_6 is a ligand] to a subject diagnosed as needing a broad spectrum antibiotic was reported (Chang *et al*., 2010). A solid dosage form of a metal complex of tetracycline for pharmaceutical administration has been proposed wherein R1 = Cl, $N(CH_3)_2$, or H; R_2 = CH_3, H, or CH_2=;R_3 = CH_3, H, OH, or absent; and R_4 = OH or H, with the provison that if R_2 is CH_3 and R_3 is H, then R_4 is not OH. *Punica granatum* L. (Punicaceae) referred to in English as pomegranates, have antimicrobial activity against a range of both Gram positive and Gram negative bacteria (Navarro *et al*., 1996; Holetz *et al*., 2002; Mathabe *et al*., 2006; Melendez and Capriles 2006 and Prashanth *et al*., 2001). The addition of vitamin C markedly enhanced the activities of both pomegranates/Fe (II) and pomegranates /Cu (II) combinations against *S. aureus*, thereby, validating the exploration of pomegranates along with additives such as metal salts and vitamin C as novel antimicrobial combinations (McCarrell *et al*., 2008).

2.10 Mixed antibiotics metal complexes

In vivo evaluation of the biological studies of the mixed antimalarial metal complexes and free ligands showed greater activity against some of the micro-organisms, when compared to the parent compounds. Toxicological studies revealed that mefloquine, chloroquine and Ni(Mef)(CQ)Cl_2 may have affected the plasma membrane integrity of the cells and were toxic to the tissues, while the mixed metal complexes of

mefloquine and chloroquine ($Co(Mef)(CQ)Cl_2$ and $Fe(Mef)(CQ)Cl_3$) would be a better therapeutic drug for malaria (Adediji *et al*., 2009). Mixed ligand metal complexes of chloramphenicol and oxytetracycline prepared by using Ni(II), Co(II) and Fe(III) metal chloride were screened for their antibacterial activity against isolated strains of *Escherichia coli*, *Staphylococcus aureus* and *Klebsiella pneumonia* by using diffusion method. The activity data showed the metal complexes to be more potent antibacterial than the parent drugs against the three species (Ogunniran et al.2008). Some new mixed ligand complexes of type ML B (M(II)=Mn(II), Co(II), Ni(II), Cu(II) and Zn(II); HL'= ovanillidene-2-aminobenzothiazole; B= 1,10-phenanthroline) and Schiff base metal complexes of types (ML 2) and (M 2 L) (HL= *o*-vanillidene-2-amino-N-(2-pyridyl)-benzene sulfonamide) synthesized and characterized by elemental analysis and spectral (IR, 1 H NMR and 13 C NMR) studies showed more potent *in vitro* biological activities against bacteria, fungi and yeast as compared with Schiff base ligands (Neelakantan *et al*., 2010).

Stability constant and thermodynamic parameters of Cd^{2+} complexes with sulfonamide (sulfadiazine, sulfisoxazole, sulfamethaxazole, sulfamethazine, sulfathiazole, sulfacetamide and sulfanilamide) as primary ligands and cephapirin as secondary ligand were determined by polarographic technique at pH = 7.30 ±0.01 and μ = 1.0 M KNO_3 at 250 ^{0}C. Cd^{2+} formed 1:1:1, 1:2:1 and 1:1:2 complexes (Parihar and Khan 2008). A mixed copper complex with deprotonated nalidixic acid (nal) and histamine (hsm) was synthesized and characterized by FTIR, UV-Vis, elemental analysis, and conductivity. The crystal structure of $[Cu(hsm)(nal)H_2O]Cl\cdot 3H_2O$ (chn) showed a pentacoordinated cooper(II) in a square pyramidal geometry surrounded by two N atoms from hsm, two O atoms from the quinolone, and one apical water oxygen. Alteration of bacterial DNA structure and/or associated functions *in vivo* by $[Cu(hsm)(nal)H_2O]Cl\cdot 3H_2O$ was demonstrated by the induction of a *recA-lacZ* fusion integrated at the *amyE* locus of a recombinant *Bacillus subtilis* strain. Results from circular dichroism and denaturation of calf thymus DNA (CT-DNA) suggested that increased amounts of copper complex were able to stabilize the double helix of DNA *in vitro* mainly by formation of hydrogen bonds between chn and the sugars of DNA minor groove. Complexes of the quinolone family drugs with copper coordinated to other amines may be active, even if the nuclease activity is not present as in those complexes with phenantroline (Bivian *et al*., 2009).

2.11 References

Abuhijleh AL. Mononuclear and binuclear copper (II) complexes of the anti-inflammatory drug ibuprofen: Synthesis, characterization and catecholase-mimetic activity. J Inorg Biochem 1994;55:255-262.

Adediji JF, Olayinka ET, Adebayo MA, Babatunde O. Antimalarial mixed ligand metal complexes: Synthesis, physicochemical and biological activities. Int J Phys Sci 2009;4:529-534.

Afanaseva IB, Ostrakhovitch EA, Mikhalchik EV, Ibragimova GA, Korkina LG. Enhancement of antioxidant and anti-inflammatory activities of bioflavonoid rutin by complexation with transition metals. Biochem Pharmacol 2001;61:677-684.

Allardyce CS, Dyson PJ, Ellis DJ, Health SL Ru (p-cymene) Cl2 (pta). A water soluble compound that exhibits pH dependent DNA binding providing selectivity for diseased cells. Chem commun 2001:1396-1397.

Allen HK, Donato J, Wang HH, Cloud-Hansen KA, Davies J Handelsman J. Call of the wild: antibiotic resistance genes in natural environments. Nature Rev Microbiol 2010;8:251-259.

Altmeyer MA, Marschner A, Schiffmann R, Klein CD. Subtype-selectivity of metal-dependent methionine aminopeptidase inhibitors. Bioorgan Med Chem Lett 2010; 20:4038-4044.

Ameerunisha Begum MS, Saha S, Nethaji M, Chakravarty AK. Iron(III) Schiff base complexes of arginine and lysine as netropsin mimics showing AT-selective DNA binding and photonuclease activity. J Inorg Biochem 2010;104:477-484.

Anacona JR, Da Silva G. Synthesis and antibacterial activity of cefotaxime metal complexes J Chil Chem Soc 2005;50:447-450.

Anderberg PI, Harding MM, Luck IJ, Turner P. Ruthenium complexes of analogues of the antitumor antibiotic streptonigrin. Inorg Chem 2002; 41;1365-1371.

Anichina J, Bohme DK. Mass-spectrometric studies of theinteractions of selected metalloantibiotics and drugs with deprotonated hexadeoxynucleotide GCATGC. J Phys Chem B 2009;113:328-335.

Annapurna MM, Bhanoji Rao ME, Ravi Kumar BVV. Synthesis, spectral characterization and evaluation ofpharmacodynamic activity of copper and nickel complexes of ethambutol dihydrochloride. E-Journal Chem 2006;3:274-277.

Anne V, Micheal H, Elizebeth A. Hillard, Emmanuel S. Selective estrogen receptor modulators in the Ruthenocene series. J Med Chem 2005;48:2814-2821.

Antonarakis ES, Emadi A. Ruthenium-based chemotherapeutics: are they ready for prime time? Cancer Chemother Pharmacol. 2010; 66(1):1-9.

Artsimovitch I, Vassylyeva MN, Svetlov D, Svetlov V, Perederina A, Igarashi N, et al. Allosteric modulation of the RNA polymerase catalytic reaction is an essential component of transcription control by rifamycins. Cell 2005;122:351–363.

Arya DP. Aminoglycoside antibiotics: from chemical biology to drug discovery. Wiley-Interscience, Hoboken, New Jersey 2007.

Bahe AR, Classen J, Williams B. Pp. 89-108 in Animal Agriculture and the Environment: National Center for Manure and Animal Waste Management White Papers. J. M. Rice, D. F. Caldwell, F. J. Humenik, eds. 2006. St. Joseph, Michigan: ASABE.

Bahrami-Samani A, Ghannadi-Maragheh M, Jalilian AR, Mazidi M. Biological studies of samarium-153 bleomycin complex in human breast cancer murine xenografts for therapeutic applications. Radiochim Acta 2010;98:237-242.

Baker-Austin C, Wright MS, Stepanauskas R, McArthur JV. Co-selection of antibiotic and metal resistance. Trends Microbiol 2006;14:176-182.

Banin E, Lozinski A, Brady KM, et al, The potential of desferrioxamine-gallium as an anti-Pseudomonas therapeutic agent. Proc Nat Acad Sci USA 2008;105:16761–16766.

Bao Y, Herrin DL. Mg2+ mimicry in the promotion of group I ribozyme activities by aminoglycoside antibiotics. Biochem Biophys Res Commun 2006;344;1246-1252.

Bartkowiak D, Stempfhuber M, Wiegel T, Bottke D. Radiation and chemoinduced multidrug resistance in colon carcinoma cells. Strahlenther Onkol 2009;185:815-820.

Bauke Albada H, Arnusch CJ, Branderhorst HM, Verel AM, Janssen WTM, Breukink E, et al. Potential scorpionate antibiotics: Targeted hydrolysis of lipid II containing model membranes by vancomycin–TACzyme conjugates and modulation of their antibacterial activity by Zn ions. Bioorg Med Chem Lett 2009;9:3721-3724.

Beckford FA. Reaction of the anticancer organometallic ruthenium compound, [ç6-p-Cymene)Ru(ATSC)Cl] PF6 with human serum albumin. Int J Inorg Chem 2010; Volume 2010 Article ID 975756, 7 pages.

Belousoff MJ, Ung P, Forsyth CM, Tor Y, Spiccia L, Graham B. New acrocyclic terbium(III) complex for use in RNA footprinting experiments. J Amer Chem Soc 2009;131:1106-1114.

Birch NJ. In: Lithium: Inorganic pharmacology and psychiatric use. Oxford: IRL Press.1988.

Bivián-Castro EY, López MG, Pedraza-Reyes M, Bernès S, Mendoza-Díaz G. Synthesis, characterization, and biological activity studies of copper(II) mixed compound with histamine and nalidixic acid. Bioinorg Chem Appl 2009; 2009: 603651.

Burger RM. Nature of activated bleomycin, Struct Bond. 2000;97:287-303.

Carter BJ, Reddy KS, Hecht SM. Polynucleotide recognition and strand scission by Fe- bleomycin. Tetrahedron. 1991;47:2463-2474.

Cary Tuckfield R, Vaun McArthur J. Spatial analysis of antibiotic resistance along metal contaminated streams. Microbial Ecol 2008;55:595-607.

Chai SC, Ye QZ. Metal-mediated inhibition is a viable approach for inhibiting cellular methionine aminopeptidase. Bioorg Med Chem Lett 2009;19:6862-6864.

Chaires JB, Waring MJ. Drug-nucleic acid interactions. Met Enzymol. San Diego, CA: Academic Press 2001;340.

Chakrabarti S, Makrigiorgos G, O'Brien K, Bump E, Kassis A. Measurement of hydroxyl radicals catalyzed in the immediate vicinity of DNA by metal-bleomycin complexes, Free Rad Biol Med 1996;20:777-783.

Chang CH, Meares. C. F. Cobalt-bleomycins and deoxyribonucleic acid: Sequence-dependent interactions, action spectrum for nicking, and indifference to oxygen. Biochemistry 1984;23:2268-2274.

Chang EL, Zabetakis D, Knight A, Van Hoek ML. Cobaltamine based metal complex as an antibacterial compound. United States Patent Application 20100004187, 01/07/2010.

Chen W. Interactions of tetracycline antibiotics with dissolved metal ions and metal oxides. Ph.D Dissertation, School of Civil and Environmental Engineering, Georgia Institute of Technology, 2008.

Chen WR, Ding Y, Johnston CT, Teppen BJ, Boyd SA, Li H. Reaction of lincosamide antibiotics with manganese oxide in aqueous solution. Environ Sci Technol 2010;44: 4486-4492.

Chohan ZH, Pervez H, Rauf A, Khan KM, Supuran CT. Antibacterial cobalt (II), copper (II), nickel (II) and zinc (II) complexes of mercaptothiadiazole—derived furanyl, thienyl, pyrrolyl, salicylyl and pyridinyl Schiff bases. J Enzyme Inhib Med Chem 2006;21:193-201.

Chohan ZH. Metal-based antibacterial and antifungal sulfonamides: synthesis, characterization, and biological properties. Trans Metal Chem 2009; 34:153-161.

Chohan ZH. Metal-based sulfonamides: Their preparation, characterization and in-vitro antibacterial, antifungal & cytotoxic properties. X-ray structure of 4-[(2-hydroxybenzylidene) amino] benzenesulfonamide. J Enz Inhib Med Chem 2008;23:120-130.

Chu DT, W. Hallas R, Clement JJ, Alder L, McDonald E, Plattner J. Synthesis and antitumor activities of quinolone antineoplastic agents, Drugs Exp Clin Res 1992;18:275–282.

Clarke MJ. Ruthenium metallopharmaceuticals. Coord Chem 2003;236:299-233.

Claussen CA, Long EC. Nucleic acid recognition by metal complexes of bleomycin. Chem Rev 1999; 99;2797–2816.

Darvesh S, Reid GA, Martin E. Biochemical and histochemical comparison of cholinesterases in normal andalzheimer brain tissues. Curr Alzheimer Res 2010;7: 386-400.

David SA, Balasubramanian KA, Mathan VI, Balaram P. Analysis of the binding of polymyxin B to endotoxic lipid A and core glycolipid using a fluorescent displacement. Probe Biochim Biophys Acta 1992;1165:145-152.

Devi PG, Chakraborty PK, Dasgupta D. Inhibition of a Zn(II)- containing enzyme, alcohol dehydrogenase, by anticancer antibiotics, mithramycin and chromomycin A3. J Biol Inorg Chem 2009;14:347-359.2009

deVries T, Gold L. Doxycycline metal complex in a solid dosage form , United States Patent 7485319, 02/03/2009.

Dorkov P, Pantcheva IN, Sheldrick WS, Mayer-Figge H, Petrova R, Mitewa M. Synthesis, structure and antimicrobial activity of manganese(II) and cobalt(II) complexes of the polyether ionophore antibiotic Sodium Monensin A. J Inorg Biochem 2008;102:26-32.

Duda AM, Kowalik-Jankowska T, Kozlowski H, Kupka T. Histamine H-2 antagonists-Powerful ligands for copper (II)- reinterpretation of the famotidin-copper (II) system. J Chem Soc Dalton Trans 1995;2909-2913.

Elsea SH, Westergaard M, Burden DA, Lomenick JP, Osheroff N. Quinolones share a common interaction domain on topoisomerase II with other DNA cleavage-enhancing antineoplastic drugs, Biochemistry 1997;36:2919-2924.

Falagas ME, Grammatikos AP, Michalopoulos A. Potential of old-generation antibiotics to address current need for new antibiotics. Expert Rev Anti Infect Ther 2008; 6:593-600.

Fan JY, Sun D, Yu H, Kerwin SM, Hurley LH. Self-assembly of a quinobenzoxazine-Mg2+ complex on DNA: A new paradigm for the structure of a drug-DNA complex and implications for the structure of the quinolone bacterial gyrase-DNA complex. J Med Chem 1995;38:408-424.

Feklistov A, Mekler V, Jiang Q, Westblade LF, Irschik H, Jansen R, et al. Rifamycins do not function by allosteric modulation of binding of Mg2+ to the RNA polymerase active center. Proc Natl Acad Sci USA 2008;105:14820-14825.

Galanski M, Arion VB, Jakupec MA, Keppler BK. Recent development in the field of tumor inhibiting metal complexes. Curr Pharm 2003;9:2078-2080.

Gokhale N, Patwardhan A, Cowan JA. Metalloaminoglycosides: chemistry and biological relevance. Chapter 8,pp 235-254. In: Dev P. Arya (ed.) Aminoglycoside antibiotics: from chemical biology to drug discovery. John Wiley & Sons, Inc, 2007.pp 235-254.

González JM, Medrano Martín FJ, Costello AL, Tierney DL,Vila AJ . The Zn2 position in metallo-â-lactamases is critical for activity: A study on chimeric metal sites on a conserved protein scaffold. J Mol Biol 2007;373:1141-1156.

Grollman AP, Takeshita M, Pillai KMR, Johnson F. Origin and cytotoxic properties of base propenals derived from DNA. Cancer Res 1985;45:1127–1131.

Guo M, Harvey I, Campopiano DJ, Sadler PJ. Short oxotitanium(IV) bond in bacterial transferrin: A protein target for metalloantibiotics. Angew Chem 2006; 118:2824 – 2827.

Guo W, Siegel D, Ross D, Stability of the Hsp90 inhibitor 17AAG hydroquinone and prevention of metal-catalyzed oxidation. J Pharma Sci 2008;97:5147-5157.

Guschlbauer W, Saenger W, DNA-ligand interactions: From drugs to proteins NATOASI Series, Series A, Life Science, New York, Plenum. 1987;Vol. 137

Hadjikakou SK, Hadjiliadis N. Antiproliferative and antitumor activity of organotin compounds. Coord Chem Rev 2009;253:235-249.

Hannon MJ. Metal–based anticancer drugs: From a past anchored in platinum chemistry to a postgenomic future of diverse chemistry and biology. Pure Appl Chem 2007;79:2243-2261.

Hawk MJ, Breece RM, Hajdin CE,. Bender KM, Hu Z , Costello AL, Bennett B, Tierney DL, Michael W. Crowder MW. Differential binding of Co(II) and Zn(II) to metalloâ- lactamase Bla2 from bacillus anthracis. J Amer Chem Soc 2009;131:10753-10762.

Hernick M, Fierke C. Mechanisms of metal-dpendent hydrolases in metabolism. Comprehensive Natural Products II, 2010, pp 547-581.

Hinton JF, Koeppe RE II. Complexing properties of gramicidins. Metal Ions Biol Syst 1985;19:173-206.

Hoffken G, Borner K, Glatzel PD, Koeppe P, Lode H. Reduced enteral absorption of ciprofloxacin in the presence of antacids. Eur J Clin Microbiol Infect Dis 1985;4:345-345.

Holetz FB, Pessini GL, Sanches NR, Cortez DAG, Nakamura CV, Filho BPD. Screening of some plants used in the Brazilian folk medicine for the treatment of infectious diseases. Memórias do Instituto Oswaldo Cruz 2002;97:1027-1031.

Hou MH, Wang AHJ. Mithramycin forms a stable dimeric complex by chelating with Fe(II): DNA-interacting characteristics, cellular permeation and cytotoxicity. Nucleic Acids Res 2005 ;33:1352-1361.

Huang M, Xie SX, Ma ZQ, Hanzlik RP, Ye QZ. Metal mediated inhibition of methionine aminopeptidase by quinolinyl sulfonamides. Biochem Biophys Res Commun 2006;339:506-513.

Jain P, Pradeep IT. Potential of silver nanoparticle-coated polyurethane foam as an antibacterial water filter. Biotechnol Bioeng 2005; 90:59-63.

Jalilian AR, Fateh B, Ghergherehchi M, Karimian A, Matlloobi M. Preparation, distribution, stability and tumor imaging properties of [62Zn] bleomycin complex in normal and tumor-bearing mice. Iran J Radiat Res 2003;1:37-44

Jamieson ER, Lippard SJ (1999). Structure, Recognition and processing of cisplatin DNA adducts. Chem Rev 1999;99:2467-2498;

Jezowska-Bojczuk M, Bal W, Kasprzak KS. Copper (II) interactions with an experimental antiviral agent, I-deoxynojirimycin, and oxygen activation by resulting complexes. J Inorg Biochem 1996;63:231-239.

Jezowska-Bojczuk M, Bal W, Kozlowski H. Kanamycin revisited: A combined potentiometric and spectroscopic study of copper (II) binding to kanamycin B. Inorg Chim Acta 1998a;275-276:541-545.

Jezowska-Bojczuk M, Karaczyn A, Bal W. Copper (II) binding to geneticin, a gentamycin analog. J Inorg Biochem 1998 c;71:129-134.

Jezowska-Bojczuk M, Karaczyn A, Kozlowski H. Copper (II) binding to tobramycin: Potentiometric and spectroscopic studies. Carbohy Res 1998 b.;313:265-269.

Kamala-Kannan S, Lee KJ. Metal tolerance and antibiotic resistance of bacillus species isolated from sunchon bay sediments, South Korea. Biotechnology 2008;7:149-152.

Kane SA, Hecht SM. Polynucleotide recognition and degradation by Bleomycin. Prog Nucl Acids Res Mol Biol 1994;49:313-352.

Kaneko Y, Thoendel M, Olakanmi O, Britigan BE, Singh PK. The transition metal gallium disrupts Pseudomonas aeruginosa iron metabolism and has antimicrobial and antibiofilm activity. J Clin Investig 2007;117:877-888.

Karver MR, Barrios AM. Identifying and characterizing the biological targets of metallotherapeutics: Two approaches using Au(I)–protein interactions as model systems. Anal Biochem 2008;382:63-65.

Kasparkova J, Suchankova T, Halamikova A, Zerzankova L, Vrana O, Margiotta N, et al. Cytotoxicity, cellular uptake, glutathione and DNA interactions of an antitumor largering PtII chelate complex incorporating the cis-1,4- diaminocyclohexane carrier ligand. Biochem Pharmacol 2019;79:552-564.

Kiat HC, Weng KL, Gerard J, Lawrence L, Siden T, Anne V. Organometallic cluster analogues of tamoxifen. J Organomet Chem 2006;69:9-19.

Kim SK , Sims CL , Wozniak SE , Drude SH, Whitson D, Shaw RW. Antibiotic resistance in bacteria: Novel metalloenzyme inhibitors. Chem Biol Drug Design 2009;74:343-348.

Kirkova M, Atanassova M, Russanov E. Effects of cimetidine and its metal complexes on nitroblue tetrazolium and ferricytochrome-c reduction by superoxide radicals. Gen Pharmacol 1999;33:271-276.

Kontoghiorghes GJ, Efstathiou A, Ioannou-Loucaides S, Kolnagou A. Chelators controlling metal metabolism and toxicity pathways: applications in cancer prevention, diagnosis and treatment. Hemoglobin 2008;32:217-227.

Kwok Y, Zeng Q, Hurley LH. Structural insight into a quinolone– topoisomerase II-DNA complex. Further evidence for a 2:2 quinobenzoxazine-Mg2+ self-assembly model formed in the presence of topoisomerase II. J Biol Chem 1999;274:17226-17235.

Ladesiae B, Kantoci D, Meider H, Hadzija O. Complexes of Fe(III) with amino sugars and small glycopeptides. J Inorg Biochem 1992;48:55-62.

Lange TS, Kim KK, Singh RK, Strongin RM, McCourt CK, Brard L. Iron (III)-salophene: an organometallic compound with selective cytotoxic and anti-proliferative properties in platinum-resistant ovarian cancer cells. PLoS One 2008;3: 2303-2305.

Lazo JS, Sebti SM, Schellens JH. Bleomycin. Cancer Chemother Biol Resp Modif 1996;16:39-47.

Lecomte S, Moreau NJ, Chenon MT. NMR investigation of pefloxacin-cation-DNA interactions: The essential role of $Mg2^{+}$. Int J Pharm 1998;164:57-65.

Lee K-B, Wang D, Lippard SJ, Sharp PA. Transcriptioncoupled and DNA damage-dependent ubiqitinition of RNA polymerase II *in vitro*. Proc Natl Acad Sci USA 2002;99:4239-4244.

Levine C, Hiasa H, Marians K. DNA gyrase and topoisomerase IV: Biochemical activities, physiological roles during chromosome replication, and drug sensitivities, Biochim. Biophys Acta 1998;1400:29-43.

Li P, Li J, Wu C, Wu Q, Li J. Synergistic antibacterial effects of â-lactam antibiotic combined with silver nanoparticles. Nanotechnology 2005;16:1912-1915.

Liang XJ, Chen C, Zhao Y, Wang PC. Circumventing tumor resistance to chemotherapy by nanotechnology Methods. Mol Biol 2010;596:467-488.

Long GV, Harding MM, Fan JY, Denny WA. Interaction of the antitumor antibiotic streptonigrin with DNA and oligonucleotides. Anti-Cancer Drug Design 1997;12:453-472.

Lu WJ, Wang HM, Yuann JMP, Huang CY, Hou MH. The impact of spermine competition on the efficacy of DNAbinding Fe(II), Co(II), and Cu(II) complexes of dimeric chromomycin A(3). J Inorg Biochem 2009;103:1626-1633.

Magliozzo RS, Peisach J, Ciriolo MR. Transfer RNAis cleaved by activated bleomycin. Mol Pharmocol 1989;35:428-432.

Marina S, Chow, LeiVLiu, Edward I, Solomon. Further insights into the mechanism of the reaction of activated bleomycin with DNA. Proc Natl Acad Sci 2008;105:13241-13245.

Masterson JG. Anti-infective agents, process for their preparation and their use in therapy. European Paten Application EP0408330, 01/16/1991.

Mathabe MC, Nikolova RV, Lall N, Nyazema NZ. Antibacterial activates of medicinal plants used for the treatment of diarrhoeas in Limpopo Province, South Africa. J Ethnopharmacol 2006;105:286-293.

McCarrell EM, Gould SWJ, Fielder MD, Kelly AF, Sankary WE, Naughton DP. Antimicrobial activities of pomegranate rind extracts: enhancement by addition of metal salts and vitamin C. BMC Complementary and Alternative Medicine 2008; 8:64-66.

Melendez PA, Capriles VA. Antibacterial properties of tropical plants from Puerto Rico. Phytomed 2006;13:272-276.

Mendoza-Diaz G, Perez-Alonso R, Moreno-Esparza R. Stability constants of copper (II) mixed complexes with some 4-quinolone antibiotics and (N–N) donors. J Inorg Biochem 1996;64:207-214.

Merryfield ML, Lardy HA. Inhibition of phosphoenolpyruvate carboxykinase by streptonigrin. Biochem Pharmacol 1982;31:1123-1129.

Miethke M, Marahiel MA. Siderophore-based iron acquisition and pathogen control Microbiol Mol Biol Rev 2007;71:413-451.

Mikkelsen NE, Johansson K, Virtanen A, Kirsebom LA. Aminoglycoside binding displaces a divalent metal ion in a tRNAneomycin B complex. Nat Struct Biol 2001;8:510–514.

Miller MJ, Zhu H, Xu Y, Wu C, Walz AJ, Vergne A, et al. Utilization of microbial iron assimilation processes for the development of new antibiotics and inspiration for the design of new anticancer agents. Biometals 2009;22:61-75.

Ming LJ, Epperson JD. Metal binding and structure–activity relationship of the metalloantibiotic peptide bacitracin. J Inorg Biochem 2002; 91: 46-58.

Mishra P, Sharma RK. Gentamicin complexes of cobalt(II),nickel(II), cadmium(II) and tin(II). Main Group Chemistry 2008;7:83-95.

Mitani Y, Sato K, Muramoto Y, Karakawa T, Kitamado M, Iwanaga T, et al. Superoxide scavenging activity of pirfenidone–iron complex. Biochem Biophys Res Commun 2008;372:19-23.

Monti E, Paracchini L, Piccinini F, Malatesta V, Morazzoni F, Supino R. Cardiotoxicity and antitumor activity of a copper(II)-doxorubicin chelate. Cancer Chemotherapy and Pharmacology 1990;25:333-336.

Mota de Freitas D. Alkali metal nuclear magnetic resonance. Meth Enzymol 1993;227:78-106.

Muranaka H, Suga M, Sato K, Nakagawa K, Akaike T, Okamoto T, Maeda H, Ando M. Superoxide scavenging activity of erythromycin-iron complex. Biochem Biophys Res Commun 1997;232:183-187.

Muranaka H, Suga M, Sato K, Nakagawa K, Akaike T, Okamoto T, Maeda H, Ando M. Superoxide scavenging activity of erythromycin-iron complex. Biochem Biophys Res Commun 1997;232:183-187.

Nacsa J, Nagy L, Molnar J, Molnar J. Trifluoperazine and its metal complexes inhibit the moloney leukemia virus reverse transcriptase. Anticancer Res 1998:18:1373-1376.

Najajreh Y, Perez JM, Navarroo-Ranninger C, Gibsin D. Novel soluble cationic trans-diaminedichloroplatinum (II) complexes that are active against cisplatin resistant ovarian cancer cell lines. J Med Chem 2002;45:5189-5195.

Najma Sultana, N, Arayne S, Sabri R. Erythromycin synergism with essential and trace elements. Pak J Pharm Sci 2005;18:35-39.

Navarro V, Villarreal ML, Rojas G, Lozoya X: Antimicrobial evaluation of some plants used in Mexican traditional medicine for the treatment of infectious diseases. J Ethnopharmacol 1996;53:143-147.

Neelakantan MA, Esakkiammal M, Mariappan SS, Dharmaraja J, Jeyakumar T. Synthesis, characterization and biocidal activities of some schiff base metal complexes. Indian J Pharm Sci 2010;72:216-222.

Ogunniran KO, Ajanaku KO, James OO, Ajani OO, Adekoya JA, Nwinyi OC. Synthesis, characterization, antimicrobial activity and toxicology study of some metal complexes of mixed antibiotics. African J Pure Appl Chem 2008;2:69-74.

Ogunniran KO, Ajanaku KO, James OO, Ajani OO, Nwinyi CO, Omonhimin CA, et al. Synthesis, physical properties, antimicrobial potentials of some mixed antibiotics complexed with transition metals and their effects on alkaline phosphatise activities of selected rat tissues. Sci Res Essay 2008;3:348-354.

Oka T, Hashizume K, Fujita H. Inhibition of peptidoglycan transpeptidase by beta-lactam antibiotics structure-activity relationships. J Antibiot 1980;33:1357-1362.

Olstein A, Dfeirtag JM. (Antibiotic-metal complexes in the detection of Gram-negative bacteria and other biological analytes, WO/2001/027628), 19.04.2001.

Olstein AD, Feirtag J. Antibiotic-metal complexes in the detection of gram-positive bacteria and other biological analytes. Patent: 20050026813, 02/03/2005.

Orvig C, Abrams MJ. Medicinal inorganic chemistry: Introduction. Chem Rev 1999;99:2201-2204.

Palm GJ, Lederer T, Orth P, Saenger W, Takahashi M, Hillen W, Hinrichs W. Specific binding of divalent metal ions to tetracycline and to the Tet repressor/tetracycline complex. J Biol Inorg Chem 2008;13:1097-1110.

Palu G, Valisena S, Ciarrocchi G, Gatto B, Palumbo M. Quinolone binding to DNA is mediated by magnesium ions. Proc Nat Acad Sci, USA.1992;89:9671-9675.

Pantcheva IN, Dorkov P, Atanasov VN, Mitewa M, Shivachev BL, Nikolova RP, Mayer-Figge H, Sheldrick WS. Crystal structure and properties of the copper(II) complex of sodium monensin A. J Inorg Biochem 2009;103:1419-1424.

Pantcheva IN, Mitewa MI, Sheldrick WS, Oppel IM, Zhorova R, Dorkov P. First divalent metal complexes of the polyether ionophore Monensin A: X-Ray structures of [Co(Mon)2(H2O)2] and [Mn(Mon)2(H2O)2] and their bactericidal properties. Curr Drug Discov Technol 2008;5:154-161.

Pantcheva IN, Zhorova R, Mitewa M, Simova S, Mayer-Figge H, Sheldrick WS. First solid state alkaline-earth complexes of monensic acid A (MonH): crystal structure of [M(Mon)2(H2O)2] (M = Mg, Ca), spectral properties and cytotoxicity against aerobic Gram-positive bacteria. Biometals 2010;23:59-70.

Parihar MS, Khan F. Stability constants and thermodynamic parameters of cadmium complexes with sulfonamides and cephapirin. Eclet Quím 2008;33: 29-34.

Parker MW, Pattus F, Tucher AD, Tsernoglou D. Structure of the membrane-pore-forming fragment of colicin-A. Nature 1989;337:93-96.

Patra AK, Bhowmick T, Roy S, RamakumarS, Chakravarty AR. Copper(II) complexes of l-arginine as netropsin mimics showing DNA cleavage activity in red light. Inor Chem 2009;48: 2932-2943.

Patra AK, Bhowmick T, Roy S, RamakumarS, Chakravarty AR. Metal-based netropsin mimics showing AT-selective DNA binding and DNA cleavage activity at red light. Inorg Chem 2007;46:9030-9032.

Peltier E, Vincent J, Finn C, Graham DW. Zinc-induced antibiotic resistance in activated sludge bioreactors. Water Res 2010;44:3829-3836.

Petering DH, Xia C, Antholine WE. Metal ion dependent antibiotics in chemotherapy. In: Metal complexes in tumor diagnosis and as anticancer agents. Sigel A, Sigel H Eds. CRC Press, 2004, Chapter 14, pp 463-498.

Petrukhin OM, Kostitsyna MV, Dzherayan TG, Shipulo EV, Vladimirova EV, AA. Dunaeva. Complexation of aminoglycoside antibiotics with metal cations as a derivatization reaction: Determination of gentamicin by equilibrium electrochemical and spectrophotometric methods. J Anal Chem 2009; 64:951-957.

Piacham T, Isarankura-Na-Ayudhya C, Nantasenamat C, Yainoy S, Ye L, Bülow L, et al. Metalloantibiotic Mn(II)– bacitracin complex mimicking manganese superoxide dismutase. Biochem Biophys Res Commun 2006;341:925-930.

Pizarro AM, Sadler PJ. Unusual DNA binding modes for metal anticancer complexes. Biochimie 2009;91:1198-1211.

Prashanth D, Asha MK, Amit A. Antibacterial activity of Punica granatum. Fitoterapia 2001;72:171-173.

Priuska EM, Schacht J. Formation of free radicals by gentamycin and iron and evidence for an iron/gentamycin complex. Biochem Pharmacol 1995.50:1749-1752.

Rafique S, Idrees M, Anwar Nasim, Akbar H, Athar A. Transition metal complexes as potential therapeutic agents. Biotechnol Mol Biol Rev 2010;5:38-45.

Rao EA, Saryan LA, Antholine WE, Petering DH. Cytotoxic and antitumor properties of bleomycin and several of its metal complexes. J Med Chem 1980;23;1310-1318.

Ray S, Mohan R, Singh JK, Samantaray MK, Shaikh MM, Panda D, et al. Anticancer and antimicrobial metallopharmaceutical agents based on palladium, gold, and silver N-heterocyclic carbene complexes. J Am Chem Soc 2007;144:125-127.

Reedijk J. Medicinal applications of metal complexes binding to biological macromolecules Macromolecular Symposia 2008;270:193-201.

Rehman SR, Ikram M, Rehman S, Faiz A, Shahnawaz. Synthesis, characterization and antimicrobial studies of transition metal complexes of imidazole derivative. Bull Chem Soc Ethiop 2010;24;201-207.

Roberts FD, Friden PM, Spacciapoli P, Nelson E. Use of locally delivered metal ions for treatment of periodontal disease. Patent 6153210, November 28, 2000.

Sadler PJ. Inorganic chemistry and drug design. Adv Inorg Chem1991;36:1-48.

Sadler PJ. Periodic iron nanomineralization in human serum transferrin fibrils. Angew Chem Int Ed 2008;47:2221-2231.

Samaha-Kfoury JN, George F, Araj GF. Recent developments in ß-lactamases and extended spectrum ß-lactamases. BMJ 2003;327:1209-1213.

Sanchez-del Grado RA, Navarro M, Perez H, Urbina JA. Toward a novel metal-based chemotherapy against tropical diseases: Synthesis and antimalarial activity in vitro and in vivo of new ruthenium- and rhodium-chloroquine complexes. J Med Chem 1996;39:1095-1099.

Saraiva R, Lopes S, Ferreira M, Novais F, Pereira E, Feio MJ, et al. Solution and biological behaviour of enrofloxacin metalloantibiotics: A route to counteract bacterial resistance? J Inorg Biochem 2010;104:843-850.

Sausville EA, Peisacti J, Horwitz B. Effect of chelating agents and metal ions on the degradation of DNA by bleomycin. Biochemistry 1978;17: 2740-2746.

Serafin A, Stañczak A. The complexes of metal ions with fluoroquinolones. Russ J Coord Chem 2009; 3:81-95.

Shaikh AR, Giridhar R, Megraud F, Yadav MR. Metalloantibiotics: Synthesis, characterization and antimicrobial evaluation of bismuth-fluoroquinolonec omplexes against He icobacterpylori. Acta Pharm 2009;59:259–271.

Shi Y, Harvey I, Campopiano D, Sadler PJ. Niobium uptake and release by bacterial ferric ion binding protein. Bioinorg Chem Applications 2010;Volume 2010, Article ID 307578, 11 pages.

Silva DO. Perspectives for novel mixed diruthenium-organic drugs as metallopharmaceuticals in cancer therapy. Anticancer Agents Med Chem 2010;10:312-323.

Silva F, Marques F, Santos IC, Paulo A, Rodrigues AS, Rueff J, et al. Synthesis, characterization and cytotoxic activity of gallium(III) complexes anchored by tridentate pyrazolebased ligands. J Inorg Biochem 2010;104:523-532.

Sissi C, Andreolli M, Cecchetti V, Fravolini A, Gatto B, Palumbo M. Mg2+-mediated binding of 6-substituted quinolones to DNA: Relevance to biological activity. Bioorg Med Chem 1998;6:1555-1561.

Smith JT. Awakening the slumbering potential of the 4-quinolone Antibacterials. Pharm J 1984;233:299-305.

Sreedhara A, Cowan JA. Catalytic hydrolysis of DNA by metal ions and complexes. J Biol Inorg Chem 2001;6:337-347.

Sreedhara A, Patwardhan A, Cowa, JA. Novel reagents for targeted cleavage of RNA sequences: Towards a new family of inorganic pharmaceuticals. Chem Commun 1999;1147-1148.

Sridevi N, Mohammed Yusuff KK. Rapid in vitro screening of drug–metal ion interactions. Toxicol Mech Methods 2007;17:559-565.

Sultana N, Arayne MS. In vitro activity of cefadroxil, cephalexin, cefatrizine and cefpirome in presence of essential and trace elements. Pak J Pharm Sci 2007;20:305-310.

Sun RW, Ma DL, Wong EL, Che CM. Some uses of transition metal complexes as anti-cancer and anti-HIV agents. Dalton Trans 2007;43:4884-4892.

Supuran CT, Scozzafava A, Saramet I, Banciu MD. Carbonic anhydrase inhibitors: Inhibition of isozymes I, II, and IV with heterocyclic mercaptans, sulfenamides, sulfonamides, and their metal complexes. J Enzy Inhib 1998;13:177-194.

Takeshita M, Grollman AP, Ohtsubo E, Ohtsubo H. Interaction of bleomycin with DNA. Proc Nat Acad Sci 1978;75:5983-5987.

Takeshita M, Horwitz SB, Grollman AP. Bleomycin, an inhibitor of vaccinia virus replication. Virology 1974;60:455-456.

Tamai K, Kawate K, Kawahara I, Takakura Y, Sakaki K. Inorganic antimicrobial coating for titanium alloy and its effect on bacteria. J Orthopaedic Sci 2009;14;204-209.

Tamilselvi A, Mugesh G. Zinc and antibiotic resistance: metallo-beta-lactamases and their synthetic analogues. J Biol Inorg Chem 2008;13:1039-1053.

Tamilselvi A, Nethaji M, Mugesh G. Antibiotic resistance: Mono- and dinuclear zinc complexes as metallo-betalactamase mimics. Chemistry-A Eur J 2006;12:7797 -7806.

Tan M, Zhu J, Pan Y, Chen Z, Liang H, Liu H, et al. Synthesis, cytotoxic activity, and DNA binding properties of copper (II) complexes with hesperetin, naringenin, and apigenin. Bioinorg Chem Appl 2009; 2009: 347872.

Tioni MF, Llarrull LI, Poeylaut-Palena AA, Mart MA, Saggu M, Periyannan GR, et al. Trapping and characterization of a reaction intermediate in carbapenem hydrolysis by B. cereus metallo-â-lactamase. J Amer Chem Soc 2008;130:15852-15863.

Tisato F, Marzano C, Porchia M, Pellei M, Santini C. Copper in diseases and treatments, and copper-based anticancer strategies. Med Res Rev 2010;30:708-749.

Top S, Vessières A, Leclercq G, Quivy J, Tang J, Vaissermann J, et al. Synthesis, biochemical properties and molecular modelling studies of organometallic specific estrogen receptor modulators (SERMs), the ferrocifens and hydroxyferrocifens: Evidence for an antiproliferative effect of hydroxyferrocifens on both hormone-dependent and hormone-independent breast cancer cell lines. Chemistry, a Eur J 2003;9: 5223-5236.

Topic A, Milenkovic M, Uskokovic-Markovic S, Vucicevic D. Insulin mimetic effect of tungsten compounds on isolated rat adipocytes. Biol Trace Elem Res 2010;134:296-306.

Tornaletti S, Pedrini AM. Studies on the interaction of 4-quinolones with DNA by DNA unwinding experiments. Biochim Biophys Acta 1988;949:279-287.

Tullius TD. In: Metal-DNA Chemistry. ACS Symposium Series, The Amer Chem Soc 1989;402.

Turel I, Bukovec N. Complex formation between some metals and a quinolone family member (ciprofloxacin). Polyhedron.1996;15:269-275.

Turel I, Leban I, Bukovec N. Synthesis, characterization, and crystal structure of a Copper (II) complex with quinolone family member (ciprofloxacin): Bis (1-cyclopropyl-6-fluoro-1,4-dihydro-4-oxo-7-piperazin-1-yl quinoline-3-carboxylate) copper(II) chloride hexahydrate. J Inorg Biochem 1994;56:273–282.

Turel I, Leban I, Klintschar G, Bukovec N, Zalar S. Synthesis, crystal structure, and characterization of two metal-quinolone compounds. J Inorg Biochem 1997;66:77-82.

Umadevi B, Muthiah PT, Shui X, Eggleston DS. Metal-drug interactions: Synthesis and crystal structure of dichlorodithiabendazolecobalt (II) monohydrate. Inorg Chim Acta1995;234:149-152.

Umezawa H, Maeda K, Takeuchi T, Okami Y. New antibiotics,bleomycin A and B.J Antibiot 1966;19:200-209.

Umezawa H, Takita T. The bleomycins: Antitumor copper-binding Antibiotics. Struct Bond 1980;40:73-99.

Underhill AE, Bougourd SA, Flugge ML, Gale SE, Gomm PS. Metal complexes of anti-inflammatory drugs. Part VIII, Suprofen complex of copper (II). Inorg Biochem 1993;52:139-144.

Underhill AE, Bury A, Odling RJ, Fleet MB, Stevens A, Gomm PS. Metal complexes of antiinflammatory drugs. Part VII: Salsalate complex of copper (II). J Inorg Biochem 1989;37:1-5.

Urbaniak B, Kokot ZJ. Analysis of the factors that significantly influence the stability of fluoroquinolone-metal complexes. Anal Chim Acta 2009;647:54-59

Vaun McArthur J, Cary Tuckfield R. Spatial patterns in antibiotic resistance among stream bacteria: Effects of industrial pollution. Appl Environ Microbiol 2000;66:3722-3726.

Vieira LMM, de Almeida MV, LourençoCS M, BezerraFAFM, Fontes APS. Synthesis and antitubercular activity of palladium and platinum complexes with fluoroquinolones. Eur J Med Chem 2009;44:4107-4111.

Wegener HC. 2003. Antibiotics in animal feed and their role in resistance development. Curr Opin Microbiol 2003;6:439-445.

Wei X, Ming LJ(a). NMR studies of metal complexes and DNA binding of the quinone-containing antibiotic streptonigrin. J Chem Soc Dalton Trans1998;2793-2798.

Wolfson JS, Hooper DC, In: Quinolone antimicrobial agents, Washington, DC: American Society for Microbiology 1993.

Wu L, Serpersu EH. Deciphering interactions of the aminoglycoside phosphotransferase(3')-IIIa with its ligands. Biopolymers 2009;91:801-809.

Xing B, Yu CW, Ho PL, Chow KH, Cheung T, Gu H, et al. Multivalent antibiotics via metal complexes: Potent divalent vancomycins against vancomycin-resistant Enterococci. J Med Chem 2003;46:4904-4909.

Yan S, Ding K, Zhang L, Sun H. Complexation of antimony (III) by Trypanothione. Angew Chem Int Ed 2000;39:4260-4262.

Yan-Guo Ren, Javier Martínez, Leif A Kirsebom, et al. Inhibition of Klenow DNA polymerase and poly(A)- specific ribonuclease by aminoglycosides. RNA 2002; 8:1393-1400.

Youngs WJ, Tessier CA, Garrison J, Quezada C Melaiye A, Panzner M, et al. Metal complexes of N-heterocyclic carbenes as radiopharmaceuticals and antibiotics. USPC Class 2010;424:169.

CHAPTER III
AIM OF PRESENT WORK

3.1 AIM OF PRESENT WORK

Tinidazole (tnz) is a therapeutic agent of choice for amoebiasis (Barnhost *et al.,* 1996) and also used in combination with other antimicrobial drugs against yeast infections (Rasmussen *et al.,* 1997). Under anaerobic conditions inside the cell, it is reduced to a cytotoxic nitro radical and binds nonspecifically to the organism's DNA and enzymes, which are thus inactivated (Edwards 1993, Castelli *et al.,* 1997, Sigeti *et al.,* 1983, Muller, 1983 and Shaw, 1999). High doses or long-term administration of tnz can cause a peripheral neuropathy with sensory disturbances and the emergence of resistance to this drug is known in many pathogenic bacteria and protozoa. Other available drugs have their own limitations and today parasite resistance is also a global problem.

Metal based drugs such as Au (I) complexes (e.g., auranofin) have been used successfully for the treatment of various diseases (Rhodes *et al.,* 1992; Best and Sadler 1996; Farrell 1989 and Mirabelli *et al.,* 1985) including P_{38} leukemia (Sadler and Sue 1994 and Matesanz *et al.,* 1999). Many neutral palladium (II) and palladium (IV) complexes were found to exhibit potential antitumour activity (Quiroga *et al.,* 1998, Sanchez *et al.,* 1996). Moreover, Ru complexes of chloroquine act as potential antimalarial agents against *P. falciparum* (Bharti *et al.,* 2002). So it was well-known that coordination of metal ion has a positive effect on drug efficacy.

A series of Pd, Pt, Cu, Au, and Ru complexes of metronidazole (mnz) were prepared (Bharti *et al.,* 2002 and Athar *et al.,* 2005) by the reaction of $[PdCl_2(DMSO)_2]$, $[PtCl_2(DMSO)_2]$, $[Cu(OAc)_2] \cdot H_2O$, $CuCl_2 \cdot 2H_2O$, $[Au(PPh_3)Cl]$, and $RuCl_3 \cdot 3H_2O$ with metronidazole, which led to the formation of $[PdCl_2(mnz)_2]$, $[PtCl_2(mnz)_2]$,$[Cu_2(OAc)_4(mnz)_2]$,$Cu(mnz)_2Cl)(H_2O)]2Cl_2$,$[Au(PPh3)(mnz)]PF_6$ and $Ru(mnz)_2(Cl)_2(H_2O)_2]$ respectively in 52-80% yield. The copper and palladium mnz complexes were considerably superior to others and demonstrated higher activity, which proved the fact that metal incorporation enhances the drug activity. Bharti et

al.(Bharti et al.2002)reported the in vivo antiamoebic activity of metronidazole metal complexes $[PdCl_2(mnz)_2]$, $[PtCl_2(mnz)_2]$ and $[Cu_2(OAc)_4(mnz)_2]$ in male golden hamsters infected by amoeba shows good activity.The above study has increased the thrust to develop the complexes related to tinidazole analogues.

In the present work the 2-substutituted nitroimidazole (tinidazole and dimetridazole) analogues were prepared and then complexed with the various transition metals like nickel, copper, cobalt, cadmium.

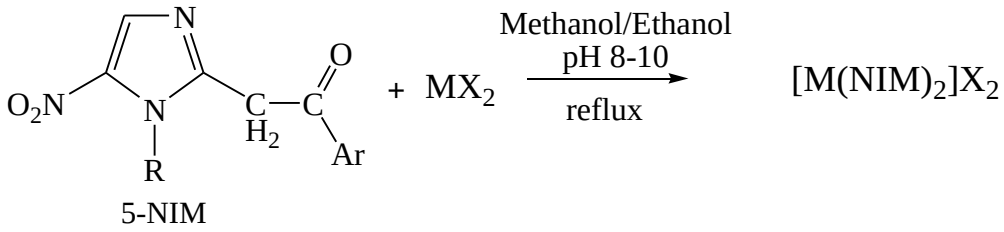

5-NIM

Ar = phenyl, *p*-cl phenyl, *m*-cl phenyl,
o-cl phenyl, furoyl

R = $-CH_3$, $-CH_2CH_2SO_2CH_2CH_3$

3.2 References

Athar F, Husain K, Abid M, Agarwal SM, Coles SJ, Hursthouse MB, Maurya MR, Azam A. Chem Biodi Vers 2005;2:1320-1325.

Barnhost DA, Jr. Foster JA, Chern KC, Meisler DM. Technology of eye drops containing metronidazole. Ophthalmology 1996;103:1880-1885.

Best SL, Sadler PJ. Recent Advances in the Chemistry of Gold(I) Complexes with C-, N- and S-Donor Ligands Part II: Sulfur Ylide, Hydrosulfido, Sulfido, Trithiocarbonato, Dithiocarbimato and 1,1-Ethylenedithiolato Derivatives. Gold Bull 1996;29: 87-92.

Bharti N, Shailendra Coles SJ, Hursthouse MB,Mayer TA,Gonzalez Garza MT,Cruz-Vega DE, Mata-Cardenas BD, Naqvi F, Maurya MR, Azam A. 1-Hydroxyethyl-2-methyl-5-nitroimidazolium 3-carboxy-4-hydroxybenzenesulfonate HelV Chim Acta 2002;85:2704-2408.

Castelli M, Malagoli M, Ruberto AI, Baggio A,Casolari C Carmelli C, Bossa MR, Rossi T, Paolucci F, Roffia SJ. Synthesis and Anti-Amoebic Activity of Gold(I), Ruthenium(II), and Copper(II) Complexes of Metronidazole Antimicrob Chemother 1997;40:19-24.

Edwards DI. Nitroimidazole drugs--action and resistance mechanisms. I. Mechanisms of action. J Antimicrob Chemother 1993;31:9-12.

Farrell N. Transition Metal Complexes as Drugs and Chemotherapeutic Agents. In Catalysis by Metal Complexes; James BR, Ugo R, Eds Kluwer: Dordrecht. The Netherlands.1989.

Matesanz AI, Perez JM, Navarro P, Moreno JM, Colocio E, Sauza PJ. Synthesis and characterization of palladium(II) complexes of thioureas. X-ray structures of [Pd(N , N'-dimethylthiourea)$_4$]$Cl_2 \cdot 2H_2O$ and [Pd(tetramethylthiourea)$_4$]Cl_2. Inorg Biochem 1999;76:29-32.

Mirabelli CK, Johnson RK, Song CM, Fancette L,Muirhead K, Crooke ST. Antitumor activity of bis(diphenylphosphino)alkanes, their gold(I) coordination complexes, and related compounds Cancer Res. 1985; 45:32-35.

Muller M. Mode of action of metronidazole on anaerobic bacteria and protozoa. Surgery. 1983;93:165-175.

Quiroga AG, Perez JM, Montero EI, Masaguer JR,Alons C, Navarro-Ranninger C. Palladated and platinated complexes derived from phenylacetaldehyde. J Inorg Biochem 1998;70:117-124.

Rasmussen BA, Bush K, Tally FP. Beta-lactamase production in anaerobic bacteria Clin Infect Dis 1997;24:5110-5120.

Rhodes MD, Sadler PJ, Scawen MD, Silyer S. Effects of gold(I) antiarthritic drugs and related compounds on Pseudomonas putida. J Inor Biochem 1992, 46, 129-139.

Sadler PJ, Sue RE. Synthesis and Structural Characterization of *N*-Heterocyclic Carbene Gold (I) Complexes. Met-Based Drugs 1994;1:107-115.

Sanchez-Delgado RA, Navarro M, Perez H, Urbina J. J Med Chem 1996;39:1095-1099.

Shaw CF. Gold (III) Compounds as Anticancer DrugsIII Chem ReV.1999;99:2589-2596.

Sigeti JS, Guiney DG, Jr. Davis CE. Mechanism of action of metronidazole on Bacteroides fragilis. J Infect Dis1983;148:1083-1087.

CHAPTER IV

SYNTHESIS OF LIGAND

INTRODUCTION

A number of 5-nitoimidazole with substitution at 2-position with various substitutes are reported recently, exhibited 100 and 50-fold increase in activity than metronidazole. In the present study the 5- nitroimidazoles like tinidazole and dimetridazole molecule is thought to be modified at 2- position.

4.1 Results and Discussion

Synthesis of 2-(1-(substituted)-5-nitro-1*H*-imidazol-2-yl)-1-(substituted) ethanone

2-(1-(substituted)-5-nitro-1H-imidazol-2-yl)-1-(substituted) ethanone **(3)** was synthesized by activation of 2-position methyl group of **(1)** by base and subsequent reaction with acid chlorides afforded **(2)** as intermediate which upon acidic hydrolysis yields the desired product (Albright et al., 1973)

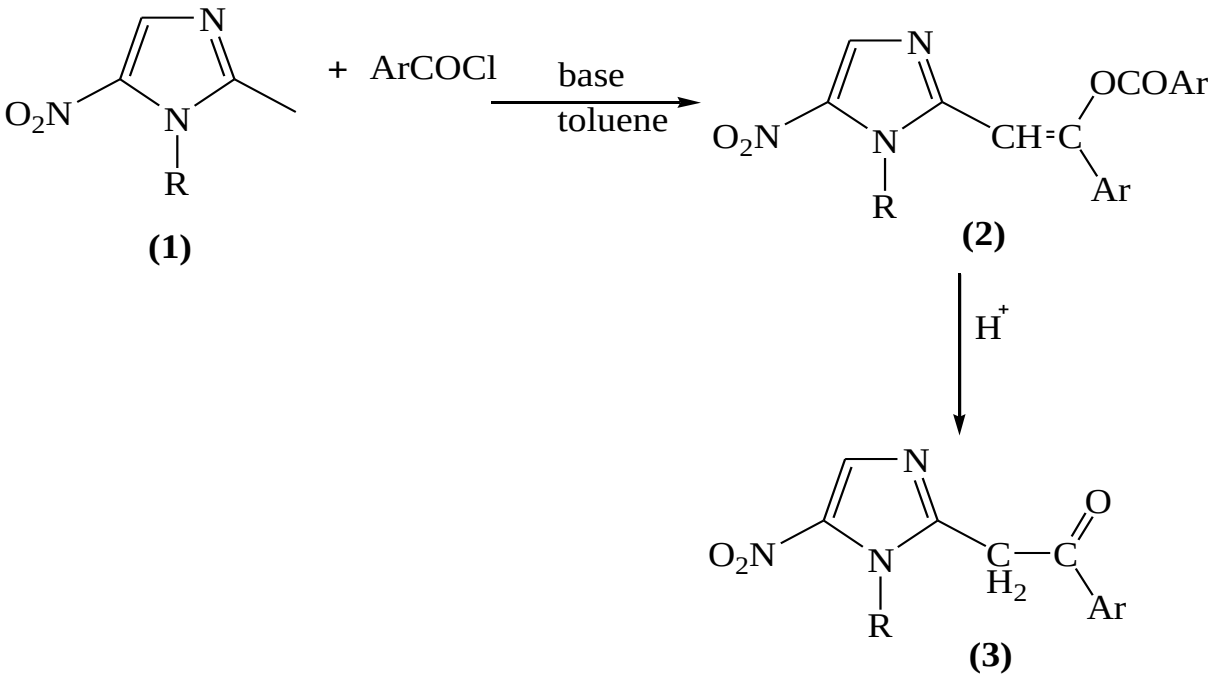

(1) **(2)** **(3)**

R = CH_3, $CH_2CH_2SO_2C_2H_5$
Ar = phenyl, *p*-chlorophenyl, *m*-chlorophenyl, *o*-chlorophenyl, furoyl

SCHEME I

4.2 Physical and spectral characteristics

All the compounds were pale yellow to yellow in color and soluble in dichloromethane, chloroform and partially soluble in methanol and ethanol. All the compounds were recrystallized from ethanol.

4.2.1 IR spectra (KBr, cm^{-1})

Peak around 3000-2800cm^{-1} was observed signify the presence CH_2. Intense absorption band around 1720-1680cm^{-1} indicates the presence of the carbonyl group. All the compounds show stretching of NO_2 1560, 1350$cm^{-1.}$

4.2.2 ^{1}H NMR spectra (DMSO-d6, δ ppm)

The ^{1}H NMR (DMSO-d_6) spectra of 2-(1-(substituted)-5-nitro-1H-imidazol-2-yl)-1-(substituted) ethanone, displays the triplet of methyl group (-$SO_2CH_2\underline{CH_3}$) resonates at δ 1.28-1.40 ppm, quartet of methylene group (-$SO_2\underline{CH_2}CH_3$) resonates at δ 3.15 ppm, triplet for(- $CH_2\underline{CH_2}SO_2CH_2CH_3$) resonates at δ 3.66-3.89 ppm, singlet for (-N=C-$\underline{CH_3}$) resonates at δ 4.26-4.30, triplet for (imidazole-$\underline{CH_2}CH\ _2SO_2CH_2CH_3$) resonates at δ 4.96 ppm, all the aromatic proton resonates between δ 6.54-7.94 , the singlet for (1H nitroimidazole ring) observed between δ 7.87-8.1ppm.

4.2.3 Mass spectra (m/z)

The molecular ions, M+1, M+2 were observed. The fragmentation routes primarily involved losses of NO (M-30), NO_2 (M-46) and HNO_2 (M-47) from the molecular ion, which are characteristic of compounds. The possible fragmentation of nitroimidazole is shown below;

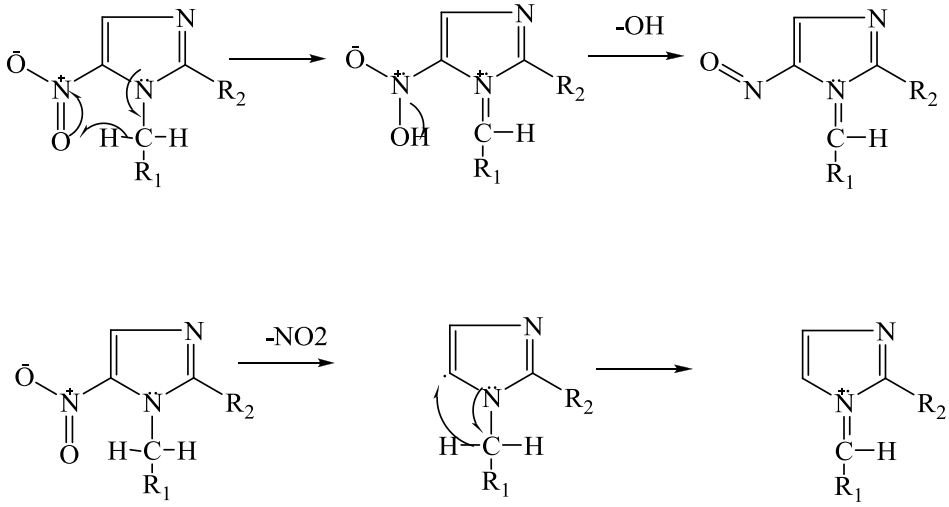

Table 1: Physical characteristics of 2-(1-(substituted)-5-nitro-1H-imidazol-2-yl)-1-(substituted)ethanone

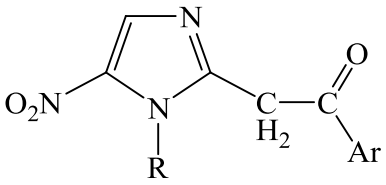

(3)

code	R	Ar	m.p. (^{0}C)	Yield (%)*	Mol. formula	Mol. weight
3-a	$-CH_2CH_2SO_2C_2H_5$	phenyl	146-148	80	$C_{15}H_{17}N_3O_5S$	351.38
3-b	$-CH_2CH_2SO_2C_2H_5$	*p*-Cl-phenyl	152-154	72	$C_{15}H_{16}ClN_3O_5S$	385.82
3-c	$-CH_2CH_2SO_2C_2H_5$	*m*-Cl-phenyl	156-158	65	$C_{15}H_{16}ClN_3O_5S$	385.82
3-d	$-CH_2CH_2SO_2C_2H_5$	*o*-Cl-phenyl	180-182	45	$C_{15}H_{16}ClN_3O_5S$	385.82
3-e	$-CH_2CH_2SO_2C_2H_5$	furoyl	165-166	75	$C_{13}H_{15}N_3O_6S$	341.34
3-f	$-CH_3$	furoyl	130-132	78	$C_{10}H_9N_3O_4$	235.20
3-g	$-CH_3$	phenyl	136-138	80	$C_{12}H_{11}N_3O_3$	245.08

*Solvent of recrystallization; methanol – chloroform

4.3 Experimental

- All the melting points were determined in open capillaries and are uncorrected.
- Thin layer chromatography was performed on microscopic slides (2x7.5cm) coated with silica gel G and spots were visualized by normal TLC and exposure to iodine vapour.
- IR spectra were recorded in KBr on SHIMADZU Fourier Transform Infrared 8400S spectrophotometer.
- Mass spectra were recorded on Micromass Q-T , TOF MS $ES^{+}4.73e^{3}$
- Nuclear Magnetic Resonance spectra (^{1}H NMR) were recorded in DMSO-d_6 on BRUKER AVANCE II at 400 MHz and the chemical shift are given in parts per million, downfield from Tetramethyl silane (TMS) was used as internal standard.

Synthesis of 2-(1-(2-(ethylsulfonyl)ethyl)-5-nitro-1*H*-imidazol-2-yl)-1-phenylethanone (3-a) (Molvi et al, 2006)

To a mixture of 4.94 g (0.020 mole) of 1-(2-(ethylsulfonyl)ethyl)-2-methyl-5-nitro-1H-imidazole **(1)**, 17.5 ml of toluene and 8.09g (0.080 mole) of triethylamine was added with occasional cooling 7.7 g (0.55 mole) of benzoyl chloride. The mixture was stirred for 22 hr, diluted with 10 ml of ether and chilled. The mixture was filtered and solid washed with three 10 ml portions ether and four 10 ml portion water. The whole crude product was taken in to 10 ml of water, 15 ml of ethanol and 10 ml of concentrated hydrochloric acid and refluxed for 2-4 hours. The solution was chilled and poured on to the ice. The solid was filtered, washed with water and recrystallized from ethanol gave 2-(1-(2-(ethylsulfonyl)ethyl)-5-nitro-1*H*-imidazol-2-yl)-1-phenylethanone **(3-a)**, m.p. 146-148 ^{0}C.

Analysis:

TLC	: Toluene: acetonitrile (4:1); Rf value: 0.67
IR (KBr, cm^{-1})	:2977-2800 (CH_2-streching), 1720 (C=O), 1560,1365 (C-NO_2)
NMR (δ, ppm, DMSO-d_6)	:δ 1.28 (t, 3H, -$SO_2CH_2\underline{CH_3}$), δ 3.15 (q, 2H, -$SO_2\underline{CH_2}CH_3$), δ 3.89 (t, 2H, -$CH_2\underline{CH_2}SO_2CH_2CH_3$), δ 4.26 (s, 3H, N=C-$\underline{CH_3}$), δ 4.96 (t, 2H, imidazole-$\underline{CH_2}CH\ _2SO_2CH_2CH_3$), δ 7.56-7.94 (m, 4H, Ar-$\underline{H}$), δ 7.81 (s,1H, nitroimidazole ring)
Mass	: 351.38 (M+1)

Synthesis of 1-(4-chlorophenyl)-2-(1-(2-(ethylsulfonyl)ethyl)-5-nitro-1*H*-imidazol-2-yl)ethanone (3-b)

To a mixture of 4.94 g (0.020 mole) of 1-(2-(ethylsulfonyl)ethyl)-2-methyl-5-nitro-1H-imidazole **(1)**, 17.5 ml of toluene and 8.09g (0.080mole) of triethylamine was added with occasional cooling 9.62 g (0.055 mole) of *p*-chlorobenzoyl chloride. The mixture was stirred for 24hr, diluted with 10 ml of ether and chilled. The mixture was filtered and the solid washed with three 10 ml portions ether and four 10 ml portion water. The whole crude product was taken in to 10 ml of water, 15 ml of ethanol and 10 ml of concentrated hydrochloric acid was refluxed for 2-4 hours. The solution was

chilled and poured on to the ice. The solid was filtered, washed with water and recrystallized from ethanol gave 1-(4-chlorophenyl)-2-(1-(2-(ethylsulfonyl)ethyl)-5-nitro-1H-imidazol-2-yl)ethanone **(3-b)**, m.p. 152-154 ^{0}C.

Analysis:

TLC	: Toluene: acetonitrile (4:1); Rf value: 0.69
IR (KBr, cm^{-1})	:2977-2800 (CH_2-streching), 1720 (C=O), 1560,1365 (C-NO_2)
NMR (δ , ppm)(DMSO-d_6)	:δ 1.28 (t, 3H, -$SO_2CH_2\underline{CH_3}$), δ 3.15 (q, 2H, -$SO_2\underline{CH_2}CH_3$), δ 3.66 (t, 2H, -$CH_2\underline{CH_2}SO_2CH_2CH_3$), δ 4.26 (s, 3H, N=C-$\underline{CH_3}$), δ 4.96 (t, 2H, imidazole-$\underline{CH_2}CH\ _2SO_2CH_2CH_3$), δ 7.60-7.84 (m, 5H, Ar-$\underline{H}$), δ 7.87 (s,1H, nitroimidazole ring)
Mass	: 385.82 (M)

Synthesis of 1-(3-chlorophenyl)-2-(1-(2-(ethylsulfonyl)ethyl)-5-nitro-1*H*-imidazol-2-yl)ethanone (3-c)

To a mixture of 4.94 g (0.020 mole) of 1-(2-(ethylsulfonyl)ethyl)-2-methyl-5-nitro-1*H*-imidazole **(1)**, 17.5 ml, of toluene, and 8.09g (0.080mole) of triethylamine was added with occasional cooling 9.62 g (0.055 mole) of *m*-Chlorobenzoyl chloride. The mixture was stirred for 24hours, diluted with 10 ml of ether and chilled. The mixture was filtered and the solid washed with three 10 ml portions ether and four 10 ml portion water. The whole crude product is taken in to 10 ml of water, 15 ml of ethanol and 10 ml of concentrated hydrochloric acid and refluxed for 2-4 hours. The solution was chilled and poured on to the ice. The solid was filtered and washed with water to give 1-(3-chlorophenyl)-2-(1-(2-(ethylsulfonyl)ethyl)-5-nitro-1*H*-imidazol-2-yl)ethanone **(3-c)**. Recrystallization from ethanol gave yellow crystals, m.p. 156^{0}C - 158^{0}C.

Analysis:

TLC	: Toluene: acetonitrile (4:1); Rf value: 0.62
IR (KBr, cm^{-1})	:2977-2800 (CH_2-streching), 1720 (C=O), 1560,1365 (C-NO_2)

NMR (δ , ppm)(DMSO-d_6)	:δ 1.40 (t, 3H, -$SO_2CH_2\underline{CH_3}$), δ 3.15 (q, 2H, -$SO_2\underline{CH_2}CH_3$), δ 3.66 (t, 2H, -$CH_2\underline{CH_2}SO_2CH_2CH_3$), δ 4.26 (s, 3H, N=C-$\underline{CH_3}$), δ 4.96 (t, 2H, imidazole-$\underline{CH_2}CH\ _2SO_2CH_2CH_3$), δ 7.50-7.86 (m, 4H, Ar-$\underline{H}$), δ 7.87 (s,1H, nitroimidazole ring)
Mass	: 385.82 (M)

Synthesis of 1-(2-chlorophenyl)-2-(1-(2-(ethylsulfonyl)ethyl)-5-nitro-1*H*-imidazol-2-yl)ethanone (3-d)

To a mixture of 4.94 g (0.020 mole) of 1-(2-(ethylsulfonyl)ethyl)-2-methyl-5-nitro-1H-imidazole **(1)**, 17.5 ml of toluene and 8.09g (0.080mole) of triethylamine was added with occasional cooling 9.62 g (0.055 mole) of o-chlorobenzoyl chloride. The mixture was stirred for 36 hr, diluted with 10 ml of ether and chilled. The mixture was filtered and the solid washed with three 10 ml portions ether and four 10 ml portion water. The whole crude product was taken in to 10 ml of water, 15 ml of ethanol and 10 ml of concentrated hydrochloric acid and refluxed for 2-4 hr. The solution was chilled and poured on to the ice. The solid was filtered, washed with water and recrystallized from ethanol gave 1-(2-chlorophenyl)-2-(1-(2-(ethylsulfonyl)ethyl)-5-nitro-1*H*-imidazol-2-yl)ethanone **(3-d)**, m.p. 180-182 ^{0}C.

Analysis:

TLC	: Toluene: acetonitrile (4:1); Rf value: 0.60
IR (KBr, cm^{-1})	:2977-2800 (CH_2-streching), 1720 (C=O), 1560,1365 (C-NO_2)
NMR (δ , ppm)(DMSO-d_6)	:δ 1.38 (t, 3H, -$SO_2CH_2\underline{CH_3}$), δ 3.15 (q, 2H, -$SO_2\underline{CH_2}CH_3$), δ 3.66 (t, 2H, -$CH_2\underline{CH_2}SO_2CH_2CH_3$), δ 4.26 (s, 3H, N=C-$\underline{CH_3}$), δ 4.96 (t, 2H, imidazole-$\underline{CH_2}CH\ _2SO_2CH_2CH_3$), δ 7.44-7.88 (m, 5H, Ar-$\underline{H}$), δ 7.87 (s,1H, nitroimidazole ring)
Mass	: 385.82 (M)

Synthesis of 2-(1-(2-(ethylsulfonyl)ethyl)-5-nitro-1*H*-imidazol-2-yl)-1-(furan-2-yl)ethanone (3-e)

To a mixture of 4.94 g (0.020 mole) of 1-(2-(ethylsulfonyl)ethyl)-2-methyl-5-nitro-1H-imidazole **(1)**, 17.5 ml of toluene and 8.09g (0.080mole) of triethylamine was added with occasional cooling 7.17 g (0.055 mole) of furoyl chloride. The mixture was stirred for 18 hr, diluted with 10 ml of ether and chilled. The mixture was filtered and the solid washed with three 10 ml portions ether and four 10 ml portion water. The whole crude product was taken in to 10 ml of water, 15 ml of ethanol and 10 ml of concentrated hydrochloric acid and refluxed for 2 hr. The solution was chilled and poured on to the ice. The solid was filtered, washed with water and recrystallized from ethanol gave 2-(1-(2-(ethylsulfonyl)ethyl)-5-nitro-1*H*-imidazol-2-yl)-1-(furan-2-yl)ethanone **(3-e)**, m.p. 165-166 ^{0}C.

Analysis:

TLC	: Toluene: acetonitrile (4:1); Rf value: 0.56
IR (KBr, cm^{-1})	:2977-2800 (CH_2-streching), 1720 (C=O), 1560,1365 (C-NO_2)
NMR (δ , ppm)(DMSO-d_6)	:δ 1.40 (t, 3H, -$SO_2CH_2\underline{CH_3}$), δ 3.15 (q, 2H, -$SO_2\underline{CH_2}CH_3$), δ 3.66 (t, 2H, -$CH_2\underline{CH_2}SO_2CH_2CH_3$), δ 4.26 (s, 3H, N=C-$\underline{CH_3}$), δ 4.96 (t, 2H, imidazole-$\underline{CH_2}CH\ _2SO_2CH_2CH_3$), δ 6.54 (d, 1H, 3-furoyl), δ 6.754 (d, 1H, 4-furoyl), δ 7.59(s, 1H, 5-furoyl), δ 7.87 (s,1H, nitroimidazole ring)
Mass	: 341.34 (M)

Synthesis of 1-(furan-2-yl)-2-(1-methyl-5-nitro-1*H*-imidazol-2-yl)ethanone (3-f)

To a mixture of 2.82 g (0.020 mole) of 1,2-dimethyl-5-nitro-1*H*-imidazole **(1)**, 17.5 ml, of toluene and 8.09g (0.080mole) of triethylamine was added with occasional cooling 7.17 g (0.055 mole) of furoyl chloride. The mixture was stirred for 18hr, diluted with 10 ml of ether and chilled. The mixture was filtered and the solid washed with three 10 ml portions ether and four 10 ml portion water. The whole crude product was taken in to 10 ml of water, 15 ml of ethanol and 10 ml of concentrated hydrochloric acid and refluxed for 2-4 hr. The solution was chilled and poured on to

the ice. The solid was filtered, washed with water and recrystallized from ethanol gave 1-(furan-2-yl)-2-(1-methyl-5-nitro-1*H*-imidazol-2-yl)ethanone **(3-f)**, m.p. 130-132 ^{0}C.

Analysis:

TLC	: Toluene: acetonitrile (4:1); Rf value: 0.50
IR (KBr, cm^{-1})	:2977-2800 (CH_2-streching), 1720 (C=O), 1560,1365 (C-NO_2)
NMR (δ , ppm)(DMSO-d_6)	:δ 4.26 (s, 3H, N=C-$\underline{CH_3}$), δ 4.96 (s, 3H, imidazole-$\underline{CH_3}$), δ 6.54 (d, 1H, 3-furoyl), δ 6.754 (d, 1H, 4-furoyl), δ 7.59(s, 1H, 5-furoyl), δ 7.87 (s,1H, nitroimidazole ring)
Mass	: 235.20 (M)

Synthesis of 2-(1-methyl-5-nitro-1*H*-imidazol-2-yl)phenylethanone (3-g)

To a mixture of 2.82 g (0.020 mole) of 1,2-dimethyl-5-nitro-1*H*-imidazole **(1)**, 17.5 ml of toluene and 8.09g (0.080mole) of triethylamine was added with occasional cooling 7.7 g (0.055 mole) of benzoyl chloride. The mixture was stirred for 18hr, diluted with 10 ml of ether and chilled. The mixture was filtered and the solid washed with three 10 ml portions ether and four 10 ml portion water. The whole crude product was taken in to 10 ml of water, 15 ml of ethanol and 10 ml of concentrated hydrochloric acid and refluxed for 2-4 hr. The solution was chilled and poured on to the ice. The solid was filtered, washed with water and recrystallized from ethanol gave 2-(1-methyl-5-nitro-1*H*-imidazol-2-yl)phenylethanone **(3-g)**, m.p. 136-138^{0}C.

Analysis:

TLC	: Toluene: acetonitrile (4:1); Rf value: 0.60
IR (KBr, cm^{-1})	:2977-2800 (CH_2-streching), 1720 (C=O), 1560, 1365 (C-NO_2)
NMR (δ , ppm)(DMSO-d_6)	:δ 4.26 (s, 3H, N=C-$\underline{CH_3}$), δ 4.96 (s, 3H, imidazole-$\underline{CH_3}$), δ 7.50-7.86 (5H, Ar-$\underline{H}$), δ 7.87 (s,1H, nitroimidazole ring)
Mass	: 245.08 (M)

4.4 References

Albright DJ and Shepherd RG: Reaction of 1,2-Dimethyl-5-nitroimidazole, Novel methods of conversion of the 2-methyl group to a nitrile. J Het Chem1973;10:899-907.

Molvi KI, Sudarsanam V and Haque N: Synthesis and Antibacterial Activity of Some 2-Substituted Tinidazole Analogues. Ethiop Pharm J 2007;25:35-42.

CHAPTER V

NITROIMIDAZOLE-NICKEL COMPLEXES

5.1 Introduction

Nickel (II) chloride (or just nickel chloride), is the chemical compound $NiCl_2$. The anhydrous salt is yellow, but the more familiar hydrate $NiCl_2 \cdot 6H_2O$ is green. It is very rarely found in nature as mineral nickelbischofite. A dihydrate is also known. In general nickel (II) chloride, in various forms, is the most important source of nickel for chemical synthesis (Pray *et al*., 1990). Nickel salts are carcinogenic. They are also deliquescent, absorbing moisture from the air to form a solution.$NiCl_2$ adopts the $CdCl_2$ structure (Wells, 1984). In this motif, each Ni^{2+} center is coordinated to six Cl^- centers, and each chloride is bonded to three Ni (II) centers. In $NiCl_2$ the Ni-Cl bonds have "ionic character". Yellow $NiBr_2$ and black NiI_2 adopt similar structures, but with a different packing of the halides, adopting the CdI_2 motif.

In contrast, $NiCl_2 \cdot 6H_2O$ consists of separated trans-$[NiCl_2(H_2O)_4]$ molecules linked more weakly to adjacent water molecules. Note that only four of the six water molecules in the formula are bound to the nickel, and the remaining two are water of crystallisation (Wells, 1984). Cobalt (II) chloride hexahydrate has a similar structure (Stucky, 1967).

Many nickel (II) compounds are paramagnetic, due to the presence of two unpaired electrons on each metal center. Square planar nickel complexes are, however, diamagnetic. Nickel (II) chloride solutions are acidic, with a pH of around 4 due to the hydrolysis of the Ni^{2+} ion.

Table 2: Properties of nickel complexes

Complex	Color	Magnetism	Geometry
$[Ni(NH_3)_6]Cl_2$	violet	paramagnetic	octahedral
$NiCl_2(dppe)$	orange	diamagnetic	square planar
$[Ni(CN)_4]^{2-}$	colorless	diamagnetic	square planar
$[NiCl_4]^{2-}$	Yellowish-Brown	paramagnetic	tetrahedral

Most of the reactions ascribed to "nickel chloride" involve the hexahydrate, although specialized reactions require the anhydrous form. Reactions starting from $NiCl_2 \cdot 6H_2O$ can be used to form a variety of nickel coordination complexes because the H_2O ligands are rapidly displaced by ammonia, amines, thioethers, thiolates, and organophosphines. In some derivative, the chloride remains within the coordination sphere, whereas chloride is displaced with highly basic ligands.

Some nickel chloride complexes exist as an equilibrium mixture of two geometries; these examples are some of the most dramatic illustrations of structural isomerism for a given coordination number. For example, $NiCl_2(PPh_3)_2$, containing four-coordinate Ni(II), exists in solution as a mixture of both the diamagnetic square planar and the paramagnetic tetrahedral isomers. Square planar complexes of nickel can often form five-coordinate adducts.

$NiCl_2$ is the precursor to acetylacetonate complexes $Ni(acac)_2(H_2O)_2$ and the benzene-soluble $(Ni(acac)_2)_3$, which is a precursor to Ni(1,5-cyclooctadiene)$_2$, an important reagent in organonickel chemistry. In the presence of water scavengers, hydrated nickel(II) chloride reacts with dimethoxyethane (dme) to form the molecular complex $NiCl_2(dme)_2$. The dme ligands in this complex are labile. For example, this complex reacts with sodium cyclopentadienide to give the sandwich compound nickelocene.

5.2 Results and discussion

5.2.1 Synthetic approach

Synthesis of $[Ni(NIM)_2]Cl_2$

The 2-(1-(substituted)-5-nitro-1*H*-imidazol-2-yl)-1-(substituted)ethanone were reacted in basic condition with nickel chloride under reflux condition yielded $[Ni(NIM)_2]Cl_2$ metal complexes as shown in scheme II.

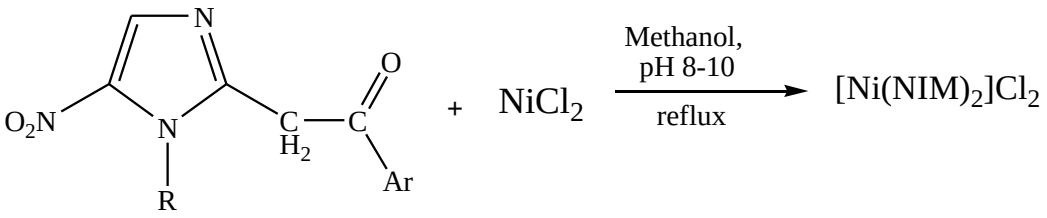

NIM

R = CH_3, $CH_2CH_2SO_2C_2H_5$
Ar = phenyl, *p*-chlorophenyl,
m-chlorophenyl, *o*-chlorophenyl,
furoyl

Scheme II

5.2.2 Physical and Spectral characteristics

All the $[Ni(NIM)_2]Cl_2$ complexes were light to dark brown in color and were soluble in DMSO, DMF and insoluble in all other solvents. The physical data for the complex presented in Table 3 represents percentage yield; melting point / decomposition temperature. The complexes are stable solid with melting point ranging from 220°C - 280°C.

5.2.2.1 IR spectra (KBr, cm^{-1})

Table 4, represents the IR frequencies of C-H streching (3096-2800 cm^{-1}), C=O (2250-2000 cm^{-1}), NO_2 (1570-1540 and 1366-1358 cm^{-1}) and M-O (600-480 cm^{-1}). The IR frequency for ligand and complex was compared; it was found that frequencies for CH_2, NO_2 was matching with peak of complex. The frequency for carbonyl is changed drastically as it is useful band in the infrared spectra of carbonyl ligand in metal complexes was that due to C–O stretching. The later gives very strong sharp bands which are separated from the bands of other ligand that may be present. The stretching wave number for a terminal carbonyl ligand in a complex correlates with the 'electron-richness' of the metal. The band position was determined by the bonding from the *d* orbital of the metal into the π^* anti-bonding Orbitals of the ligand (known as *backbonding*). The bonding weakens the C–O bond and lowers the wave number value from its value in free CO thus its show lower frequency ranging 2250-2000 cm^{-1}. The M-O (metal-oxygen) streching was observed near 600-480 cm^{-1}.

5.2.2.2 UV-Visible spectra (λ max, nm)

The UV spectra reveal three (λ max nm) peaks for the 2-substituted nitroimidazole complexes at 240,256 and 352.

5.2.2.3 Molar conductance (cm^2mol^{-1})

The molar conductance values of the synthesized mixed ligand complexes with the mentioned metal ions under investigation were determined using 10^{-3} M DMF solvent, as shown in Table 5, were in the range of 0.83 - 1.65 cm^2mol^{-1}. These values suggest the presence of a non-electrolyte nature.

5.2.2.4 ^{1}HNMR spectra (DMSO-d_6, δ ppm)

The ^{1}HNMR (DMSO-d_6) spectra of nitroimidazole-nickel complex, displays the triplet of methyl group (-$SO_2CH_2\underline{CH_3}$) resonates at δ 1.28-1.40 ppm, quartet of methylene group (-$SO_2\underline{CH_2}CH_3$) resonates at δ 3.15 ppm, triplet for(-$CH_2\underline{CH_2}SO_2CH_2CH_3$) resonates at δ 3.66-3.89 ppm, singlet for (-N=C-$\underline{CH_3}$) resonates at δ 4.26-4.30, triplet for (imidazole-$\underline{CH_2}CH_2SO_2CH_2CH_3$) resonates at δ 4.96 ppm, all the aromatic proton resonates between δ 6.54-7.94 , the singlet for (^{1}H nitroimidazole ring) observed between δ 7.87-8.1ppm.

5.2.2.5 Mass spectra (m/z)

The molecular ions were observed. The fragmentation routes primarily involved losses of, NO (M-30), NO_2 (M-46) and HNO_2 (M-47) from the molecular ion, which are characteristic of compounds. The higher molecular weight of the complex (double than ligand) indicates the Metal: Lignads;1:2 ratio.

Table 3: Physical characteristics of $[Ni(NIM)_2]Cl_2$

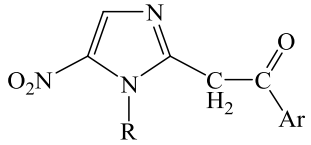

NIM = 5-Nitroimidazoles

Ligand / Complex	Color	R	Ar	m.p. (^{0}C)	Yield (%)	Mol. formula	Mol. weight
NIMP (Ligand)	Yellow	$-C_2H_4SO_2C_2H_5$	phenyl	146-148	80	$C_{15}H_{17}N_3O_5S$	351.38
$[Ni(NIMP)_2]Cl_2$	Dark brown	$-C_2H_4SO_2C_2H_5$	phenyl	262-264	85	$C_{30}H_{34}N_6Cl_2O_{10}S_2Ni$	831.76
NIMPCl (Ligand)	Light yellow	$-C_2H_4SO_2C_2H_5$	*p*-Cl- phenyl	152-154	72	$C_{15}H_{16}ClN_3O_5S$	385.82
$[Ni(NIMPCl)_2]Cl_2$	Brown	$-C_2H_4SO_2C_2H_5$	*p*-Cl- phenyl	280-282	90	$C_{30}H_{32}Cl_3N_6O_{10}S_2Ni$	865.76
NIMMCl(Ligand)	Yellow	$-C_2H_4SO_2C_2H_5$	*m*-Cl- phenyl	156-158	65	$C_{15}H_{16}ClN_3O_5S$	385.82
$[Ni(NIMMCl)_2]Cl_2$	Red- brown	$-C_2H_4SO_2C_2H_5$	*m*- Cl- phenyl	242-245	70	$C_{30}H_{32}Cl_3N_6O_{10}S_2Ni$	865.76
[NIMOCl(Ligand)	Yellow	$-C_2H_4SO_2C_2H_5$	*o*- Cl- phenyl	180-182	45	$C_{15}H_{16}ClN_3O_5S$	385.82
$[Ni(NIMOCl)_2]Cl_2$	Red	$-C_2H_4SO_2C_2H_5$	*o*- Cl- phenyl	261-264	65	$C_{30}H_{32}Cl_3N_6O_{10}S_2Ni$	865.76
NIMF(Ligand)	Yellow	$-C_2H_4SO_2C_2H_5$	furoyl	165-166	75	$C_{13}H_{15}N_3O_6S$	341.34
$[Ni(NIMF)_2]Cl_2$	Red	$-C_2H_4SO_2C_2H_5$	furoyl	232-235	75	$C_{26}H_{30}N_6Cl_2O_{12}S_2Ni$	811.68
NIMDF(Ligand)	Yellow	$-CH_3$	furoyl	130-132	78	$C_{10}H_9N_3O_4$	235.20
$[Ni(NIMDF)_2]Cl_2$	Brown	$-CH_3$	furoyl	278-280	72	$C_{20}H_{18}N_6Cl_2O_8Ni$	533.34
NIMDP(Ligand)	Yellow	$-CH_3$	phenyl	140-143	78	$C_{12}H_{11}N_3O_3$	245.23
$[Ni(NIMDP)_2]Cl_2$	Red	$-CH_3$	phenyl	222-225	82	$C_{24}H_{22}N_6Cl_2O_6Ni$	619.46

Table 4: Spectral characteristics of $[Ni(NIM)_2]Cl_2$

Ligand / Complex	IR (Cm^{-1})			
	v (CH_2)	**v(C=O)**	**v(NO_2)**	**v(M-O)**
NIMP (Ligand)	2977-2800	1720	1570,1365	--
$[Ni(NIMP)_2]Cl_2$	2977-2800	2270	1570,1365	495
NIMPCl (Ligand)	2977-2850	1700	1565,1365	---
$[Ni(NIMPCl)_2]Cl_2$	2980-2850	2250	1558,1361	484
NIMMCL(Ligand)	2977-2850	1700	1565,1365	---
$[Ni(NIMMCL)_2]Cl_2$	2900-2850	2248	1570,1350	500
NIMOCl (Ligand)	2977-2850	1700	1565,1365	---
$[Ni(NIMOCl)_2]Cl_2$	2900-2850	2230	1550,1345	520
NIMF (Ligand)	2977-2850	1690	1550.1360	---
$[Ni(NIMF)_2]Cl_2$	2980-2900	2270	1545,1360	510
NIMDF (Ligand)	2977-2850	1700	1555,1362	---
$[Ni(NIMDF)_2]Cl_2$	2980-2900	2270	1545,1360	525
NIMDP (Ligand)	3000-2950	1705	1572,1360	---
$[Ni(NIMDP)_2]Cl_2$	2980-2900	2270	1555,1340	512

Table 5: Spectral and conductance characteristics of $[Ni(NIM)_2]Cl_2$

Complex	^{1}HNMR	Molar Cond. $cm^2\ mol^{-1}$	UV (λ max nm)	Mass (m/z)
$[Ni(NIMP)_2]Cl_2$	δ 1.28(t,3H,$SO_2CH_2\underline{CH_3}$), δ 3.15 (q, 2H, -$SO_2\underline{CH_2}CH_3$), δ 3.89 (t, 2H, -$CH_2\underline{CH_2}SO_2CH_2CH_3$), δ 4.26 (s, 3H, N=C-$\underline{CH_3}$), δ 4.96 (t, 2H, imidazole-$\underline{CH_2}CH_2SO_2CH_2CH_3$), δ 7.56-7.94 (m, 4H, Ar-$\underline{H}$), δ 7.81 (s,1H, nitroimidazole)	1.20	240, 256, 352	831.76
$[Ni(NIMPCl)_2]Cl_2$	δ1.28(t,3H,$SO_2CH_2\underline{CH_3}$), δ 3.20 (q, 2H, -$SO_2\underline{CH_2}CH_3$), δ 3.72 (t, 2H,-$CH_2\underline{CH_2}SO_2CH_2CH_3$), δ 4.30 (s, 3H, N=C-$\underline{CH_3}$), δ 4.90 (t, 2H, imidazole-$\underline{CH_2}CH_2SO_2CH_2CH_3$), δ 7.60-7.84 (m, 5H, Ar-$\underline{H}$), δ 7.87 (s,1H, nitroimidazole)	1.6	240, 280, 352	----
$[Ni(NIMMCL)_2]Cl_2$	-----	1.25	240, 256, 352	----
$[Ni(NIMOCl)_2]Cl_2$	----	1.10	240, 256, 352	866.50 (M+1)
$[Ni(NIMF)_2]Cl_2$	δ 1.40 (t,3H,-$SO_2CH_2\underline{CH_3}$), δ 3.15 (q, 2H, -$SO_2\underline{CH_2}CH_3$), δ 3.66 (t, 2H, -$CH_2\underline{CH_2}SO_2CH_2CH_3$), δ 4.26 (s, 3H, N=C-$\underline{CH_3}$), δ 4.96 (t, 2H, imidazole-$\underline{CH_2}CH_2SO_2CH_2CH_3$), δ 6.54 (d, 1H, 3-furoyl), δ 6.754 (d, 1H, 4-furoyl), δ 7.59(s, 1H, 5-furoyl), δ 8.1 (s,1H, nitroimidazole)	2.0	240, 320, 365	811.68
$[Ni(NIMDF)_2]Cl_2$	δ 4.30 (s, 3H, N=C-$\underline{CH_3}$), δ 4.96 (s, 3H, imidazole-$\underline{CH_3}$), δ 6.54 (d, 1H, 3-furoyl), δ 6.754 (d, 1H, 4-furoyl), δ 7.59(s, 1H, 5-furoyl), δ 7.98 (s,1H, nitroimidazole)	1.30	240, 328, 490	----
$[Ni(NIMDP)_2]Cl_2$	-----	1.20	240, 256, 352	831.76

5.3 Experimental

- All the melting points were determined in open capillaries and are uncorrected.
- IR spectra were recorded in KBr on SHIMADZU Fourier Transform Infrared 8400S spectrophotometer.
- Mass spectra were recorded on Micromass Q-T , TOF MS $ES^{+}4.73e^{3}$
- Nuclear Magnetic Resonance spectra (^{1}H NMR) were recorded in DMSO-d_6 on BRUKER AVANCE II at 400 MHz and the chemical shift are given in parts per million, downfield from Tetramethyl silane (TMS) was used as internal standard.
- Molar conductivity is taken on conductivity bridge

Synthesis of $[Ni(NIMP)_2]Cl_2$

Nickel chloride (II) 0.650g,(0.005 mol) was dissolved in 50 ml hot methanol and hot solution of 3.51g,(0.010 mole), 2-(1-(2-(ethylsulfonyl) ethyl)-5-nitro-1*H*-imidazol-2-yl)-1-phenylethanone was added. The solution mixture was adjusted to pH 8-10 with concentrated ammonia. The brown colored solution was refluxed for 4-5 hr and then allowed to stand at room temp for 24 hrs. The dark brown crystals were filtered off, dried in vacuo yielding 85%, $[Ni(NIMP)_2]Cl_2$, m.p. 262^0C -264^0C.

Synthesis of $[Ni(NIMPCl)_2]Cl_2$

Nickel chloride (II) 0.650g(0.005 mol) was dissolved in 50 ml hot methanol and hot solution of 3.86g,(0.010 mole) 1-(4-chlorophenyl)-2-(1-(2-(ethylsulfonyl)ethyl)-5-nitro-1*H*-imidazol-2-yl)ethanone was added. The solution mixture was adjusted to pH 8-10 with concentrated ammonia. The brown colored solution was refluxed for 4-5 hours and then allowed to stand for 24 hr. The brown crystals were filtered off, dried in vacuo yielding 90%, $[Ni(NIMPCl)_2]Cl_2$, m.p. 280-282 ^0C.

Synthesis of $[Ni(NIMMCl)_2]Cl_2$

Nickel chloride (II) 0.650g(0.005 mol) was dissolved in 50 ml hot methanol and hot solution of 3.86g,(0.010 mole), 1-(3-chlorophenyl)-2-(1-(2-(ethylsulfonyl)ethyl)-5-nitro-1H-imidazol-2-yl)ethanone was added. The solution mixture was adjusted to pH 8-10 with concentrated ammonia. The brown colored solution was refluxed for 4-5 hrs and then allowed to stand at room temp. for 24 hr. The reddish-brown crystals were filtered off, dried in vacuo yielding 70%, $[Ni(NIMMCl)_2]Cl_2$,m.p. 242^0C -245^0C.

Synthesis of $[Ni(NIMOCl)_2]Cl_2$

Nickel chloride (II) 0.650g,(0.005 mol) was dissolved in 50 ml hot methanol and hot solution of 3.86g,(0.010 mole) 1-(2-chlorophenyl)-2-(1-(2-(ethylsulfonyl)ethyl)-5-nitro-1*H*-imidazol-2-yl)ethanone was added. The solution mixture was adjusted to pH 8-10 with concentrated ammonia. The reddish brown colored solution was refluxed for 4-5 hr and then allowed to stand for 24 hr. The dark brown crystals were filtered off, dried in vacuo yielding 65%, $[Ni(NIMOCl)_2]Cl_2$,m.p. 261^0C -264^0C.

Synthesis of $[Ni(NIMF)_2]Cl_2$

Nickel chloride (II) 0.650g,(0.005 mol) was dissolved in 50 ml hot methanol and hot solution of 3.41g,(0.010 mole) 2-(1-(2-(ethylsulfonyl)ethyl)-5-nitro-1*H*-imidazol-2-yl)-1-(furan-2-yl)ethanone was added. The solution mixture was adjusted to pH 8-10 with concentrated ammonia. The brown colored solution was refluxed for 4-5 hours and then allowed to stand for 24 hr. The reddish color crystals were filtered off, dried in vacuo yielding 75%, $[Ni(NIMF)_2]Cl_2$, m.p. 232^0C -235^0C.

Synthesis of $[Ni(NIMDF)_2]Cl_2$

Nickel chloride (II) 0.650g,(0.005 mol) was dissolved in 50 ml hot methanol and hot solution of 2.35g,(0.010 mole) 1-(furan-2-yl)-2-(1-methyl-5-nitro-1*H*-imidazol-2-yl)ethanone was added. The solution mixture was adjusted to pH 8-10 with concentrated ammonia. The brown colored solution was refluxed for 4-5 hr and then allowed to stand for 24 hr. The brown crystals were filtered off, dried in vacuo yielding 72%, $[Ni(NIMDF)_2]Cl_2$, m.p. 278^0C -280^0C.

Synthesis of $[Ni(NIMDP)_2]Cl_2$

Nickel chloride (II) 0.650g (0.005 mol) was dissolved in 50 ml hot methanol and hot solution of 2.45g,(0.010 mole) 2-(1-methyl-5-nitro-1*H*-imidazol-2-yl)-1-phenylethanone was added. The solution mixture was adjusted to pH 8-10 with concentrated ammonia. The brown colored solution was refluxed for 4-5 hr and then allowed to stand for 24 hr. The dark brown crystals were filtered off, dried in vacuo yielding 82%, $[Ni(NIMDP)_2]Cl_2$, m.p. 222^0C -225^0C.

5.4 References

Pray AP, Tyree SY, Martin Dean F, Cook James R. Anhydrous Metal Chlorides. Inorganic Syntheses 1990;28:321–2.

Wells AF. Structural Inorganic Chemistry, Oxford Press, Oxford, United Kingdom, 1984.

Stucky JB. The Crystal and Molecular Structure of Tetraethylammonium Tetrachloronickelate (II). Acta Crystallographica 1967;23:1064–1070.

CHAPTER VI
NITROIMIDAZOLE-COBALT COMPLEXES

6.1 Introduction

The two most stable oxidation states of cobalt are the +2 (cobaltous) and +3 (cobaltic). The cobaltous ion is labile and may have either a tetrahedral or octahedral geometry. Common salts include cobalt chloride hexahydrate and cobalt nitrate hexahydrate, which have the formulas $[Co(H_2O)_6]Cl_2$ and $[Co(H_2O)_6](NO_3)_2$.In solution, cobalt(II) forms the octahedral $[Co(H_2O)_6]^{2+}$ ion, which is pale pink in color. Addition of concentrated HCl results in the formation of the complex ion $[CoCl_4]^{2-}$, which has a tetrahedral geometry. Addition of the SCN^- ion results in the formation of $[Co(SCN)_4]^{2-}$, which is also tetrahedral (Radostina *et al*., 2008).

Cobalt is one of the most important trace elements in the world of animals and humans. In the form of vitamin B_{12} (Cobalamin), this metal plays a number of crucial roles in many biological functions. Cobalamin is necessary for DNA synthesis, formation of red blood cells, and maintenance of the nervous system, growth and development of children. There is evidence to support the importance of cobalt for immune processes. The following main factors stimulate the increasing interest to the putative anticancer properties of this metal: 1) It has been found that the disturbed balance in the essential metal metabolism of mammals increases susceptibility to infections and malignancies; 2) Being involved in the regulation of some definite processes of the animal organisms, cobalt behaves like biological response modifier; 3) Like an essential element cobalt may be less toxic than non-essential metals such as platinum. Different cobalt containing compounds have been proved to express antineoplastic activity. It has recently been reported that cobalt (II) is a topoisomerase II position. It was found that some complexes of cobalt(II) with different ligands (cholic acids, Mannich bases, mixed ligands) reduced significantly viability and proliferation of cultured tumor cells and induced DNA damages in the treated cells (Radostina *et al*., 2008).

6.2 Results and Discussion

6.2.1 Synthetic approach

Synthesis of $[Co(NIM)_2(NO_3)_2]6H_2O$

The 2-(1-(substituted)-5-nitro-1*H*-imidazol-2-yl)-1-(substituted)ethanone [NIM] were reacted with Cobalt nitrate hexahydrate under reflux yielded the $[Co(NIM)_2(NO_3)_2]6H_2O$ metal complexes as shown in the scheme III

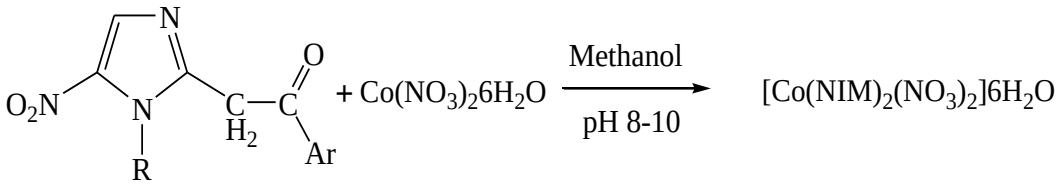

NIM

Ar = phenyl, *p*-cl phenyl, *o*-cl phenyl,
m-cl Phenyl,furoyl
R = CH_3, $CH_2CH_2SO_2CH_2CH_3$

Scheme III

6.2.2 Physical and Spectral characteristics

All the $[Co(NIM)_2(NO_3)_2]6H_2O$ complexes were light to dark brown in color and were soluble in DMSO, DMF and insoluble in all other solvents. The physical data for the complexes presented in Table 6 and 6a represents percentage yield; melting point / decomposition temperature, as well as their color. The complexes were stable solid with melting point ranging from 205^0C -280^0C.

6.2.2.1 IR spectra (KBr, cm^{-1})

Table 7, represents the IR frequencies of the complexes, broad peak near 3600-3500 cm^{-1} indicates water of crystallization of cobalt nitrate salt, C-H streching (3096-2800 cm^{-1}), C=O (2250-2000 cm^{-1}), NO_2 (1570-1540 and 1366-1358cm^{-1}), M-O (600-480 cm^{-1}). The IR frequency for ligand and complex was compared; it was found that frequencies for CH_2, NO_2 was matching with peak of complex. The frequency for carbonyl was changed drastically as it was useful band in the infrared spectra of carbonyl ligand in metal complexes was that due to C–O stretching. The later gives very strong sharp bands which are separated from the bands of other ligand that may be present. The stretching wave number for a terminal carbonyl ligand in a complex correlates with the 'electron-richness' of the metal. The band position is determined by the bonding from the *d* orbitals of the metal into the π^* anti-bonding Orbitals of the ligand (known as *backbonding*). The bonding weakens the C–O bond and lowers the wave number value from its value in free CO thus its show lower frequency ranging 2250-2000cm^{-1}. The M-O streching was observed near 600-480 cm^{-1}.

6.2.2.2 UV-Visible spectra (λ max, nm)

The UV spectra reveal three (λ max, nm) for the 2-substituted nitroimidazole complexes shows three peaks at 240,315 and 480.

6.2.2.3 Molar conductance (cm^2mol^{-1})

The molar conductance values of the synthesized ligand complexes with the cobalt were determined using 10^{-3} M DMF solvent, as shown in Table 8, were in the range of 0.55 - 1.50 cm^2mol^{-1}. These values suggest the presence of a non-electrolyte nature.

6.2.2.4 ^{1}H NMR spectra (DMSO-d6, δ ppm)

The ^{1}HNMR (DMSO-d_6) spectra of complex, displays the triplet of methyl group (-$SO_2CH_2\underline{CH_3}$) resonates at δ 1.28-1.40 ppm, quartet of methylene group (-$SO_2\underline{CH_2}CH_3$) resonates at δ 3.15 ppm, triplet for(- $CH_2\underline{CH_2}SO_2CH_2CH_3$) resonates at δ 3.66-3.89 ppm, singlet for (-N=C-$\underline{CH_3}$) resonates at δ 4.26-4.30, triplet for (imidazole-$\underline{CH_2}CH_2SO_2CH_2CH_3$) resonates at δ 4.96 ppm, all the aromatic proton resonates between δ 6.54-7.94 , the singlet for (^{1}H nitroimidazole ring) observed between δ 7.87-8.1ppm.

6.2.2.5 Mass spectra (m/z)

The molecular ions were observed. The fragmentation routes primarily involved losses of, NO (M-30), NO_2 (M-46) and HNO_2 (M-47) from the molecular ion, which are characteristic of compounds. The higher molecular weight of the complex (double than ligand) indicates the Metal: Lignads; 1:2 ratio.

Table 6: Physical characteristics of $[Co(NIM)_2(NO_3)_2]6H_2O$

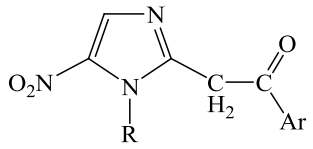

NIM = 5-Nitroimidazoles

Ligand / Complex	Color	R	Ar	m.p. (^{0}C)	Yield (%)*	Molecular formula	Mol. weight
NIMP (Ligand)	Yellow	$-C_2H_4SO_2C_2H_5$	Phenyl	146-148	80	$C_{15}H_{17}N_3O_5S$	351.38
$[Co(NIMP)_2(NO_3)_2]6H_2O$	Dark brown	$-C_2H_4SO_2C_2H_5$	Phenyl	262-264	75	$C_{30}H_{46}CoN_8O_{22}S_2$	993.15
NIMPCl (Ligand)	Light yellow	$-C_2H_4SO_2C_2H_5$	*p*-Cl-phenyl	152-154	72	$C_{15}H_{16}ClN_3O_5S$	385.82
$[Co(NIMPCl)_2(NO_3)_2]6H_2O$	Light Brown	$-C_2H_4SO_2C_2H_5$	*p*-Cl-phenyl	275-277	87	$C_{30}H_{44}CoCl_2N_8O_{22}S_2$	1062.68
NIMMCl(Ligand)	Yellow	$-C_2H_4SO_2C_2H_5$	*m*-Cl-phenyl	156-158	65	$C_{15}H_{16}ClN_3O_5S$	385.82
$[Co(NIMMCl)_2(NO_3)_2]6H_2O$	Earthy brown	$-C_2H_4SO_2C_2H_5$	*m*-Cl-phenyl	237-239	72	$C_{30}H_{38}CoCl_3N_8O_{22}S_2$	1062.68
NIMOCl(Ligand)	Yellow	$-C_2H_4SO_2C_2H_5$	*o*-Cl-phenyl	180-182	45	$C_{15}H_{16}ClN_3O_5S$	385.82

Table 6 a: Physical characteristics of $[Co(NIM)_2(NO_3)_2]6H_2O$

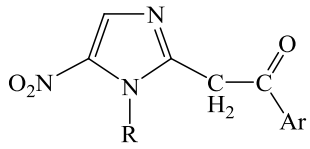

NIM = 5-Nitroimidazoles

Ligand / Complex	**Color**	**R**	**Ar**	**m.p. (^{0}C)**	**Yield (%)***	**Molecular formula**	**Mol. weight**
$[Co(NIMOCl)_2(NO_3)_2]6H_2O$	Red	$-C_2H_4SO_2C_2H_5$	*o*-Cl-phenyl	211-213	69	$C_{30}H_{38}Co\ Cl_3N_8O_{22}S_2$	1062.68
NIMF(Ligand)	Yellow	$-C_2H_4SO_2C_2H_5$	furoyl	165-166	75	$C_{13}H_{15}N_3O_6S$	341.34
$[Co(NIMF)_2(NO_3)_2]6H_2O$	Dark brown	$-C_2H_4SO_2C_2H_5$	furoyl	208-209	72	$C_{26}H_{36}\ CoN_8O_{24}S_2$	967.06
NIMDF(Ligand)	Yellow	$-CH_3$	furoyl	130-132	78	$C_{10}H_9N_3O_4$	235.20
$[Co(NIMDF)_2(NO_3)_2]6H_2O$	Brown	$-CH_3$	furoyl	205-207	72	$C_{20}H_{30}\ CoN_8\ O_{20}S_2$	825.56
NIMDP(Ligand)	Yellow	$-CH_3$	phenyl	140-143	78	$C_{12}H_{11}N_3O_3$	245.23
$[Co(NIMDP)_2(NO_3)_2]6H_2O$	Red	$-CH_3$	phenyl	222-225	85	$C_{24}H_{34}\ Co\ N_8O_{18}$	781.50

Table 7: Spectral characteristics of $[Co(NIM)_2(NO_3)_2]6H_2O$

Ligand / Complex	IR (Cm^{-1})				
	v (OH)	**v (CH_2)**	**v(C=O)**	**v(NO_2)**	**v(M-O)**
NIMP (Ligand)	---	2977-2800	1720	1570,1365	--
$[Co(NIMP)_2(NO_3)_2]6H_2O$	3650-3500	2977-2800	2270	1570,1365	495
NIMPCl (Ligand)	---	2977-2850	1700	1565,1365	---
$[Co(NIMPCl)_2(NO_3)_2]6H_2O$	3600-3500	2980-2850	2250	1500,1365	550
NIMMCl(Ligand)	---	2977-2850	1700	1565,1365	---
$[Co(NIMMCl)_2(NO_3)_2]6H_2O$	3610-3300	2900-2850	2250	1570,1350	516
NIMOCl(Ligand)	---	2977-2850	1700	1565,1365	---
$[Co(NIMOCl)_2(NO_3)_2]6H_2O$	3650-3450	2900-2850	2230	1550,1345	520
NIMF(Ligand)	---	2977-2850	1690	1550.1360	---
$[Co(NIMF)_2(NO_3)_2]6H_2O$	3630-3430	2980-2900	2250	1545,1360	510
NIMDF(Ligand)	---	2977-2850	1700	1555,1362	---
$[Co(NIMDF)_2(NO_3)_2]6H_2O$	3500-3300	2980-2900	2270	1545,1360	525
NIMDP (Ligand)	---	3000-2950	1705	1572,1360	---
$[Co(NIMDP)_2(NO_3)_2]6H_2O$	3500-3400	2980-2900	2280	1555,1340	512

Table 8: Spectral and conductance characteristics of $[Co(NIM)_2(NO_3)_2]6H_2O$

Complex	^{1}HNMR	Molar Cond. $cm^2mol.^{-1}$	UV (λmax, nm)	Mass (m/z)
$[Co(NIMP)_2(NO_3)_2]6H_2O$	----	1.4	240, 315, 484	----
$[Co(NIMPCl)_2(NO_3)_2]6H_2O$	----	0.7	240, 305, 484	----
$[Co(NIMMCl)_2(NO_3)_2]6H_2O$	δ1.28(t,3H,$SO_2CH_2\underline{CH_3}$), δ 3.20 (q, 2H, -$SO_2\underline{CH_2}CH_3$), δ 3.72 (t, 2H,-$CH_2\underline{CH_2}SO_2CH_2CH_3$), δ 4.30 (s, 3H, N=C-$\underline{CH_3}$), δ 4.90 (t, 2H, imidazole-$\underline{CH_2}CH_2SO_2CH_2CH_3$), δ 7.60-7.84 (m, 5H, Ar-$\underline{H}$), δ 7.87 (s,1H, nitroimidazole)	0.55	240, 305, 484	-----
$[Co(NIMOCl)_2(NO_3)_2]6H_2O$	----	0.67	240, 305, 464	1064.68 (M+2)
$[Co(NIMF)_2(NO_3)_2]6H_2O$	δ 1.40 (t,3H,-$SO_2CH_2\underline{CH_3}$), δ 3.15 (q, 2H, -$SO_2\underline{CH_2}CH_3$), δ 3.66 (t, 2H, -$CH_2\underline{CH_2}SO_2CH_2CH_3$), δ 4.26 (s, 3H, N=C-$\underline{CH_3}$), δ 4.96 (t, 2H, imidazole-$\underline{CH_2}CH_2SO_2CH_2CH_3$), δ 6.54 (d, 1H, 3-furoyl), δ 6.754 (d, 1H, 4-furoyl), δ 7.59(s, 1H, 5-furoyl), δ 8.1 (s,1H, nitroimidazole)	0.69	240, 345, 484	-----
$[Co(NIMDF)_2(NO_3)_2]6H_2O$	δ 4.30 (s, 3H, N=C-$\underline{CH_3}$), δ 4.96 (s, 3H, imidazole-$\underline{CH_3}$), δ 6.54 (d, 1H, 3-furoyl), δ 6.754 (d, 1H, 4-furoyl), δ 7.59(s, 1H, 5-furoyl), δ 7.98 (s,1H, nitroimidazole)	1.30	240, 315, 484	----
$[Co(NIMDP)_2(NO_3)_2]6H_2O$	-----	1.20	240, 300, 484	780 (M)

6.3 Experimental

- All the melting points were determined in open capillaries and are uncorrected.
- IR spectra were recorded in KBr on SHIMADZU Fourier Transform Infrared 8400S spectrophotometer.
- Mass spectra were recorded on Micromass Q-T , TOF MS $ES^{+}4.73e^{3}$
- Nuclear Magnetic Resonance spectra (^{1}H NMR) were recorded in DMSO-d_6 on BRUKER AVANCE II at 400 MHz and the chemical shift are given in parts per million, downfield from Tetramethyl silane (TMS) was used as internal standard.
- Molar conductivity is taken on conductivity bridge

Synthesis of $[Co(NIMP)_2(NO_3)_2]6H_2O$

Cobalt nitrate hexahydrate (II) 1.45g, (0.005 mole) was dissolved in hot methanol (50ml) and hot solution of 3.51g, (0.010 mole) 2-(1-(2-(ethylsulfonyl) ethyl)-5-nitro-1*H*-imidazol-2-yl)-1-phenylethanone was added. The solution mixture was adjusted to pH 8-10 with concentrated ammonia. The brown colored solution was refluxed for 4-5 hr and then allowed to stand for 24 hr. The dark brown crystals were filtered, dried in vacuo yielding 75%, $[Co(NIMP)_2(NO_3)_2]6H_2O$, m.p. 262^0C -264^0C.

Synthesis of $[Co(NIMPCl)_2(NO_3)_2]6H_2O$

Cobalt nitrate hexahydrate (II) 1.45g,(0.005 mole) was dissolved in hot methanol (50ml) and hot solution of 3.86g,(0.010 mole) 1-(4-chlorophenyl)-2-(1-(2-(ethylsulfonyl)ethyl)-5-nitro-1*H*-imidazol-2-yl)ethanone was added. The solution mixture was adjusted to pH 8-10 with concentrated ammonia. The brown colored solution was refluxed for 4-5 hr and then allowed to stand for 24 hr. The light brown crystals were filtered, dried in vacuo yielding 87%, $[Co(NIMPCl)_2(NO_3)_2]6H_2O$, m.p. 275^0C -277^0C.

Synthesis of $[Co(NIMMCl)_2(NO_3)_2]6H_2O$

Cobalt nitrate hexahydrate (II) 1.45g,(0.005 mol) was dissolved in hot methanol (50ml) and hot solution of 3.86g,(0.010 mole) 1-(3-chlorophenyl)-2-(1-(2-(ethylsulfonyl)ethyl)-5-nitro-1*H*-imidazol-2-yl)ethanone was added. The solution mixture was adjusted to pH 8-10 with concentrated ammonia. The brown colored solution was refluxed for 4-5 hr and then allowed to stand for 24 hr. The dark brown crystals were filtered, dried in vacuo yielding 72%, $[Co(NIMMCl)_2(NO_3)_2]6H_2O$, m.p. 237^0C -239^0C.

Synthesis of $[Co(NIMOCl)_2(NO_3)_2]6H_2O$

Cobalt nitrate hexahydrate (II) 1.45g,(0.005 mol) was dissolved in hot methanol (50ml) and hot solution of 3.86g,(0.010 mole) 1-(2-chlorophenyl)-2-(1-(2-(ethylsulfonyl)ethyl)-5-nitro-1*H*-imidazol-2-yl)ethanone was added. The solution mixture was adjusted to pH 8-10 with concentrated ammonia. The brown colored solution was refluxed for 4-5 hr and then allowed to stand for 24 hr. The dark brown crystals were filtered off, dried in vacuo yielding 69%, $[Co(NIMOCl)_2(NO_3)_2]6H_2O$,m.p. 211^0C -213^0C.

Synthesis of $[Co(NIMF)_2(NO_3)_2]6H_2O$

Cobalt nitrate hexahydrate (II) 1.45g,(0.005 mole) was dissolved in hot methanol (50ml) and hot solution of 3.41g,(0.010 mole) 2-(1-(2-(ethylsulfonyl)ethyl)-5-nitro-1*H*-imidazol-2-yl)-1-(furan-2-yl)ethanone was added. The solution mixture was adjusted to pH 8-10 with concentrated ammonia. The brown colored solution was refluxed for 4-5 hr and then allowed to stand for 24 hr. The dark brown crystals were filtered, dried in vacuo yielding 72%, $[Co(NIMF)_2(NO_3)_2]6H_2O$, m.p. 208^0C -209^0C.

Synthesis of $[Co(NIMDF)_2(NO_3)_2]6H_2O$

Cobalt nitrate hexahydrate (II) 1.45g,(0.005 mole) was dissolved in hot methanol (50ml) and hot solution of 2.35g,(0.010 mole) 1-(furan-2-yl)-2-(1-methyl-5-nitro-1*H*-imidazol-2-yl)ethanone was added. The solution mixture was adjusted to pH 8-10 with concentrated ammonia. The brown colored solution was refluxed for 4-5 hours and then allowed to stand for 24 hr. The dark brown crystals were filtered, dried in vacuo yielding 72%, $[Co(NIMDF)_2(NO_3)_2]6H_2O$, m.p. 205^0C -207^0C.

Synthesis of $[Co(NIMDP)_2(NO_3)_2]6H_2O$

Cobalt nitrate hexahydrate (II) 1.45g,(0.005 mole) was dissolved in hot methanol (50ml) and hot solution of 2.45g,(0.010 mole) 2-(1-methyl-5-nitro-1*H*-imidazol-2-yl)phenylethanone was added. The solution mixture was adjusted to pH 8-10 with concentrated ammonia. The brown colored solution was refluxed for 4-5 hr and then allowed to stand for 24 hr. The dark brown crystals were filtered, dried in vacuo yielding 85 %, $[Co(NIMDP)_2(NO_3)_2]6H_2O$, m.p. 222^0C -225^0C.

6.4 References

Radostina A, Reni K, Milena K, Petya G, Georgi M, Otilia C, *et al.* Cobalt and cobalt compounds -biological activity and potential antitumour properties. New trends and strategies in the chemistry of advance materials with relevance in biological systems, technique and environmental protection 6-7 November, 2008. Timisora, Romania.

Introduction to coordination chemistry
http://www.uncp.edu/home/mcclurem/courses/chm226/introduction_Coordination_Chemistry.

CHAPTER VII
NITROIMIDAZOLE-CADMIUM COMPLEXES

7.1 Introduction

Cadmium chloride is a white crystalline compound of cadmium and chlorine, with the formula $CdCl_2$. It is a hygroscopic solid that is highly soluble in water and slightly soluble in alcohol. Although it is considered to be ionic, it has considerable covalent character to its bonding. The crystal structure of cadmium chloride composed of two-dimensional layers of ions. It is also known as $CdCl_2.H_2O$ and $CdCl_2{\cdot}5H_2O$ (Lide, 1998).

Cadmium chloride forms crystals with rhombohedral symmetry. Cadmium iodide, CdI_2, has a very similar crystal structure to $CdCl_2$. The individual layers in the two structures are identical, but in $CdCl_2$ the chloride ions are arranged in a CCP lattice, whereas in CdI_2 the iodide ions are arranged in a HCP lattice (Greenwood *et al*,. 1997 and Wells, 1984).

Cadmium chloride dissolves well in water and other polar solvents. In water, its high solubility is due in part to formation of complex ions such as $[CdCl_4]^{2-}$. Because of this behavior, $CdCl_2$ is a mild Lewis acid (Greenwood *et al*,.1997).

$$CdCl_2 + 2\ Cl^- \rightarrow [CdCl_4]^{2-}$$

With large cations, it is possible to isolate the trigonal bipyramidal $[CdCl_5]^{3-}$ ion Cadmium chloride is used for the preparation of cadmium sulfide, used as "Cadmium Yellow", a brilliant-yellow stable inorganic pigment.

$$CdCl_2 + H_2S \rightarrow CdS + 2\ HCl$$

In the laboratory, anhydrous $CdCl_2$ can be used for the preparation of organocadmium compounds of the type R_2Cd, where R is an aryl or a primary alkyl. These were once used in the synthesis of ketones from acyl chlorides (March, 1992).

7.2 Results and Discussion

7.2.1 Synthetic approach

Synthesis of $[Cd(NIM)_2]Cl_2$

The 2-(1-(substituted)-5-nitro-1*H*-imidazol-2-yl)-1-(substituted)ethanone [NIM] were reacted with Cadmium chloride under reflux condition yielded $[Cd(NIM)_2]Cl_2$ metal complexes as shown in the scheme IV.

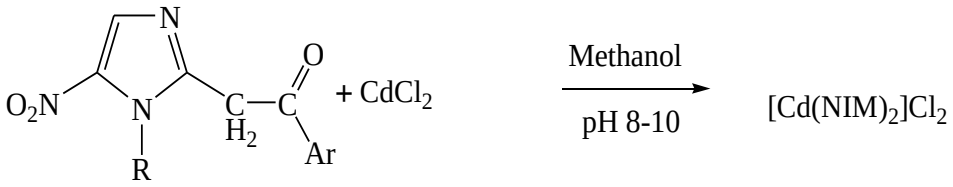

NIM

Ar = phenyl, *p*-cl phenyl, *o*-cl phenyl,
m-cl Phenyl,furoyl
R = CH_3, $CH_2CH_2SO_2CH_2CH_3$

Scheme IV

7.2.2 Physical and Spectral characteristics

All the $[Cd(NIM)_2]Cl_2$ complexes were light yellow to dark brown in color and soluble in DMSO, DMF and insoluble in all other solvents. The physical data for the complexes presented in Table 9; represents percentage yield; melting point / decomposition temperature as well as their color. The complexes are stable solid with melting point ranging from 208^0C -248^0C.

7.2.2.1 IR spectra (KBr,cm^{-1})

Table 10; represents the IR frequencies of the complexes shows, C-H streching (3096-2800 cm^{-1}), C=O (2250-2000 cm^{-1}), NO_2 (1570-1540 and 1366-1358cm^{-1}) and M-O (600-480 cm^{-1}). The IR frequency for ligand and complex was compared; it was found that frequencies for CH_2, NO_2 is matching with peak of complex. The frequency for carbonyl was changed drastically as it was useful band in the infrared spectra of carbonyl ligand in metal complexes is that due to C–O stretching. The later gives very strong sharp bands which are separated from the bands of other ligand that may be present. The stretching wave number for a terminal carbonyl ligand in a complex correlates with the 'electron-richness' of the metal. The band position was determined by the bonding from the *d* orbitals of the metal into the π^* anti-bonding Orbitals of the ligand (known as *backbonding*). The bonding weakens the C–O bond and lowers the wave number value from its value in free CO thus its show lower frequency ranging 2250-2000cm^{-1}. The M-O streching was observed near 600-480 cm^{-1}.

7.2.2.2 UV-Visible spectra (λ max, nm)

The UV spectra reveal three (λ max nm) for the 2-substituted nitroimidazole complexes shows three peaks at 240,260 and 330.

7.2.2.3 Molar conductance (cm^2mol^{-1})

The molar conductance values of the synthesized mixed ligand complexes with the mentioned metal ions under investigation were determined using 10^{-3} M DMF solvent, as shown in Table 11; were in the range of 1.10-2.60 $cm^2mol.^{-1}$. These values suggest the presence of a non-electrolyte nature.

7.2.2.4 ^{1}H NMR spectra (DMSO-d_6, δ ppm)

The ^{1}HNMR (DMSO-d_6) spectra of complex, displays the triplet of methyl group (-$SO_2CH_2\underline{CH_3}$) resonates at δ 1.28-1.40 ppm, quartet of methylene group (-$SO_2\underline{CH_2}CH_3$) resonates at δ 3.15 ppm, triplet for(- $CH_2\underline{CH_2}SO_2CH_2CH_3$) resonates at δ 3.66-3.89 ppm, singlet for (-N=C-$\underline{CH_3}$) resonates at δ 4.26-4.30, triplet for (imidazole-$\underline{CH_2}CH_2SO_2CH_2CH_3$) resonates at δ 4.96 ppm, all the aromatic proton resonates between δ 6.54-7.94 , the singlet for (^{1}H nitroimidazole ring) observed between δ 7.87-8.1ppm..

7.2.2.5 Mass spectra (m/z)

The molecular ions were observed. The fragmentation routes primarily involved losses of, NO (M-30), NO_2 (M-46) and HNO_2 (M-47) from the molecular ion, which are characteristic of compounds. Also the higher molecular weight of the compound indicates complex formed as, Metal: Ligand; 1:2 ratio.

Table 9: Physical characteristics of $[Cd(NIM)_2]Cl_2$

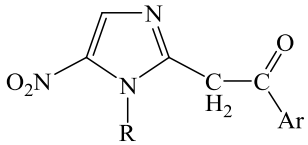

NIM = 5-Nitroimidazoles

Ligand / Complex	Color	R	Ar	m.p. (^{0}C)	Yield (%)*	Molecular formula	Mol. weight
NIMP (Ligand)	Yellow	$-C_2H_4SO_2C_2H_5$	phenyl	146-148	80	$C_{15}H_{17}N_3O_5S$	351.38
$[Cd(NIMP)_2]Cl_2$	Blue	$-C_2H_4SO_2C_2H_5$	phenyl	212-214	87	$C_{30}H_{34}\,Cd\,Cl_2N_6\,O_{10}S_2$	886.07
NIMPCl (Ligand)	Light yellow	$-C_2H_4SO_2C_2H_5$	*p*-Cl-phenyl	152-154	72	$C_{15}H_{16}\,ClN_3O_5S$	385.82
$[Cd(NIMPCl)_2]Cl_2$	Brown	$-C_2H_4SO_2C_2H_5$	*p*- Cl-phenyl	208-210	82	$C_{30}H_{32}\,Cd\,Cl_3N_6O_{10}S_2$	919.51
NIMMCl(Ligand)	Yellow	$-C_2H_4SO_2C_2H_5$	*m*-Cl-phenyl	156-158	65	$C_{15}H_{16}ClN_3O_5S$	385.82
$[Cd(NIMMCl)_2]Cl_2$	Reddish brown	$-C_2H_4SO_2C_2H_5$	*m*-Cl-phenyl	240-243	72	$C_{30}H_{32}\,Cd\,Cl_3N_6O_{10}S_2$	919.51
NIMOCl(Ligand)	Yellow	$-C_2H_4SO_2C_2H_5$	*o*-Cl-phenyl	180-182	45	$C_{15}H_{16}ClN_3O_5S$	385.82
$[Cd(NIMOCl)_2]Cl_2$	Red	$-C_2H_4SO_2C_2H_5$	*o*-Cl-phenyl	246-248	62	$C_{30}H_{32}\,Cd\,Cl_3N_6O_{10}S_2$	919.51
NIMF(Ligand)	Yellow	$-C_2H_4SO_2C_2H_5$	furoyl	165-166	75	$C_{13}H_{15}N_3O_6S$	341.34
$[Cd(NIMF)_2]Cl_2$	Dark brown	$-C_2H_4SO_2C_2H_5$	furoyl	232-235	73	$C_{26}H_{30}N_6\,Cd\,Cl_2O_{12}S_2$	866.00
NIMDF(Ligand)	Yellow	CH_3	furoyl	130-132	78	$C_{10}H_9N_3O_4$	235.20
$[Cd(NIMDF)_2]Cl_2$	Brown	CH_3	furoyl	217-218	72	$C_{20}H_{18}\,Cd\,Cl_2N_6\,O_8$	533.34
NIMDP(Ligand)	Yellow	CH_3	phenyl	140-143	78	$C_{12}H_{11}N_3O_3$	245.23
$[Cd(NIMDP)_2]Cl_2$	Red	$-CH_3$	phenyl	222-225	78	$C_{24}H_{22}\,Cd\,Cl_2N_6\,O_6$	673.79

Table 10: Spectral characteristics of $[Cd(NIM)_2]Cl_2$

Ligand / Complex	IR (Cm^{-1})			
	v (CH_2)	**v(C=O)**	**v(NO_2)**	**v(M-O)**
NIMP (Ligand)	2977-2800	1720	1570,1365	--
$[Cd(NIMP)_2]Cl_2$	2977-2800	2270	1570,1365	495
NIMPCl (Ligand)	2977-2850	1700	1565,1365	---
$[Cd(NIMPCl)_2]Cl_2$	2980-2850	2250	1558,1361	484
NIMMCL(Ligand)	2977-2850	1700	1565,1365	---
$[Cd(NIMMCL)_2]Cl_2$	2900-2850	2248	1570,1350	500
NIMOCl (Ligand)	2977-2850	1700	1565,1365	---
$[Cd(NIMOCl)_2]Cl_2$	2900-2850	2230	1550,1345	520
NIMF (Ligand)	2977-2850	1690	1550.1360	---
$[Cd(NIMF)_2]Cl_2$	2980-2900	2270	1545,1360	510
NIMDF (Ligand)	2977-2850	1700	1555,1362	---
$[Cd(NIMDF)_2]Cl_2$	2980-2900	2270	1545,1360	525
NIMDP (Ligand)	3000-2950	1705	1572,1360	---
$[Cd(NIMDP)_2]Cl_2$	2980-2900	2270	1555,1340	512

Table 11: Spectral and conductance characteristics of $[Cd(NIMM)_2]Cl_2$

Complex	^{1}HNMR	Molar Cond. $cm^2mol.^{-1}$	UV (λ max nm)	Mass (m/z)
$[Cd(NIMP)_2]Cl_2$	---	2.20	238,255, 330	887.07
$[Cd(NIMPCl)_2]Cl_2$	δ1.28(t,3H,$SO_2CH_2\underline{CH_3}$), δ 3.20 (q, 2H, -$SO_2\underline{CH_2}CH_3$), δ 3.72 (t, 2H,-$CH_2\underline{CH_2}SO_2CH_2CH_3$), δ 4.30 (s, 3H, N=C-$\underline{CH_3}$), δ 4.90 (t, 2H, imidazole-$\underline{CH_2}CH_2SO_2CH_2CH_3$), δ 7.60-7.84 (m, 5H, Ar-$\underline{H}$), δ 7.87 (s,1H, nitroimidazole)	1.6	210,222, 245	----
$[Cd(NIMMCL)_2]Cl_2$		1.25	---	920.00
$[Cd(NIMOCl)_2]Cl_2$	----	1.10	----	
$[Cd(NIMF)_2]Cl_2$	δ 1.40 (t,3H,-$SO_2CH_2\underline{CH_3}$), δ 3.15 (q, 2H, -$SO_2\underline{CH_2}CH_3$), δ 3.66 (t, 2H, -$CH_2\underline{CH_2}SO_2CH_2CH_3$), δ 4.26 (s, 3H, N=C-$\underline{CH_3}$), δ 4.96 (t, 2H, imidazole-$\underline{CH_2}CH_2SO_2CH_2CH_3$), δ 6.54 (d, 1H, 3-furoyl), δ 6.754 (d, 1H, 4-furoyl), δ 7.59(s, 1H, 5-furoyl), δ 8.1 (s,1H, nitroimidazole)	1.50	240,265, 328	---
$[Cd(NIMDF)_2]Cl_2$	δ 4.30 (s, 3H, N=C-$\underline{CH_3}$), δ 4.96 (s, 3H, imidazole-$\underline{CH_3}$), δ 6.54 (d, 1H, 3-furoyl), δ 6.754 (d, 1H, 4-furoyl), δ 7.59(s, 1H, 5-furoyl), δ 7.98 (s,1H, nitroimidazole)	2.60	235,265, 340	----
$[Cd(NIMDP)_2]Cl_2$	-----	2.00	236,260, 330	674.00

7.3 Experimental

- All the melting points were determined in open capillaries and are uncorrected.
- IR spectra were recorded in KBr on SHIMADZU Fourier Transform Infrared 8400S spectrophotometer.
- Mass spectra were recorded on Micromass Q-T , TOF MS $ES^{+}4.73e^{3}$
- Nuclear Magnetic Resonance spectra (^{1}H NMR) were recorded in DMSO-d_6 on BRUKER AVANCE II at 400 MHz and the chemical shift are given in parts per million, downfield from Tetramethyl silane (TMS) was used as internal standard.
- Molar conductivity is taken on conductivity bridge

Synthesis of $[Cd(NIMP)_2]Cl_2$

Cadmium chloride (II) 0.920g,(0.005 mol) was dissolved in hot methanol (50ml) and hot solution of 3.51g,(0.010 mole) 2-(1-(2-(ethylsulfonyl)ethyl)-5-nitro-1*H*-imidazol-2-yl)-1-phenylethanone was added. The solution mixture was adjusted to pH 8-10 with concentrated ammonia. The brown colored solution was refluxed for 6 hr and then allowed to stand for 24 hr. The dark brown crystals were filtered, dried in vacuo yielding 87%, $[Cd(NIMP)_2]Cl_2$,m.p. 212^0C -214^0C.

Synthesis of $[Cd(NIMPCl)_2]Cl_2$

Cadmium chloride (II) 0.920g,(0.005 mol) was dissolved in hot methanol (50ml) and hot solution of 3.86g,(0.010 mole) 1-(4-chlorophenyl)-2-(1-(2-(ethylsulfonyl)ethyl)-5-nitro-1*H*-imidazol-2-yl)ethanone was added. The solution mixture was adjusted to pH 8-10 with concentrated ammonia. The brown colored solution was refluxed for 8 hr and then allowed to stand for 24 hr. The dark brown crystals were filtered, dried in vacuo yielding 82%, $[Cd(NIMPCl)_2]Cl_2$,m.p. 208^0C -210^0C.

Synthesis of $[Cd(NIMMCl)_2]Cl_2$

Cadmium chloride (II) 0.920g,(0.005 mol) was dissolved in hot methanol (50ml) and hot solution of 3.86g,(0.010 mole) 1-(3-chlorophenyl)-2-(1-(2-(ethylsulfonyl)ethyl)-5-nitro-1*H*-imidazol-2-yl)ethanone was added. The solution mixture is adjusted to pH 8-10 with concentrated ammonia. The brown colored solution was refluxed for 6 hr and then allowed to stand for 24 hrs. The dark brown crystals were filtered, dried in vacuo yielding 72%, $[Cd(NIMMCl)_2]Cl_2$,m.p. 240^0C -243^0C.

Synthesis of $[Cd(NIMOCl)_2]Cl_2$

Cadmium chloride (II) 0.920g,(0.005 mol) was dissolved in hot methanol (50ml) and hot solution of 3.86g,(0.010 mole) 1-(2-chlorophenyl)-2-(1-(2-(ethylsulfonyl)ethyl)-5-nitro-1*H*-imidazol-2-yl)ethanone was added. The solution mixture was adjusted to pH 8-10 with concentrated ammonia. The brown colored solution was refluxed for 4-5 hr and then allowed to stand for 24 hr. The dark brown crystals were filtered, dried in vacuo yielding 62%, $[Cd(NIMOCl)_2]Cl_2$,m.p. 246^0C -248^0C.

Synthesis of $[Cd(NIMF)_2]Cl_2$

Cadmium chloride (II) 0.920g,(0.005 mol) was dissolved in hot methanol (50ml) and hot solution of 3.41g,(0.010 mole) 2-(1-(2-(ethylsulfonyl)ethyl)-5-nitro-1*H*-imidazol-2-yl)-1-(furan-2-yl)ethanone was added. The solution mixture was adjusted to pH 8-10 with concentrated ammonia. The brown colored solution was refluxed for 4-5 hr and then allowed to stand for 24 hr. The dark brown crystals were filtered, dried in vacuo yielding 73%, $[Cd(NIMF)_2]Cl_2$, m.p. 232^0C -235^0C.

Synthesis of $[Cd(NIMDF)_2]Cl_2$

Cadmium chloride (II) 0.920g,(0.005 mol) was dissolved in hot methanol (50ml) and hot solution of 2.35g,(0.010 mole) 1-(furan-2-yl)-2-(1-methyl-5-nitro-1*H*-imidazol-2-yl)ethanone was added. The solution mixture was adjusted to pH 8-10 with concentrated ammonia. The brown colored solution was refluxed for 4-5 hours and then allowed to stand for 24 hr. The dark brown crystals were filtered, dried in vacuo yielding 72%, $[Cd(NIMDF)_2]Cl_2$, m.p. 217^0C -218^0C.

Synthesis of $[Cd(NIMDP)_2]Cl_2$

Cadmium chloride (II) 0.920g,(0.005 mol) was dissolved in hot methanol (50ml) and hot solution of 2.45g,(0.010 mole) 2-(1-methyl-5-nitro-1*H*-imidazol-2-yl)phenylethanone was added. The solution mixture is adjusted to pH 8-10 with concentrated ammonia. The red colored solution was refluxed for 4-5 hours and then allowed to stand for 24 hr. The reddish crystals were filtered, dried in vacuo yielding 78%, $[Cd(NIMDP)_2]Cl_2$,m.p. 222^0C-225^0C.

7.4 References

Greenwood NN, Earnshaw A. Chemistry of the Elements, 1997, 2nd ed., Butterworth-Heinemann, Oxford, UK.

Lide DR. Handbook of Chemistry and Physics 1998; 87th ed., Boca Raton, FL: CRC Press, pp. 4–67.

March J. Advanced Organic Chemistry, 4th ed., p. 723, Wiley, New York, 1992.

Wells AF. Structural Inorganic Chemistry, 1984. 5th ed., Oxford University Press, Oxford, UK, Nicholls D. Complexes and First-Row Transition Elements, Macmillan Press, London, 1973.

CHAPTER VIII
NITROIMIDAZOLE-COPPER COMPLEXES

8.1 Introduction

The two most important oxidation states of copper are the +1 (cuprous) and +2 (cupric). The +2 ion is more stable and by far the most common. Commonly encountered copper salts include copper sulfate pentahydrate and copper chloride dihydrate, which have the formulas $CuSO_4 5H_2O$ and $CuCl_2 2H_2O$. The former is pale blue in color, and the latter is blue-green in color.

Copper sulfate pentahydrate contains copper (II) in a geometry best described as distorted octahedral. The copper (II) is bound to four water molecules in a square-planar geometry and two oxygen atoms from two sulfate ions. This salt dissolves in water to produce the pale-blue $[Cu(H_2O)_6]^{2+}$ ion, in which two of the water molecules are less tightly held and have longer bond distances. The blue-green color of cobalt chloride dihydrate is due to the presence of some $CuCl_4^{2-}$, which is yellow in color and has a square planar geometry. Concentrated solutions of copper chloride may appear blue-green in color, but dilution results in the formation of the pale-blue $[Cu(H_2O)_6]^{2+}$ ion.

Addition of NH_3 to solutions containing the $[Cu(H_2O)_6]^{2+}$ ion results in successive replacement of the first four H_2O molecules. Replacement of the fifth and six water molecules does not occur to an appreciable extent in aqueous solution, and replacement of the sixth only occurs in liquid ammonia.

$$[Cu(H_2O)_6] + NH_3 \rightarrow [Cu(H_2O)_5(NH_3)]^{2+} + H_2O$$
$$[Cu(H_2O)_5(NH_3)]^{2+} + NH_3 \rightarrow [Cu(H_2O)_4(NH_3)_2]^{2+} + H_2O$$
$$[Cu(H_2O)_4(NH_3)_2]^{2+} + NH_3 \rightarrow [Cu(H_2O)_3(NH_3)_3]^{2+} + H_2O$$
$$[Cu(H_2O)_3(NH_3)_3]^{2+} + NH_3 \rightarrow [Cu(H_2O)_2(NH_3)_4]^{2+} + H_2O$$

A similar series of reactions occur when ethylenediamine is added to a solution containing the $[Cu(H_2O)_6]^{2+}$ ion. Addition of the first two ethylenediamine molecules occurs readily, but addition of a third only occurs when the concentration is very high.

$$[Cu(H_2O)_6]^{2+} + en \rightarrow [Cu(H_2O)_4(en)]^{2+} + 2H_2O$$

$$[Cu(H_2O)_4(en)]^{2+} + en \rightarrow [Cu(H_2O)_2(en)_2]^{2+} + 2H_2O$$

Addition of HCl to a solution containing the $[Cu(H_2O)_6]^{2+}$ ion results in the formation of $[CuCl_4]^{2-}$ which, as previously mentioned, is yellow in color and has square planar geometry. Salts containing this ion may be isolated with bulky cations, as in $(NH_4)_2[CuCl_4]$. Addition of OH^- to $[Cu(H_2O)_6]^{2+}$ results in the initial formation of solid. $Cu(OH)_2$, but with further additions the solid dissolves to form the complex ion $[Cu(OH)_4]^{2-}$. Addition of NO_2^- to a solution containing the $[Cu(H_2O)_6]^{2+}$ ion results in the formation of a solution which probably contains the $[Cu(NO_2)_4]^{2-}$ ion.

Many classes of transition metal complexes are able to enhance cellular radiation damage both in vitro and in vivo. Three principal mechanisms have been suggested for radiosensitization by metal complexes: DNA-binding with subsequent consequences to repair processes, thiol depletion and electron-affinic mechanism implying reduction of the metal complex and subsequent fixation of damage on the intracellular target of radiation, the DNA (Farrel, 1989). Copper (II) ion is well known to modify the radiation response in both mammalian and bacterial cells (Kirschner, 1970 and Hesslewood *et al.,* 1978). The radiosensitizing mechanism in mammalian cells may involve reduction of copper (II) to copper (I) (Kirschner, 1970). More recently, it has been found that: radiosensitization process may be related to radiation induced DNA damage (Savoye, 1996); biological damage sensitized by copper ions might involve nucleobases (Chabita *et al.,* 1996); and copper complexes with different structural features can bind with double-helical DNA and promote double-strand DNA damage (Liu *et al.,* 1999).

8.2 Results and Discussion

8.2.1 Synthetic approach

Synthesis of $[Cu(NIM)_2Cl_2]2H_2O$

The 2-(1-(substituted)-5-nitro-1H-imidazol-2-yl)-1-(substituted) ethanone [NIM] were reacted with Copper chloride dihydrate under reflux yielded, $[Cu(NIM)_2Cl_2]2H_2O$ metal complexes as shown in the scheme V.

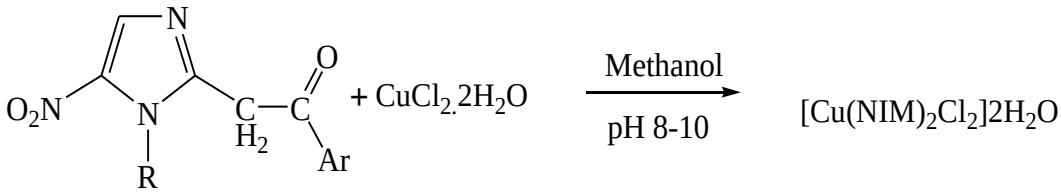

NIM

Ar = phenyl, *p*-cl phenyl, *o*-cl phenyl,
m-cl Phenyl,furoyl
R = CH_3, $CH_2CH_2SO_2CH_2CH_3$

Scheme V

8.2.2 Physical and Spectral characteristics

All the $[Cu(NIM)_2Cl_2]2H_2O$ complexes were greenish yellow in color and soluble in DMSO, DMF and insoluble in all other solvents. The physical data for the complexes presented in Table 12; represents percentage yield; melting point / decomposition temperature, as well as their color. The complexes are stable solid with melting point ranging from, 210^0C-244^0C.

8.2.2.1 IR spectra (KBr, cm^{-1})

Table 13; represents the IR frequencies of the complexes shows the, the broad peak near 3700-3500 cm^{-1} which indicates the water of crystallization of cobalt nitrate salt, C-H streching (3096-2800 cm^{-1}), C=O (2100-1900cm^{-1}), NO_2 (1570-1540 and 1366-1358cm^{-1}) and M-O (600-480 cm^{-1}). The IR frequency for ligand and complex was compared; it was found that frequencies for CH_2, NO_2 was matching with peak of complex. The frequency for carbonyl was changed drastically as it was useful band in the infrared spectra of carbonyl ligand in metal complexes was that due to C–O stretching. The later gives very strong sharp bands which are separated from the bands of other ligand that may be present. The stretching wave number for a terminal carbonyl ligand in a complex correlates with the 'electron-richness' of the metal. The band position is determined by the bonding from the d orbitals of the metal into the π^* anti-bonding Orbital of the ligand (known as *backbonding*). The bonding weakens the C–O bond and lowers the wave number value from its value in free CO thus its show lower frequency ranging 2100-1900cm^{-1}. The M-O streching is observed near 600-480 cm^{-1}.

8.2.2.2 UV-Visible spectra (λ max nm)

The UV spectra reveal three (λ max nm) for the 2-substituted nitroimidazole complexes shows three peaks at 240,330 and 457.

8.2.2.3 Molar conductance (cm^2mol^{-1})

The molar conductance values of the synthesized mixed ligand complexes with the mentioned metal ions under investigation were determined using 10^{-3} M DMF solvent, as shown in Table 14; were in the range of 0.50-2.0 cm^2mol^{-1}. These values suggest the presence of a non-electrolyte nature.

8.2.2.4 1H NMR spectra (DMSO-d_6, δ ppm)

The ^{1}HNMR (DMSO-d_6) spectra of complex, displays the triplet of methyl group (-$SO_2CH_2\underline{CH_3}$) resonates at δ 1.28-1.40 ppm, quartet of methylene group (-$SO_2\underline{CH_2}CH_3$) resonates at δ 3.15 ppm, triplet for(- $CH_2\underline{CH_2}SO_2CH_2CH_3$) resonates at δ 3.66-3.89 ppm, singlet for (-N=C-$\underline{CH_3}$) resonates at δ 4.26-4.30, triplet for (imidazole-$\underline{CH_2}CH_2SO_2CH_2CH_3$) resonates at δ 4.96 ppm, all the aromatic proton resonates between δ 6.54-7.94 , the singlet for (^{1}H nitroimidazole ring) observed between δ 7.87-8.1 ppm..

8.2.2.5 Mass spectra (m/z)

The molecular ions were observed. The fragmentation routes primarily involved losses of, NO (M-30), NO_2 (M-46) and HNO_2 (M-47) from the molecular ion, which are characteristic of compounds. Also the higher molecular weight of the compound indicates complex formed as, Metal: Ligand; 1:2 ratio.

Table 12: Physical characteristics of $[Cu(NIM)_2Cl)_2]2H_2O$

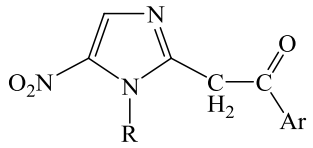

NIM = 5-Nitroimidazoles

Ligand / Complex	**Color**	**R**	**Ar**	**m.p. (^{0}C)**	**Yield (%)***	**Molecular formula**	**Mol. weight**
NIMP (Ligand)	Yellow	$-C_2H_4SO_2C_2H_5$	phenyl	146-148	80	$C_{15}H_{17}N_3O_5S$	351.38
$[Cu(NIMP)_2Cl_2]2H_2O$	yellow	$-C_2H_4SO_2C_2H_5$	phenyl	242-244	78	$C_{30}H_{38}Cl_2\ Cu\ N_6\ O_{12}S_2$	873.24
NIMPCl (Ligand)	Light yellow	$-C_2H_4SO_2C_2H_5$	*p*-Cl-phenyl	152-154	72	$C_{15}H_{16}\ ClN_3O_5S$	385.82
$[Cu(NIMPCl)_2\ Cl_2]2H_2O$	yellow	$-C_2H_4SO_2C_2H_5$	*p*-Cl-phenyl	213-215	76	$C_{30}H_{37}\ Cl_3\ Cu\ N_6O_{12}S_2$	907.68
NIMMCl(Ligand)	Yellow	$-C_2H_4SO_2C_2H_5$	*m*-Cl-phenyl	156-158	65	$C_{15}H_{16}ClN_3O_5S$	385.82
$[Cu(NIMMCl)_2Cl_2]2H_2O$	Greenish yellow	$-C_2H_4SO_2C_2H_5$	*m*-Cl-phenyl	224-226	76	$C_{30}H_{37}\ Cl_3\ Cu\ N_6O_{12}S_2$	907.68
NIMOCl(Ligand)	Yellow	$-C_2H_4SO_2C_2H_5$	*o*-Cl-phenyl	180-182	45	$C_{15}H_{16}ClN_3O_5S$	385.82

Table 12a: Physical characteristics of $[Cu(NIM)_2Cl)_2]2H_2O$

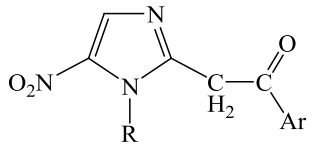

NIM = 5-Nitroimidazoles

Ligand / Complex	Color	R	Ar	m.p. (^{0}C)	Yield (%)*	Molecular formula	Mol. weight
$[Cu(NIMOCl)_2Cl_2]2H_2O$	Red	$-C_2H_4SO_2C_2H_5$	*o*-Cl-phenyl	237-240	68	$C_{30}H_{37}Cl_3CuN_6O_{12}S_2$	907.68
NIMF(Ligand)	Yellow	$-C_2H_4SO_2C_2H_5$	furoyl	165-166	75	$C_{13}H_{15}N_3O_6S$	341.34
$[Cu(NIMF)_2Cl_2]2H_2O$	Greenish yellow	$-C_2H_4SO_2C_2H_5$	furoyl	232-235	75	$C_{26}H_{34}Cl_2CuN_6O_{14}S_2$	853.16
NIMDF(Ligand)	Yellow	$-CH_3$	furoyl	130-132	78	$C_{10}H_9N_3O_4$	235.20
$[Cu(NIMDF)_2Cl_2]2H_2O$	Greenish yellow	$-CH_3$	furoyl	210-212	55	$C_{20}H_{22}Cl_2CuN_6O_{10}S_2$	705.00
NIMDP(Ligand)	Yellow	$-CH_3$	phenyl	140-143	78	$C_{12}H_{11}N_3O_3$	245.23
$[Cu(NIMDP)_2Cl_2]2H_2O$	Greenish yellow	$-CH_3$	phenyl	218-222	78	$C_{24}H_{26}Cl_2CuN_6O_8S_2$	725.08

Table 13: Spectral characteristics of $[Cu(NIM)_2Cl)_2]2H_2O$

Ligand / Complex	IR (Cm^{-1})				
	v (OH)	**v (CH_2)**	**v(C=O)**	**v(NO_2)**	**v(M-O)**
NIMP (Ligand)	---	2977-2800	1720	1570,1365	--
$[Cu(NIMP)_2Cl_2]2H_2O$	3747-3600	2977-2800	2110	1546,1338	472
NIMPCl (Ligand)	---	2977-2850	1700	1565,1365	---
$[Cu(NIMPCl)_2\ Cl_2]2H_2O$	3750-3660	2980-2850	1990	1542,1365	550
NIMMCl(Ligand)	---	2977-2850	1700	1565,1365	---
$[Cu(NIMMCl)_2Cl_2]2H_2O$	3650-3450	2900-2850	1950	1550,1345	520
NIMOCl(Ligand)	---	2977-2850	1700	1565,1365	---
$[Cu(NIMOCl)_2Cl_2]2H_2O$	3610-3500	2900-2850	2000	1556,1345	516
NIMF(Ligand)	---	2977-2850	1690	1550.1360	---
$[Cu(NIMF)_2Cl_2]2H_2O$	3630-3430	2980-2900	1970	1545,1360	510
NIMDF(Ligand)	---	2977-2850	1700	1555,1362	---
$[Cu(NIMDF)_2Cl_2]2H_2O$	3500-3300	2980-2900	2100	1545,1360	525
NIMDP(Ligand)	---	3000-2950	1705	1572,1360	---
$[Cu(NIMDP)_2Cl_2]2H_2O$	3500-3400	2980-2900	2010	1555,1340	512

Table 14: Spectral and conductance characteristics of $[Cu(NIM)_2Cl)_2]2H_2O$

Complex	^{1}HNMR	Molar Cond. cm^2mol^{-1}	UV (λmax nm)	Mass (m/z)
$[Cu(NIMP)_2Cl_2]2H_2O$	----	0.50	240,330	875.24
$[Cu(NIMPCl)_2\ Cl_2]2H_2O$	----	0.6	240,280, 454	----
$[Cu(NIMMCl)_2Cl_2]2H_2O$	----	1.25	240,310, 460	910.00 (M+2)
$[Cu(NIMOCl)_2Cl_2]2H_2O$	δ1.28(t,3H,$SO_2CH_2\underline{CH_3}$), δ 3.20 (q, 2H, -$SO_2\underline{CH_2}CH_3$), δ 3.72 (t, 2H,-$CH_2\underline{CH_2}SO_2CH_2CH_3$), δ 4.30 (s, 3H, N=C-$\underline{CH_3}$), δ 4.90 (t, 2H, imidazole-$\underline{CH_2}CH\ _2SO_2CH_2CH_3$), δ 7.60-7.84 (m, 5H, Ar-$\underline{H}$), δ 7.87 (s,1H, imidazole)	1.10	240,340, 445	---
$[Cu(NIMF)_2Cl_2]2H_2O$	δ 1.40 (t,3H,-$SO_2CH_2\underline{CH_3}$), δ 3.15 (q, 2H, -$SO_2\underline{CH_2}CH_3$), δ 3.66 (t, 2H, -$CH_2\underline{CH_2}SO_2CH_2CH_3$), δ 4.26 (s, 3H, N=C-$\underline{CH_3}$), δ 4.96 (t, 2H, imidazole-$\underline{CH_2}CH\ _2SO_2CH_2CH_3$), δ 6.54 (d, 1H, 3-furoyl), δ 6.754 (d, 1H, 4-furoyl), δ 7.59(s, 1H, 5-furoyl), δ 8.1 (s,1H, nitroimidazole)	2.0	240,335, 455	---
$[Cu(NIMDF)_2Cl_2]2H_2O$	δ 4.30 (s, 3H, N=C-$\underline{CH_3}$), δ 4.96 (s, 3H, imidazole-$\underline{CH_3}$), δ 6.54 (d, 1H, 3-furoyl), δ 6.754 (d, 1H, 4-furoyl), δ 7.59(s, 1H, 5-furoyl), δ 7.98 (s,1H, nitroimidazole)	1.85	240,332, 440	706.00 (M+1)
$[Cu(NIMDP)_2Cl_2]2H_2O$	-----	1.20	240,304, 457	

8.3 Experimental

- All the melting points were determined in open capillaries and are uncorrected.
- IR spectra were recorded in KBr on SHIMADZU Fourier Transform Infrared 8400S spectrophotometer.
- Mass spectra were recorded on Micromass Q-T , TOF MS $ES^{+}4.73e^{3}$
- Nuclear Magnetic Resonance spectra (^{1}H NMR) were recorded in DMSO-d_6 on BRUKER AVANCE II at 400 MHz and the chemical shift are given in parts per million, downfield from Tetramethyl silane (TMS) was used as internal standard.
- Molar conductivity is taken on conductivity bridge

Synthesis of $[Cu(NIMP)_2Cl_2]2H_2O$

Copper chloride dehydrate (II) 0.850g,(0.005 mole) was dissolved in hot methanol (50ml) and hot solution of 3.51g,(0.010 mole), 2-(1-(2-(ethylsulfonyl) ethyl)-5-nitro-1*H*-imidazol-2-yl)-1-phenylethanone was added. The solution mixture was adjusted to pH 8-10 with concentrated ammonia. The greenish yellow colored solution was refluxed for 4-5 hr and then allowed to stand for 24 hr. The greenish yellow crystals were filtered, dried in vacuo yielding 78%, $[Cu(NIMP)_2Cl_2]2H_2O$,m.p. 242^0C-244^0C.

Synthesis of $[Cu(NIMPCl)_2\ Cl_2]2H_2O$

Copper chloride dehydrate (II) 0.850g,(0.005 mole) was dissolved in hot methanol (50ml) and hot solution of 3.86g,(0.010 mole) 1-(4-chlorophenyl)-2-(1-(2-(ethylsulfonyl)ethyl)-5-nitro-1*H*-imidazol-2-yl)ethanone was added. The solution mixture is adjusted to pH 8-10 with concentrated ammonia. The greenish yellow colored solution was refluxed for 4-5 hr and then allowed to stand for 24 hr. The greenish yellow crystals were filtered, dried in vacuo yielding 76%, $[Cu(NIMPCl)_2\ Cl_2]2H_2O$,m.p. 213^0C-215^0C.

Synthesis of $[Cu(NIMMCl)_2Cl_2]2H_2O$

Copper chloride dehydrate (II) 0.850g,(0.005 mole) was dissolved in hot methanol (50ml) and hot solution of 3.86g,(0.010 mole) 1-(3-chlorophenyl)-2-(1-(2-(ethylsulfonyl)ethyl)-5-nitro-1*H*-imidazol-2-yl)ethanone was added. The solution mixture was adjusted to pH 8-10 with concentrated ammonia. The greenish yellow colored solution was refluxed for 4-5 hr and then allowed to stand for 24 hr. The greenish yellow crystals were filtered, dried in vacuo yielding 76%, $[Cu(NIMMCl)_2Cl_2]2H_2O$,m.p. 224^0C-226^0C.

Synthesis of $[Cu(NIMOCl)_2Cl_2]2H_2O$

Copper chloride dehydrate (II) 0.850g,(0.005 mole) was dissolved in hot methanol (50ml) and hot solution of 3.86g,(0.010 mole) 1-(2-chlorophenyl)-2-(1-(2-(ethylsulfonyl)ethyl)-5-nitro-1*H*-imidazol-2-yl)ethanone was added. The solution mixture was adjusted to pH 8-10 with concentrated ammonia. The greenish yellow colored solution was refluxed for 4-5 hr and then allowed to stand for 24 hr. The greenish yellow crystals were filtered, dried in vacuo yielding 68%, $[Cu(NIMOCl)_2Cl_2]2H_2O$,m.p. 237^0C-240^0C.

Synthesis of $[Cu(NIMF)_2Cl_2]2H_2O$

Copper chloride dehydrate (II) 0.850g,(0.005 mole) was dissolved in hot methanol (50ml) and hot solution of 3.41g,(0.010 mole) 2-(1-(2-(ethylsulfonyl)ethyl)-5-nitro-1H-imidazol-2-yl)-1-(furan-2-yl)ethanone was added. The solution mixture was adjusted to pH 8-10 with concentrated ammonia. The greenish yellow colored solution was refluxed for 4-5 hr and then allowed to stand for 24 hr. The greenish yellow crystals were filtered, dried in vacuo yielding 75%, $[Cu(NIMF)_2Cl_2]2H_2O$,m.p. 232^0C-235^0C.

Synthesis of $[Cu(NIMDF)_2Cl_2]2H_2O$

Copper chloride dehydrate (II) 0.850g,(0.005 mole) was dissolved in hot methanol (50ml) and hot solution of 2.35g,(0.010 mole) 1-(furan-2-yl)-2-(1-methyl-5-nitro-1*H*-imidazol-2-yl)ethanone was added. The solution mixture was adjusted to pH 8-10 with concentrated ammonia. The greenish yellow colored solution was refluxed for 4-5 hr and then allowed to stand for 24 hr. The greenish yellow crystals were filtered, dried in vacuo yielding 55%, $[Cu(NIMDF)_2Cl_2]2H_2O$,m.p. 210^0C-212^0C.

Synthesis of $[Cu(NIMDP)_2Cl_2]2H_2O$

Copper chloride dihydrate (II) 0.850g,(0.005 mole) was dissolved in hot methanol (50ml) and hot solution of 2.45g,(0.010 mole) 2-(1-methyl-5-nitro-1*H*-imidazol-2-yl)phenylethanone was added. The solution mixture was adjusted to pH 8-10 with concentrated ammonia. The greenish yellow colored solution was refluxed for 4-5 hr and then allowed to stand for 24 hr. The greenish yellow crystals were filtered, dried in vacuo yielding 78%, $[Cu(NIMDP)_2Cl_2]2H_2O$, m.p. 218^0C-222^0C.

8.4 References

Chabita K, Saha A, Mandal PC, Bhattacharyya SN, Rath MC, Mukherjee T. Reactions of OH and eaq- adducts of cytosine and its nucleosides or nucleotides with Cu (II) ions in dilute aqueous solutions: a steady-state and pulse radiolysis study. Res Chem Intermed.1996; 22:225.

Farrel N. Metal complexes as radiosensitizers. Prog Clin Biochem Med. 1989; 10 : 89.

Hesslewood IP, Cramp WA, McBrien DC, Williamson P, Lott AK. Copper as a hypoxic cell sensitizer of mammalian cells. Br J Cancer 1978; 37(Suppl.): 95.

Kirschner I, Citri N, Levitzki A, Anbar M. The effect of copper on the radiosensitivity of bacteria. Int J Radiat Biol 1970;17: 81.

Liu C, Zhou J, Li Q, Wang L, Liao Z, Xu HJ. Synthesis, DNA-binding and cleavage studies of macrocyclic copper. Inorg Biochem 1999; 75:233.

Savoye C, Sabattier R., Charlier M, Spotheim-Maurizot M. Calculated radiosensitivities of different forms of copper complexes Int J Radiat Biol 1996;70: 189.

CHAPTER IX
ANTIMICROBIAL

9.1 Introduction

The microbiological assay of an antibiotic is based upon a comparison of the inhibition of growth of micro-organisms by measured concentrations of the antibiotics under examination with that produced by known concentrations of a standard preparation of the antibiotic having a known activity. Two general methods are usually employed, the cylinder-plate (or cup-plate) method and the turbidimetric (or tube assay) method (Indian Pharmacopoeia, 2007).

The cylinder-plate method (Method A) depends upon diffusion of the antibiotic from a vertical cylinder through a solidified agar layer in a Petri dish or plate to an extent such that growth of the added micro-organism is prevented entirely in a zone around the cylinder containing a solution of the antibiotic.

The turbidimetric method (Method B) depends upon the inhibition of growth of a microbial culture in a uniform solution of the antibiotic in a fluid medium that is favorable to its rapid growth in the absence of the antibiotic The assay is designed in such a way that the mathematical model on which the potency equation is based can be proved to be valid. If a parallel-line model is chosen, the two log dose response lines of the preparation under examination and the standard preparation should be parallel; they should be rectilinear over the range of doses used in the calculation. These conditions should be verified by validity tests for a given probability.

Media preparation

The media required is prepared for the test organism inocula from the ingredients listed in Table 15. Minor modifications of the individual ingredients may be made, or reconstituted dehydrated media may be used provided the resulting media have equal or better growth-promoting properties and give a similar standard curve response.

Dissolve the ingredients in sufficient water to produce 1000 ml and add sufficient 1 M sodium hydroxide or 1 M hydrochloric acid, as required so that after sterilization the pH is as given in Table 15.

Table 15: Media preparation

Media: Quantities in g of ingredients per 1000 ml

Ingredient	Medium									
	A	B	C	D	E	F	G	H	I	J
Peptone	6.0	6.0	5.0	6.0	6.0	6.0	9.4	–	10.0	–
Pancreatic digest of casien	4.0	–	–	4.0	–	–	–	17.0	–	15.0
Yeast extract	3.0	3.0	1.5	3.0	3.0	3.0	4.7	–	–	–
Beef extract	1.5	1.5	1.5	1.5	1.5	1.5	2.4	–	10.0	–
Dextrose	1.0	–	1.0	1.0	–	–	10.0	2.5	–	–
Papaic digest of soyabean	–	–	–	–	–	–	–	3.0	–	5.0
Agar	15.0	15.0		15.0	15.0	15.0	23.5	12.0	17.0	15.0
Glycerin	–	–	–	–	–	–	–	–	10.0	–
Polysorbate 80	–	–	–	–	–	–	–	10.0*	–	–
Sodium chloride	–	–	3.5	–	–	–	10.0	5.0	3.0	5.0
Dipotassium Hydrogen Phosphate	–	–	3.68	–	–	–	–	2.5	–	–
Potassium dihydrogen phosphate	–	–	1.32	–	–	–	–	–	–	–
Final pH (after sterilisation)	6.5 - 6.6	6.5 - 6.6	6.95 - 7.05	7.8 - 8.0	7.8 - 8.0	5.8 - 6.0	6.0 - 6.2	7.1 - 7.3	6.9 - 7.1	7.2 - 7.4

* Quantity in ml, to be added after boiling the media to dissolve the agar.

Buffer Solutions.

Prepare by dissolving the required quantities of dipotassium hydrogen phosphate and potassium dihydrogen phosphate in sufficient water to produce 1000 ml after sterilisation, adjusting the pH with 8 M phosphoric acid or 10 M potassium hydroxide.

Preparation of the Standard Solution.

A stock solution, was prepared by dissolving a quantity of the Standard Preparation of a given antibiotic (Ciprofloxacin and Tinidazole) accurately weighed and previously dried in the solvent ; DMF and then dilute to the required concentration. Store in a refrigerator and use within the period indicated.

Preparation of the Sample Solution:

The test samples of 2-substituted nitroimidazole complex were dissolved in 4% DMF and diluted with distilled water to attain the different concentration.

Test Organisms.

The test organism for, activity is obtained as American Type Culture Collection (ATCC).Gram positive bacteria *B. Pumilus* ATCC 14884, *S. aureus* ATCC 29737and gram negative bacteria *S. aboney* NCTC 6017

Preparation of inoculum.

The microbial suspensions for the inoculum were prepared by standard method. Growth characteristics are sufficiently uniform so that the inoculum can be adequately determined by the trials given below.

9.2 Method

Cylinder-plate or Cup-plate method

Inoculate a previously liquefied medium appropriate nutrient agar, requisite quantity of suspension of the micro organism, add the suspension to the medium at a temperature between 40ºC and 50ºC and immediately pour the inoculated medium into the petridishes. Ensure that the layers of medium are uniform in thickness, by placing the dishes or plates on a level surface. Store the prepared dishes or plates in a manner so as to ensure that no significant growth or death of the test organism occurs before the dishes or plates are used and that the surface of the agar layer is dry at the time of use.

Apply the standard and test solutions in cavities prepared in the agar. The volume of solution added to each cylinder or cavity must be uniform and sufficient almost to fill the holes when these are used. The plates were incubated for 24 hr and zone of inhibition is measured. (Indian Pharmacopoeia, 2007)

9.3 Results & Discussion

The result of zone of inhibition against Gram positive Bacteria Gram negative Bacteria were represented in Table no. 16,17,18 and 19.

Table 16: Zone of inhibition of $[Ni(NIM)_2]Cl_2$

Complex	Gram positive bacteria		Gram negative bacteria
	B. Pumilus ATCC 14884 Zone of inhibiton (mm)	*S. aureus* ATCC 29737 Zone of inhibiton (mm)	*S. aboney* NCTC 6017 Zone of inhibiton (mm)
$[Ni(NIMP)_2]Cl_2$	---	---	---
$[Ni(NIMPCl)_2]Cl_2$	---	---	---
$[Ni(NIMMCL)_2]Cl_2$	---	---	---
$[Ni(NIMOCl)_2]Cl_2$	---	---	---
$[Ni(NIMF)_2]Cl_2$	15	10	
$[Ni(NIMDF)_2]Cl_2$	25	23	---
$[Ni(NIMDP)_2]Cl_2$	13	20	---
Tinidazole (Control)	---	---	---
Ciprofloxacin (Control)	30	29	31

Figure 12: Zone of inhibition against *B. Pumilus* for $[Ni(NIM)_2]Cl_2$

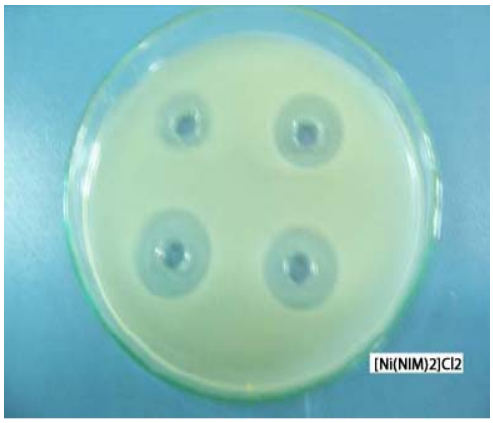

Figure 13: Zone of inhibition against *S. aureus* $[Ni(NIM)_2]Cl_2$

Table 17: Zone of inhibition of $[Co(NIM)_2(NO_3)_2]6H_2O$

Complex	Gram positive bacteria		Gram negative bacteria
	B. Pumilus ATCC 14884 Zone of inhibiton (mm)	*S. aureus* ATCC 29737 Zone of inhibiton (mm)	*S. aboney* NCTC 6017 Zone of inhibiton (mm)
$[Co(NIMP)_2(NO_3)_2]6H_2O$	---	---	---
$[Co(NIMPCl)_2(NO_3)_2]6H_2O$	---	---	---
$[Co(NIMMCl)_2(NO_3)_2]6H_2O$	---	---	---
$[Co(NIMOCl)_2(NO_3)_2]6H_2O$	---	---	---
$[Co(NIMF)_2(NO_3)_2]6H_2O$	15	10	---
$[Co(NIMDF)_2(NO_3)_2]6H_2O$	12	12	---
$[Co(NIMDP)_2(NO_3)_2]6H_2O$	13	13	---
Tinidazole (Control)	---	---	---
Ciprofloxacin (Control)	30	29	31

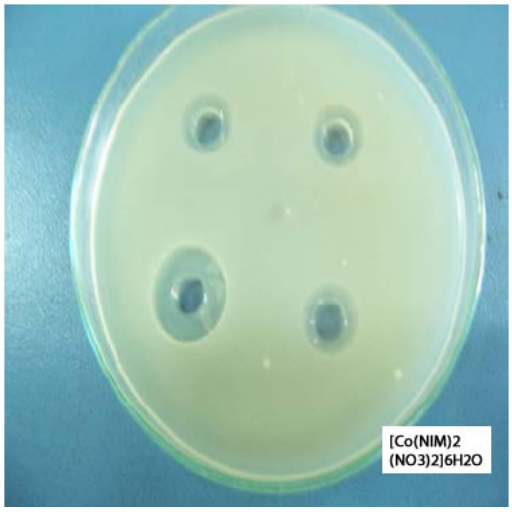

Figure 14: Zone of inhibition against *B. Pumilus* $[Co(NIM)_2(NO_3)_2]6H_2O$

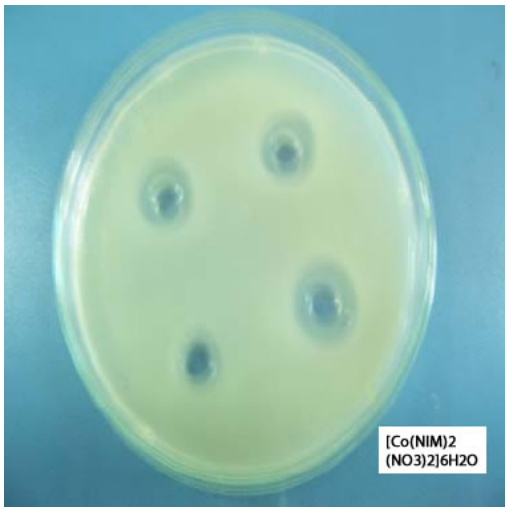

Figure 15: Zone of inhibition against *S. aureus* $[Co(NIM)_2(NO_3)_2]6H_2O$

Table 18: Zone of inhibition of $[Cd(NIM)_2]Cl_2$

Complex	Gram positive bacteria		Gram negative bacteria
	B. Pumilus ATCC 14884 Zone of inhibiton (mm)	*S. aureus* ATCC 29737 Zone of inhibiton (mm)	*S. aboney* NCTC 6017 Zone of inhibiton (mm)
$[Cd(NIMP)_2]Cl_2$	---	---	---
$[Cd(NIMPCl)_2]Cl_2$	---	---	---
$[Cd(NIMMCL)_2]Cl_2$	---	---	---
$[Cd(NIMOCl)_2]Cl_2$	---	---	---
$[Cd(NIMF)_2]Cl_2$	12	10	---
$[Cd(NIMDF)_2]Cl_2$	10	08	---
$[Cd(NIMDP)_2]Cl_2$	12	20	---
Tinidazole (Control)	---	---	---
Ciprofloxacin (Control)	28	32	31

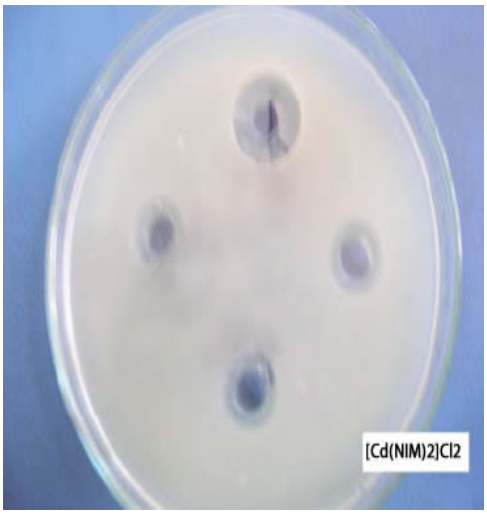

Figure 16: Zone of inhibition against *B. Pumilus* $[Cd(NIM)_2]Cl_2$

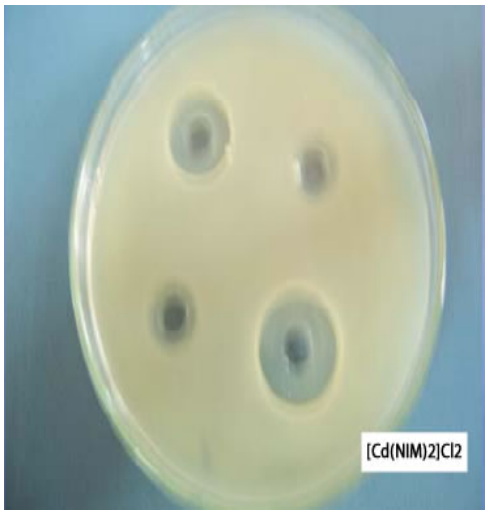

Figure 17: Zone of inhibition against *S. aureus* $[Cd(NIM)_2]Cl_2$

Table 19: Zone of inhibition of $[Cu(NIM)_2Cl_2]2H_2O$

Complex	Gram positive bacteria		Gram negative bacteria
	B. Pumilus ATCC 14884 Zone of inhibiton (mm)	*S. aureus* ATCC 29737 Zone of inhibiton (mm)	*S. aboney* NCTC 6017 Zone of inhibiton (mm)
$[Cu(NIMP)_2Cl_2]2H_2O$	---	---	---
$[Cu(NIMPCl)_2 Cl_2]2H_2O$	---	---	---
$[Cu(NIMMCl)_2Cl_2]2H_2O$	---	---	---
$[Cu(NIMOCl)_2Cl_2]2H_2O$	---	---	---
$[Cu(NIMF)_2Cl_2]2H_2O$	12	8	
$[Cu(NIMDF)_2Cl_2]2H_2O$	8	22	---
$[Cu(NIMDP)_2Cl_2]2H_2O$	8	20	---
Tinidazole (Control)	---	---	---
Ciprofloxacin (Control)	32	26	31

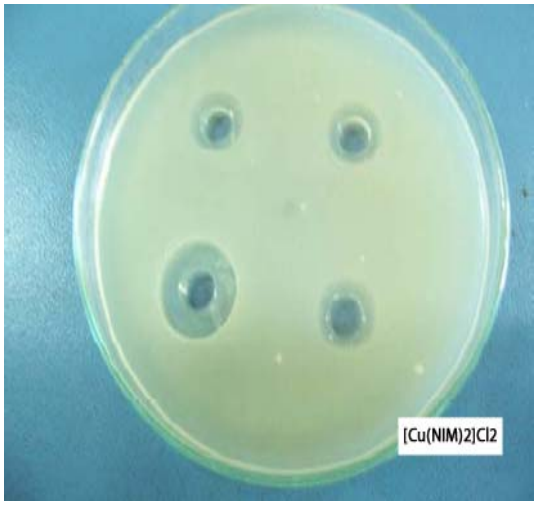

Figure 18 : Zone of inhibition against *B. Pumilus* $[Cu(NIM)_2Cl_2]2H_2O$

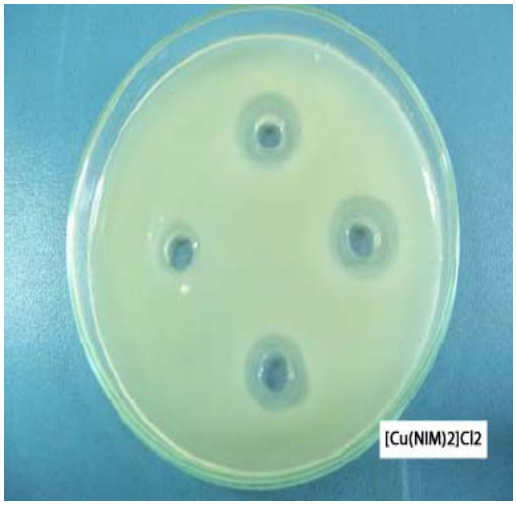

Figure 19: Zone of inhibition against *S. aureus* $[Cu(NIM)_2Cl_2]2H_2O$

Discussion

All the synthesized complexes from each series were screened for their antibacterial activity against Gram negative and Gram positive bacteria by cylinder plate method using tinidazole and ciprofloxacin as standard control. The results were expressed in zone of inhibiton (mm) at 100 µ/ml concentration.

The complexes from each series having the ligand NIMF, NIMDF and NIMDP that mean complex $[Ni(NIMF)_2]Cl_2$, $[Ni(NIMDF)_2]Cl_2$, $[Ni(NIMDP)_2]Cl_2$ with Nickel as metal, $[Co(NIMF)_2(NO_3)_2]6H_2O$,$[Co(NIMDF)_2(NO_3)_2]6H_2O$, $[Co(NIMDP)_2(NO_3)_2]6H_2O$ having Cobalt as metal, $[Cd(NIMF)_2]Cl_2$, $[Cd(NIMDF)_2]Cl_2$, $[Cd(NIMDP)_2]Cl_2$ with Cadmium as metal and $[Cu(NIMF)_2Cl_2]2H_2O$, $[Cu(NIMDF)_2Cl_2]2H_2O$, $[Cu(NIMDP)_2Cl_2]2H_2O$ with Copper as metal were found to be active against Gram positive bacteria (*B. Pumulis and S. aureus*)

Among all the synthesized complex, $[Ni(NIMDF)_2]Cl_2$ was found most active and having zone of inhibition (25mm) comparable to the standard ciprofloxacin having zone of inhibition (30) as show in the chart 1

It was also observed out that all the metal complexes of 2-substituted nitroimidazole were remain inactive against the gram negative bacteria.

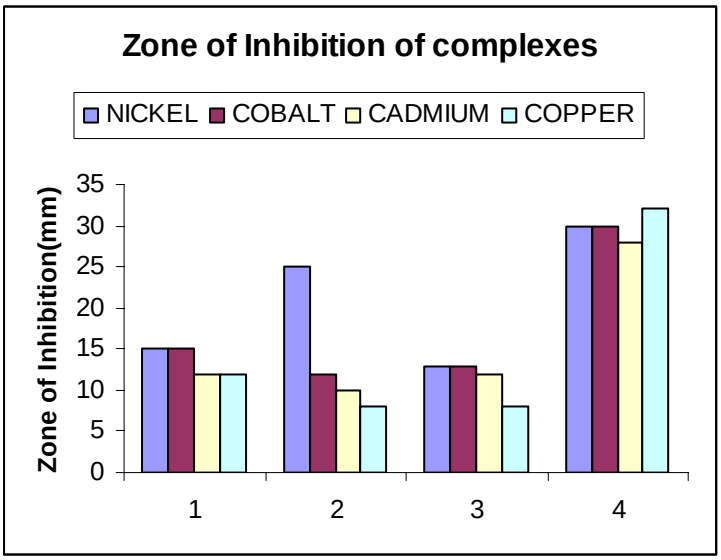

Chart 1: Zone of inhibition of active Complexes(*B. Pumilus*)
(Where 1; NIMF, 2: NIMDF 3: NIMDP and 4: Ciprofloxacin)

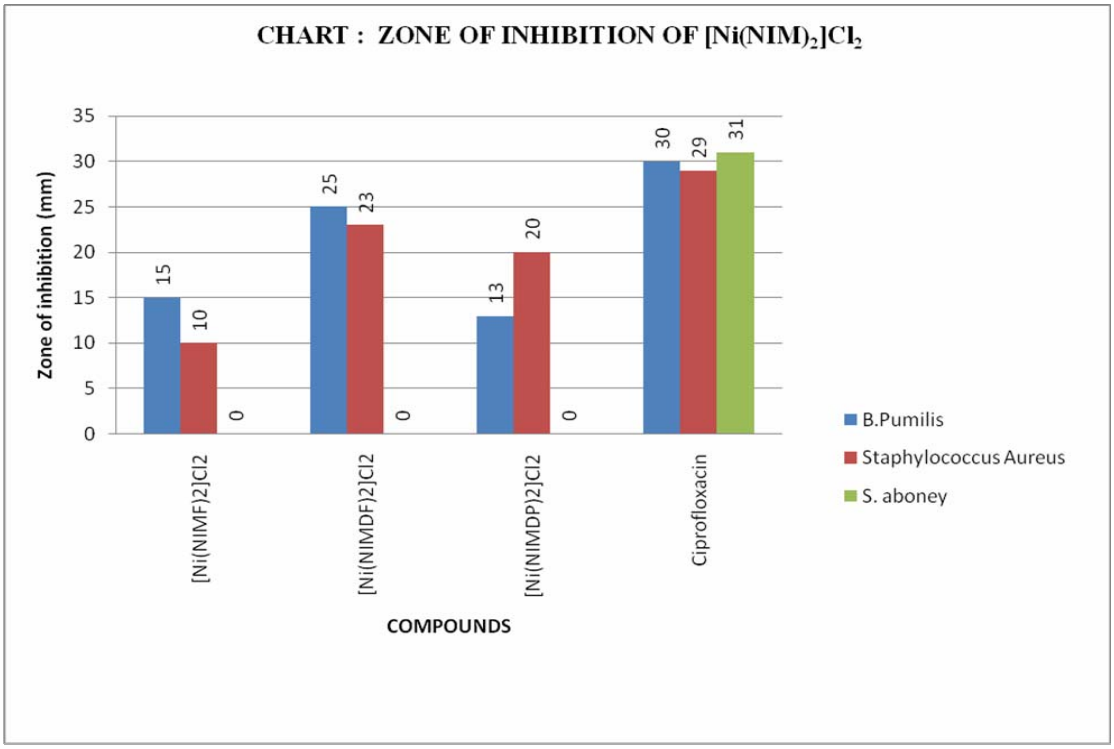

Chart-2

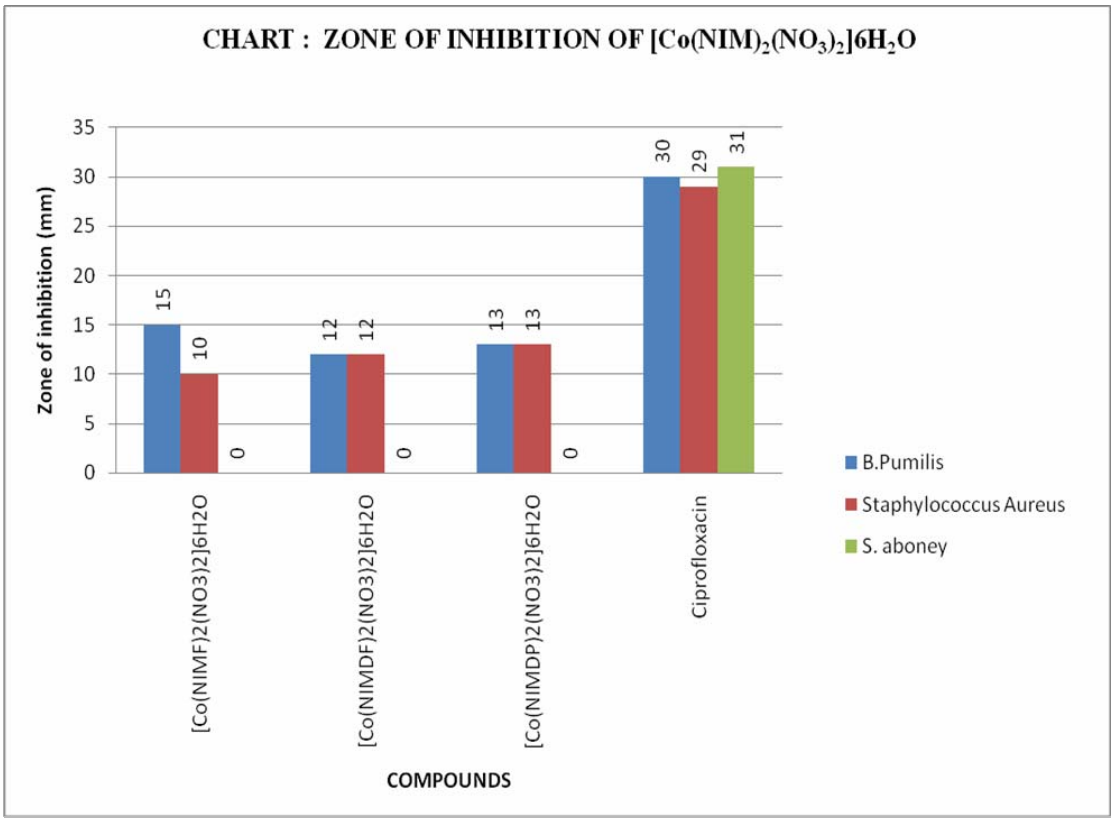

Chart-3

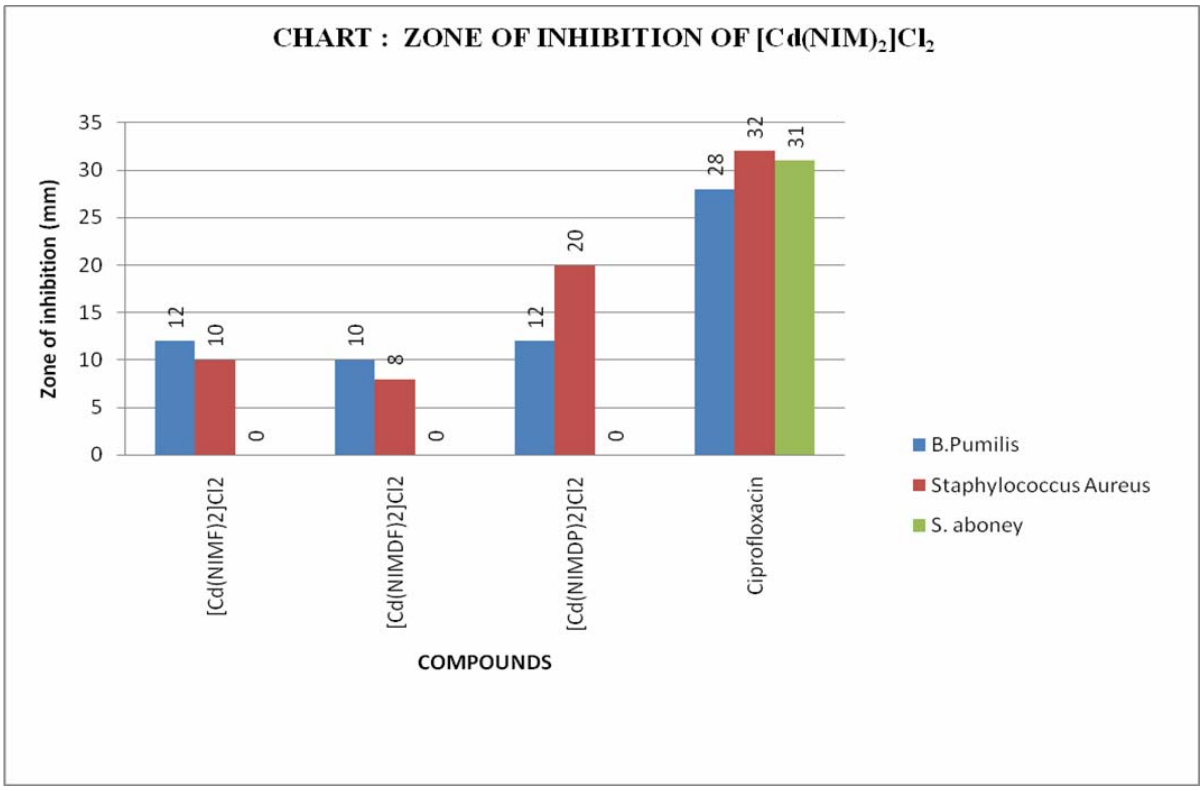

Chart-4

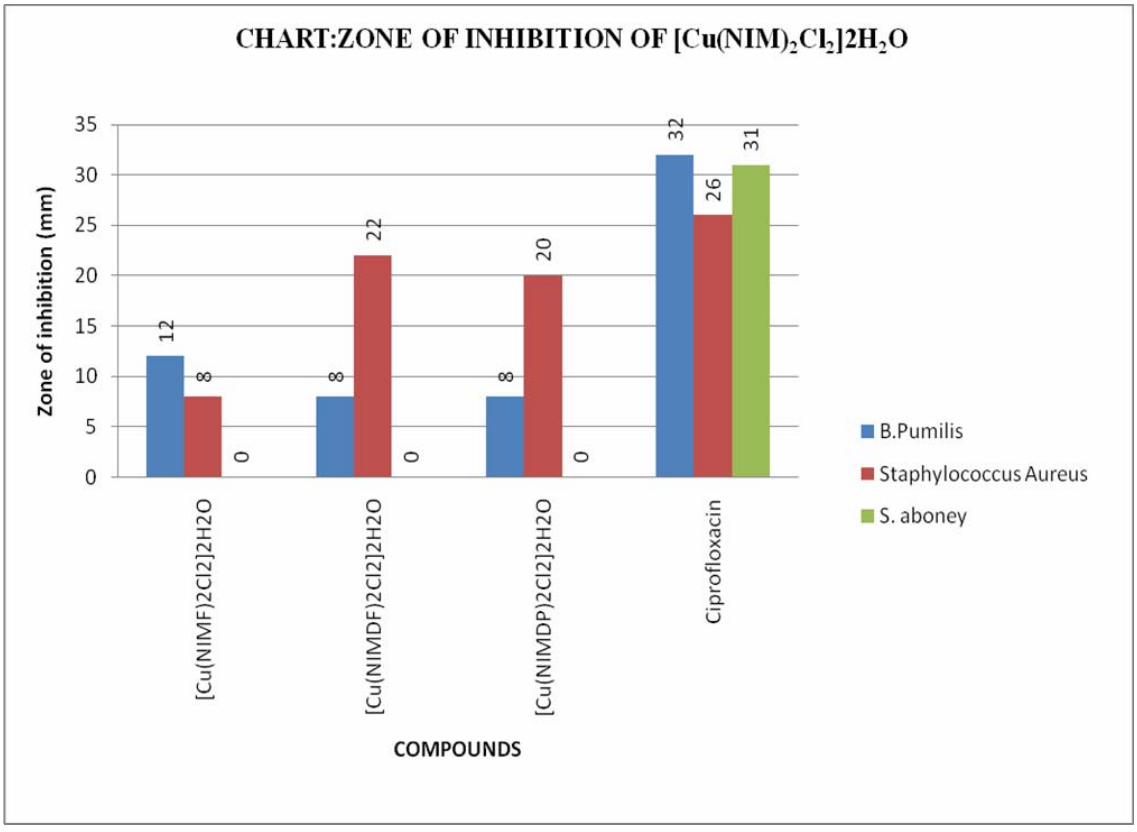

Chart-5

9.4 References

The Indian Pharmacopoeia 2007, published by the Indian Pharmacopoeia Commission (IPC) on behalf of the Government of India, Ministry of Health & Family Welfare, March 2005;Volume I, P. 45-50.

CHAPTER X
CONCLUSION

It was the observed that metal complexes of nitroimidazole shows tetrahedral structures with divalent transition metals observed in the ratio of [M: L; 1:2]. The double molecular weight of the complex compared to ligand shows the binding of two mole of ligand with metal.

Thus the proposed structure of the complex may be,

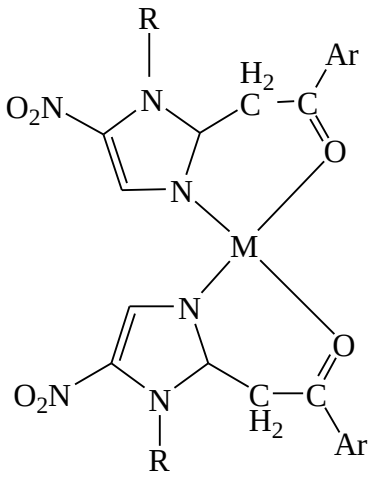

M = NiCl2
CuCl2
CdCl2
Co(NO3)2

The antimicrobial study shows the most potent activity was observed in the nickel metal amongst all the divalent transition metal against Gram positive bacteria. Nitroimidazoles were drug specifically used for the treatment of anaerobic bacteria; surprisingly the preparation of its nickel complex shows good aerobic antibacterial activity against gram positive bacteria which was almost comparable to standard drug ciprofloxacin. Thus the nitroimidazole complex of nitroimidazole may be considered as better choice for treatment of anaerobic as well as aerobic infections.

CHAPTER XI
SUMMARY

Nitroimidazoles, especially tinidazole (tnz) is a therapeutic agent of choice for amebiasis and is also used in combination with other antimicrobial drugs against yeast infections. Under anaerobic conditions inside the cell, it is reduced to a cytotoxic nitro radical and binds nonspecifically to the organism's DNA and enzymes, which are thus inactivated. High doses or long-term administration of tinidazole can cause a peripheral neuropathy with sensory disturbances, and the emergence of resistance to this drug is known in many pathogenic bacteria and protozoa. Other available drugs have their own limitations, and today, parasite resistance is also a global problem. Metal based drugs such as Au (I) complexes have been used successfully for the treatment of various diseases including P_{38} leukemia. Many neutral palladium(II) and palladium(IV) complexes were found to exhibit potential antitumour activity. Moreover, Ru complexes of chloroquine act as potential antimalarial agents against *P. falciparum*. So it is well-known that coordination of metal ion has a positive effect on drug efficacy. A series of Pd, Pt, Cu, Au, and Ru complexes of metronidazole (mnz) was prepared showed good activity.

The Nickel complex with 2-substituted nitroimidazoles were designed, synthesized and characterized by IR, ^{1}HNMR, MASS, UV and conductivity measurements. The IR frequency for ligand and complex was compared; it was found that frequencies for CH_2, NO_2 is matching with peak of complex. The frequency for carbonyl is changed drastically as it is useful band in the infrared spectra of carbonyl ligand in metal complexes is that due to C–O stretching. The later gives very strong sharp bands which are separated from the bands of other ligand that may be present. The stretching wave number for a terminal carbonyl ligand in a complex correlates with the 'electron-richness' of the metal. The band position is determined by the bonding from the d Orbitals of the metal into the π^* anti-bonding Orbitals of the ligand (known as *backbonding*). The bonding weakens the C–O bond and lowers the wave number value from its value in free CO thus its show lower frequency ranging 2250-2000cm^{-1} The M-O streching is observed near 600-480 Cm^{-1}. Characterization by spectral

analysis reveals that divalent nickel transition metal binds the bidentate ligand (2-substituted nitroimidazoles) in the ratio of [M:L;1:2] was confirmed by the MASS, which shows the double in the mass of the molecules. The conductivity measurement shows negligible conductance which is indication of non electrolytic behavior of the complex. Thus characterization shows that the nickel complexes of nitroimidazoles may be tetrahedral in nature.

Cobalt complex with 2-substituted nitroimidazoles were designed, synthesized and characterized by IR, ^{1}HNMR, MASS, UV and conductivity measurements. IR frequencies of the complexes shows, the broad peak near 3600-3500 cm^{-1} which indicates the water of crystallization of cobalt nitrate salt, C-H streching (3096-2800 cm^{-1}), >C=O (2250-2000 cm^{-1}) , NO_2 (1570-1540 and 1366-1358cm^{-1}), M-O (600-480 cm^{-1}) indicates the coordinate covalent bond formed between ligand and metal. All other characteristics were same as the metal complexes of nickel. The cobalt complex also reveals the tetrahedral structure of complex due to binding of metal to ligand in the ratio of 1:2

All the $[Cd(NIM)_2]Cl_2$ complexes were light yellow to dark brown in color and are soluble in DMSO and insoluble in all other solvents. The complexes are stable solid with melting point ranging from 212 - 248°C. IR frequencies of the complexes shows the C-H streching (3096-2800 cm^{-1}), >C=O (2250-2000 cm^{-1}), NO_2 (1570-1540 and 1366-1358cm^{-1}), M-O (600-480 cm^{-1}) indicates the coordinate covalent bond formed between ligand and metal in the ratio of 1:2.

Copper (II) ion is well known to modify the radiation response in both mammalian and bacterial cells. The radiosensitizing mechanism in mammalian cells may involve reduction of copper(II) to copper(I). More recently, it has been found that: radiosensitization process may be related to radiation induced DNA damage, biological damage sensitized by copper ions might involve nucleobases; and copper complexes with different structural features can bind with double-helical DNA and promote double-strand DNA damage. Copper complex with 2-substituted nitroimidazoles were designed, synthesized and characterized by IR, ^{1}HNMR, MASS, UV and conductivity measurements. IR frequencies of the complexes shows the, the broad peak near 3700-3500 cm^{-1} which indicates the water of crystallization of copper

chloride salt, C-H streching (3096-2800 cm^{-1}), >C=O (2100-1900cm^{-1}) , NO_2 (1570-1540 and 1366-1358cm^{-1}), M-O (600-480 cm^{-1}) indicates the coordinate covalent bond formed between ligand and metal. It is also confirms that copper -nitroimidazole complex having tetrahedral structure.

All the synthesized and characterized compounds of 2-subtitutednitroimidazole complexes of metals were studied for their antimicrobial activity against Gram negative bacteria (*S. aboney*) and Gram positive bacteria (*S. auerues and B. pumulis*) using tinidazole and ciprofloxacin as standard control drug by cylinder plate method. The results were expressed in zone of inhibiton (mm) at 100 µ/ml concentration.

The complexes from each series having the ligand NIMF, NIMDF and NIMDP that mean complex $[Ni(NIMF)_2]Cl_2$, $[Ni(NIMDF)_2]Cl_2$, $[Ni(NIMDP)_2]Cl_2$ with Nickel as metal, $[Co(NIMF)_2(NO_3)_2]6H_2O$,$[Co(NIMDF)_2(NO_3)_2]6H_2O$, $[Co(NIMDP)_2(NO_3)_2]6H_2O$ having Cobalt as metal, $[Cd(NIMF)_2]Cl_2$, $[Cd(NIMDF)_2]Cl_2$, $[Cd(NIMDP)_2]Cl_2$ with Cadmium as metal and $[Cu(NIMF)_2Cl_2]2H_2O$, $[Cu(NIMDF)_2Cl_2]2H_2O$, $[Cu(NIMDP)_2Cl_2]2H_2O$ with Copper as metal were found to be active against Gram positive bacteria (*B. pumulis and S. aureus*). Among all the synthesized complex, $[Ni(NIMDF)_2]Cl_2$ were found most active and having zone of inhibition (25mm) comparable to the standard ciprofloxacin having zone of inhibition (30) as show in the figure and graph 1. It was also observed out that all the metal complexes of 2-substitutednitroimidazole were remain inactive against the gram negative bacteria.

PHARMA SCIENCE MONITOR
AN INTERNATIONAL JOURNAL OF PHARMACEUTICAL SCIENCES

SYNTHESIS AND ANTIBACTERIAL ACTIVITY OF NICKEL COMPLEX OF SOME NOVEL NITROIMIDAZOLE

D.G. Desai*[1], A.K.Seth[2], K.I.Molvi[3], M.M.Mansuri[4], B.R.Prajapati [5]

[1,4] P&M Kansara Pharmacy College, Pipariya, Gujarat –India.
[2] Department of Pharmacy, Sumandeep Vidyapeeth, Pipariya, Gujarat-India.
[3] Ali-Allana College of Pharmacy, Department of Pharmaceutical Medicinal Chemistry, Akkalkuawa, Nandurbar, 425415 – India.
[5] L.M.College of Pharmacy, Navrangpura, Ahmedabad-09, Gujarat-India.

ABSTRACT

The Ni(II) complex of novel, 2-(1-(substituted)-5-nitro-1H-imidazol-2-yl)-1-(substituted) ethanone have been synthesized and characterized by FTIR, molar conductivity, ^{1}HNMR, MASS. Novel 2-nitroimidazole act as a bidentate ligand through the 3-N of imidazole ring and C=O, at 2-position of nitroimidazole, which coordinate the metal ion give rise to 4-coordinate tetrahedral Ni(II) complex. The in vitro antimicrobial activity was determined by using cylinder plate method. The compounds were found to be more active than ligand against Gram-positive bacteria, *B. Pumilus* ATCC 14884, *S. aureus* ATCC 29737 and Gram negative bacteria, *S. aboney* NCTC 6017.

Keywords: nitroimidazole, complex, Nickel chloride, ligands.

INTRODUCTION

At present, disease-causing microbes that have become resistant to antibiotic drug therapy are on the increase and resistance against antimicrobial agents is becoming a public health problem worldwide [1,2 & 3] . In the search for novel therapy against resistant organism, the modification of existing drug by combination to a metal centre has gained attention in recent years [4,5]. The efficacies of some therapeutic agents are known to increase upon co-ordination, thus metal-based drug is seen as promising alternatives for possible replacement for some of the current drugs. A number of antibiotics such as bleomycin, streptonigrin and bactracin have been reported to function properly upon coordination with metal ions [6]. Metal complexes as pharmaceuticals have received considerable attention in the development of anticancer agents using platinum, ruthenium and other metals, with greater efficacy and reduced toxic side effects [7]. Vanadium compounds, either alone or in combination with other agents, have the potential to serve as anti-diabetic agents [8].

Nitroimidazoles is a therapeutic agent of choice for amoebiasis [9] and is also used in combination with other antimicrobial drugs against yeast infections [10]. Under anaerobic conditions inside the cell, it is reduced to a cytotoxic nitro radical and binds nonspecifically to the organism's DNA and enzymes, which are thus inactivated[11,12]. High doses or long-term administration of nitroimidazole can cause a peripheral neuropathy with sensory disturbances, and the emergence of resistance to this drug is known in many pathogenic bacteria and protozoa. A series of Pd, Pt, Cu, Au, and Ru complexes of metronidazole was prepared by Bharti and others [13,14] The copper and palladium metronidazole complexes were considerably superior to others and demonstrated higher activity, which proved the fact that metal incorporation enhances the drug activity [13].

In the present work the some novel nitroimidazole analogues were synthesized by modification at 2-position and then complexed with the transition metals Ni(II).

MATERIAL AND METHODS

Materials

Nickel salt, reagents and chemicals are of analytical grade and they were used without further purification. All the melting points were determined in open capillaries and are uncorrected. IR spectra were recorded in KBr on SHIMADZU Fourier Transform Infrared 8400S spectrophotometer. Mass spectra were recorded on Micromass Q-T , TOF MS $ES^{+}4.73e^{3}$ Nuclear Magnetic Resonance spectra (^{1}H NMR) were recorded in DMSO-d_6 on BRUKER AVANCE II at 400 MHz and the chemical shift are given in parts per million, downfield from Tetramethyl silane (TMS) was used as internal standard. Molar conductance was obtained on conductivity bridge, Systronics. *B. Pumilus* ATCC 14884, *S. aureus* ATCC 29737 and *S. aboney* NCTC 6017 typed cultures as obtained from the American Typed Culture Collection (ATCC) were used.

Synthesis of the metal complexes

Nickel chloride (II) (0.635g, 0.005 mol) was dissolved in hot ethanol (50ml) and hot solution of 0.010mole, 2-(1-(substituted)-5-nitro-1H-imidazol-2-yl)-1-(substituted) ethanone was added. The solution is adjusted to pH 8-10, with concentrated ammonia. The brown colored solution was refluxed for 4-5 hours and then

allowed to stand for 24 hrs. The dark brown crystals were filtered off, dried in vacuo yielding 70-90 % yield.

Antimicrobial study

The metal complexes were dissolved in minimum amount of dimethylformamide and diluted with water. Agar medium suitable for testing the sensitivity of clinically important pathogens towards antibiotics, and nutrient broth were prepared with the standard preparatory techniques. All the synthesized complexes of 2-substituted nitroimidazole were screened for antimicrobial activity by Cylindrical Plate method using Ciprofloxacin and Tinidazole as a standard drugs against gram positive bacteria,(*B. pumilus, S. aureus*) and gram negative bacteria *S. aboney* The result were expressed in the form of zone of inhibition at 100µg/ml concentration.[14]

RESULTS AND DISCUSSION

The physical data for the complexes are presented in Table I represent, percentage yield; melting point / decomposition temperature, as well as their color. The complexes are stable solid with melting point ranging from 220 - 280°C. Table II represent the IR frequencies of the complexes shows the C-H streching (3096-2800 cm^{-1}), >C=O (2250-2000 cm^{-1}) due, NO2 (1570-1540 and 1366-1358cm^{-1}), M-O (600-480 cm^{-1}) indicates the coordinate covalent bond formed between ligand and metal. Conductivity measurements, NMR and MASS (m/z) of the complexes as presented in Table III, which shows that the complexes are non-electrolytes in solution. The ^{1}HNMR (DMSO-d_6) spectra of complex, displays the triplet of methyl group (-$SO_2CH_2\underline{CH_3}$) resonates at δ 1.28-1.40 ppm, quartet of methylene group (-$SO_2\underline{CH_2}CH_3$) resonates at δ 3.15 ppm, triplet for(-$CH_2\underline{CH_2}SO_2CH_2CH_3$) resonates at δ 3.66-3.89 ppm, singlet for (-N=C-$\underline{CH_3}$) resonates at δ 4.26-4.30, triplet for (imidazole-$\underline{CH_2}CH\ _2SO_2CH_2CH_3$) resonates at δ 4.96 ppm, all the aromatic proton resonates between δ 6.54-7.94 , the singlet for (1H nitroimidazole ring) observed between δ 7.87-8.1ppm. The molecular ions were observed. The fragmentation routes primarily involved losses of, NO (M-30), NO_2 (M-46) and HNO_2 (M-47) from the molecular ion, which are characteristic of compounds which indicates the complex formed as, Metal: Lignads; 1:2 ratio.

TABLE 1: PHYSICAL CHARACTERISTICS OF $[Ni(NIM)_2]Cl_2$

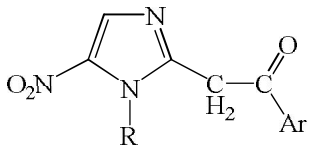

NIM = 5-Nitroimidazoles

Ligand / Complex	Color	R	Ar	m.p. (^{0}C)	Yield (%)*	Molecular formula	Mol. weight
NIMP (Ligand)	Yellow	$-C_2H_4SO_2C_2H_5$	phenyl	146-148*	80	$C_{15}H_{17}N_3O_5S$	351.38
$[Ni(NIMP)_2]Cl_2$	Dark brown	$-C_2H_4SO_2C_2H_5$	phenyl	262-264	85	$C_{30}H_{34}N_6Cl_2O_{10}S_2Ni$	831.76
NIMPCl (Ligand)	Light yellow	$-C_2H_4SO_2C_2H_5$	*p-cl* phenyl	152-154	72	$C_{15}H_{16}ClN_3O_5S$	385.82
$[Ni(NIMPCl)_2]Cl_2$	Brown	$-C_2H_4SO_2C_2H_5$	*p-cl* phenyl	280-282	90	$C_{30}H_{32}Cl_3N_6O_{10}S_2Ni$	865.76
NIMMCL(Ligand)	Yellow	$-C_2H_4SO_2C_2H_5$	*m-cl* phenyl	156-158	65	$C_{15}H_{16}ClN_3O_5S$	385.82
$[Ni(NIMMCL)_2]Cl_2$	Reddish brown	$-C_2H_4SO_2C_2H_5$	*m-cl* phenyl	240-243	70	$C_{30}H_{32}Cl_3N_6O_{10}S_2Ni$	865.76
NIMOCl(Ligand)	Yellow	$-C_2H_4SO_2C_2H_5$	*o- cl* phenyl	180-182	45	$C_{15}H_{16}ClN_3O_5S$	385.82
$[Ni(NIMOCl)_2]Cl_2$	Red	$-C_2H_4SO_2C_2H_5$	*o- cl* phenyl	260-264	65	$C_{30}H_{32}Cl_3N_6O_{10}S_2Ni$	865.76
NIMF(Ligand)	Yellow	$-C_2H_4SO_2C_2H_5$	furoyl	165-166*	75	$C_{13}H_{15}N_3O_6S$	341.34
$[Ni(NIMF)_2]Cl_2$	Red	$-C_2H_4SO_2C_2H_5$	furoyl	232-235	75	$C_{26}H_{30}N_6Cl_2O_{12}S_2Ni$	811.68
NIMDF(Ligand)	Yellow	CH_3	furoyl	130-132	78	$C_{10}H_9N_3O_4$	235.20
$[Ni(NIMDF)_2]Cl_2$	Brown	CH_3	furoyl	278-280	72	$C_{26}H_{30}N_6Cl_2O_{12}S_2Ni$	599.40
NIMDP(Ligand)	Yellow	CH_3	phenyl	140-143	78	$C_{12}H_{11}N_3O_3$	245.23
$[Ni(NIMDP)_2]Cl_2$	Red	$-CH_3$	phenyl	222-225	82	$C_{24}H_{22}N_6Cl_2O_6Ni$	619.46

TABLE 2: SPECTRAL DATA OF $[Ni(NIM)_2]Cl_2$

Ligand / Complex	IR (Cm^{-1})			
	v (CH_2)	v(C=O)	v(NO_2)	v(M-O)
NIMP (Ligand)	2977-2800	1720	1570,1365	--
$[Ni(NIMP)_2]Cl_2$	2977-2800	2270	1570,1365	495
NIMPCl (Ligand)	2977-2850	1700	1565,1365	---
$[Ni(NIMPCl)_2]Cl_2$	2980-2850	2250	1558,1361	484
NIMMCL(Ligand)	2977-2850	1700	1565,1365	---
$[Ni(NIMMCL)_2]Cl_2$	2900-2850	2248	1570,1350	500
NIMOCl (Ligand)	2977-2850	1700	1565,1365	---
$[Ni(NIMOCl)_2]Cl_2$	2900-2850	2230	1550,1345	520
NIMF (Ligand)	2977-2850	1690	1550.1360	---
$[Ni(NIMF)_2]Cl_2$	2980-2900	2270	1545,1360	510
NIMDF (Ligand)	2977-2850	1700	1555,1362	---
$[Ni(NIMDF)_2]Cl_2$	2980-2900	2270	1545,1360	525
NIMDP (Ligand)	3000-2950	1705	1572,1360	---
$[Ni(NIMDP)_2]Cl_2$	2980-2900	2270	1555,1340	512

The IR frequency for ligand and complex was compared; it was found that frequencies for CH_2, NO_2 is matching with frequency of complex. The frequency for carbonyl is changed drastically as it is useful band in the infrared spectra of carbonyl ligand in metal complexes is that due to C–O stretching. The latter gives very strong sharp bands which are separated from the bands of other ligand that may be present. The

stretching wave number for a terminal carbonyl ligand in a complex correlates with the 'electron-richness' of the metal. The band position is determined by the bonding from the d orbitals of the metal into the π* anti-bonding Orbitals of the ligand (known as *backbonding*). The bonding weakens the C–O bond and lowers the wave number value from its value in free CO thus its show lower frequency ranging 2250-1700cm^{-1}[15] The M-O streching is observed near 600-480 Cm^{-1}.

TABLE 3: SPECTRAL DATA OF [NI(NIM)$_2$]Cl$_2$

Complex	1HNMR	Molar Cond. (µS)	Mass (m/z)
[Ni(NIMP)$_2$]Cl$_2$	δ 1.28(t,3H,$SO_2CH_2\underline{CH_3}$), δ 3.15 (q, 2H, -$SO_2\underline{CH_2}CH_3$), δ 3.89 (t, 2H, -$CH_2\underline{CH_2}SO_2CH_2CH_3$), δ 4.26 (s, 3H, N=C-$\underline{CH_3}$), δ 4.96 (t, 2H, imidazole-$\underline{CH_2}CH\ _2SO_2CH_2CH_3$), δ 7.56-7.94 (m, 4H, Ar-H), δ 7.81 (s,1H, nitroimidazole)	3.20	831.76
[Ni(NIMPCl)$_2$]Cl$_2$	δ1.28(t,3H,$SO_2CH_2\underline{CH_3}$), δ 3.20 (q, 2H, -$SO_2\underline{CH_2}CH_3$), δ 3.72 (t, 2H,-$CH_2\underline{CH_2}SO_2CH_2CH_3$), δ 4.30 (s, 3H, N=C-$\underline{CH_3}$), δ 4.90 (t, 2H, imidazole-$\underline{CH_2}CH\ _2SO_2CH_2CH_3$), δ 7.60-7.84 (m, 5H, Ar-H), δ 7.87 (s,1H, nitroimidazole)	1.6	----
[Ni(NIMMCL)$_2$]Cl$_2$	-----	1.25	-----
[Ni(NIMOCl)$_2$]Cl$_2$	----	1.10	866.50 (M+1)
[Ni(NIMF)$_2$]Cl$_2$	δ 1.40 (t,3H,-$SO_2CH_2\underline{CH_3}$), δ 3.15 (q, 2H, -$SO_2\underline{CH_2}CH_3$), δ 3.66 (t, 2H, -$CH_2\underline{CH_2}SO_2CH_2CH_3$), δ 4.26 (s, 3H, N=C-$\underline{CH_3}$), δ 4.96 (t, 2H, imidazole-$\underline{CH_2}CH\ _2SO_2CH_2CH_3$), δ 6.54 (d, 1H, 3-furoyl), δ 6.754 (d, 1H, 4-furoyl), δ 7.59(s, 1H, 5-furoyl), δ 8.1 (s,1H, nitroimidazole)	2.0	811.68
[Ni(NIMDF)$_2$]Cl$_2$	δ 4.30 (s, 3H, N=C-$\underline{CH_3}$), δ 4.96 (s, 3H, imidazole-$\underline{CH_3}$), δ 6.54 (d, 1H, 3-furoyl), δ 6.754 (d, 1H, 4-furoyl), δ 7.59(s, 1H, 5-furoyl), δ 7.98 (s,1H, nitroimidazole)	1.30	----
[Ni(NIMDP)$_2$]Cl$_2$	-----	1.20	831.76

TABLE 4: ZONE OF INHIBITION OF $[Ni(NIM)_2]Cl_2$

Complex	Gram positive bacteria		Gram negative bacteria
	B. Pumilus ATCC 14884 Zone of inhibiton (mm)	*S. aureus* ATCC 29737 Zone of inhibiton (mm)	*S. aboney* NCTC 6017 Zone of inhibiton (mm)
$[Ni(NIMP)_2]Cl_2$	---	---	---
$[Ni(NIMPCl)_2]Cl_2$	---	---	---
$[Ni(NIMMCL)_2]Cl_2$	---	---	---
$[Ni(NIMOCl)_2]Cl_2$	---	---	---
$[Ni(NIMF)_2]Cl_2$	15	10	
$[Ni(NIMDF)_2]Cl_2$	25	23	---
$[Ni(NIMDP)_2]Cl_2$	13	20	---
Tinidazole (Control)	---	---	---
Ciprofloxacin (Control)	30	29	31

The complex compound $[Ni(NIMF)_2]Cl_2$, $[Ni(NIMDF)_2]Cl_2$, $[Ni(NIMDP)_2]Cl_2$ were found active against gram positive bacteria (*B. Pumilus* , *S. aureus*) but are less than control drug ciprofloxacin. The above compounds were more active against aerobic bacteria as compared to tinidazole. All the synthesized complex remains found inactive against gram negative bacteria (*S.aboney*).

CONCLUSION

The compound were found active against aerobic bacteria containing furoyl ring in the ligand, it is concluded on this basis that furoyl side chain enhances the activity due to the presence of electro negative oxygen atom.

AKNOWLEDGEMENT

The authors are thankful to Pharmacy Department, Sumandeep Vidyapeeth and Prashant and Mittal Kansara Pharmacy College, Pipaliya for providing the facilities for this research work.

REFERENCES

1. Levy SB: The Challenge of Antibiotic Resistance. Scientific American 1998.
2. Cohen ML: Epidemiology of drug resistance: implications for a post-antimicrobial era. Sci 1992; 257:1050-1055.
3. Neu HC : The crisis in antibiotic resistance. Sci 1992;257:1064-1073.
4. Navarro M, Perez H, Sanchez-Delgado RA: Toward a novel metal based chemotherapy against tropical diseases . Synthesis and antimalarial activity in vitro and in vivo of the new goldchloroquine complex [Au(PPh3)(CQ)]PF6. J Med Chem 1997;40:1937-1939.
5. Delhaes L, Abessolo H, Biot C, Berry L, Delcourt P, Maciejewski L, Brocard J, Camus D and Dive D: In vitro and in vivo antimalarial activity of ferrochloroquine, a ferrocenyl analogue of chloroquine against chloroquine-resistant malaria parasites. Parasitol. Res 2001;87: 239.
6. Li-june M: Structure and function of metallo-antibiotics. Med Res Rev 2003;6(23): 697-762.
7. Timerbaev AR, Hartinger CG and Keppler BK : Metallodrug research and analysis using capillary electrophoresis. TrAC Trends Anal Chem 2006;25(9): 868-875.
8. Srivastava AK : Potential use of vanadium compounds in the treatment of diabetes mellitus. Exp Opin Invest Drugs 1995; 4: 525-536.
9. Freeman CD, Klutman NE and Lamp KC: Metronidazole. A Therapeutic Review and Update. Drugs 1997, 54, 679.
10. Barnhost DA, Jr, Foster JA, Chern KC and Meisler DM: The efficacy of topical metronidazole Ophthalmology 1996, 103, 1880.
11. Rasmussen BA, Bush K and Tally FP: Antimicrobial resistance in *Bacteroides.* Clin Infect Dis 1997;24.

12. Edwards, DI: Nitroimidazole drugs - action and resistance mechanisms I. Mechanism of action. J Antimicrob Chemother 1993;31:9.
13. Bharti N, Shailendra, Coles SJ, Hursthouse MB, Mayer TA, Gonzalez Garza MT, Cruz-Vega DE, Mata-Cardenas BD, Naqvi F, Maurya MR and Azam A: Synthesis, crystal structure, and enhancement of the efficacy of metronidazole against *Entamoeba histolytica* by complexation with palladium(II), platinum(II), or copper(II). HelV Chim Acta 2002;85:2704.
14. Athar F, Husain K, Abid M, Agarwal SM, Coles SJ, Hursthouse MB, Maurya MR, and Azam A: Synthesis and anti-amoebic activity of gold(I), ruthenium(II), and copper(II) complexes of metronidazole Chem BiodiVers 2005;2:1320.
15. Stuart B, Infrared Spectroscopy: Fundamentals and Applications, John Wiley & Sons, 2004.

For Correspondence:
Dinesh Chandra G. Desai,
P& M Kansara Pharmacy College,
Pipariya, waghodiya,
Vadodara
Gujarat-India.
Mobile No. +91-
E-mail: dinesh_desai50@yahoo.com